United States Environmental Protection Agency

Final Report

Evaluation of the Emissions from Low-Sulfur and Biodiesel Fuel Used in a Heavy-Duty Diesel Truck during On-Road Operation

Evaluation of the Emissions from Low-Sulfur and Biodiesel Fuel Used in a Heavy-Duty Diesel Truck during On-Road Operation

Final Report

John S. Kinsey

Office of Research and Development

National Risk Management Research Laboratory

Research Triangle Park, NC 27711

Yuanji Dong, Craig Williams, and Russell Logan

ARCADIS U.S., Inc.

4915 Prospectus Drive

Durham, NC 27713

EPA Review Notice

This report has been peer and administratively reviewed by the U.S. Environmental Protection Agency and approved for publication. Mention of trade names or commercial products does not constitute endorsement or recommendation for use.

This document is available to the public through the National Technical Information Service, Springfield, Virginia 22161.

Foreword

The U.S. Environmental Protection Agency (EPA) is charged by Congress with protecting the Nation's land, air, and water resources. Under a mandate of national environmental laws, the Agency strives to formulate and implement actions leading to a compatible balance between human activities and the ability of natural systems to support and nurture life. To meet this mandate, EPA's research program is providing data and technical support for solving environmental problems today and building a science knowledge base necessary to manage our ecological resources wisely, understand how pollutants affect our health, and prevent or reduce environmental risks in the future.

The National Risk Management Research Laboratory (NRMRL) is the agency's center for investigation of technological and management approaches for preventing and reducing risks from pollution that threaten human health and the environment. The focus of the laboratory's research program is on methods and their cost-effectiveness for prevention and control of pollution to air, land, water, and subsurface resources; protection of water quality in public water systems; remediation of contaminated sites, sediments and ground water; prevention and control of indoor air pollution; and restoration of ecosystems. NRMRL collaborates with both public and private sector partners to foster technologies that reduce the cost of compliance and to anticipate emerging problems. NRMRL's research provides solutions to environmental problems by: developing and promoting technologies that protect and improve the environment; advancing scientific and engineering information to support regulatory and policy decisions; and providing the technical support and information transfer to ensure implementation of environmental regulations and strategies at the national, state, and community levels.

This publication has been produced as part of the laboratory's strategic long-term research plan. It is published and made available by EPA's Office of Research and Development to assist the user community and to link researchers with their clients.

Sally Gutierrez, Director
National Risk Management Research Laboratory

Abstract

In October of 2004, the Air Pollution Prevention and Control Division of the U.S. EPA's National Risk Management Research Laboratory investigated the emissions from a diesel-powered tractor-trailer operating along a highway at near-zero grade. In place of a dynamometer and standard dilution tunnel, the Diesel Emissions Aerosol Laboratory (DEAL) was used to sample both the exhaust plume of the truck and the background environment, which eliminated the contributions of other vehicle emissions to the plume measurements. The primary thrust of the research was to compare the truck's emissions when using low sulfur (15 ppm) diesel fuel (base fuel) with those when using a 20% soy-based biodiesel blend (B20). These comparisons were made for two speeds (56 and 105 km/h) and load conditions—21,350 and 33,850 kg gross vehicle weight (GVW). Each time the fuel was changed, the truck was returned to the dealer to have the filters replaced, the old fuel removed, and the new fuel added. The highway traversed during the bulk of the measurements was a level section of US-70 in eastern North Carolina near the town of New Bern. After 20 days of primary experiments near New Bern were completed, an additional two days were spent driving a section of Virginia's I-77 between Exits 1 and 8, which is near the town of Fancy Gap, VA, to investigate the effect of road grade on diesel emissions. The truck used standard pump fuel during this phase of the research. The DEAL was instrumented to measure total hydrocarbons (THC), carbon monoxide (CO), carbon dioxide (CO_2), oxides of nitrogen (NO_X), fine particulate matter (PM-2.5—PM with an aerodynamic diameter equal to or less than 2.5 µm) and the chemical composition of selected gas- and particle-phase air pollutants. Using B20 in place of the base fuel reduced nearly all emissions under nearly all combinations of speed and GVW examined, but the greatest reduction was in PM emission factors. For example, at the higher GVW and 56 km/h, using B20 reduced emissions of NO_X by 9%, CO by 8%, THC by 20%, and PM by 68% compared with the base fuel. At the lower GVW and 105 km/h, using B20 reduced emissions of NO_X by 5%, CO by 13%, THC by 18%, and PM by 19% compared with the base fuel. Changes in GVW at a given speed and fuel type had a smaller effect on emissions than changes in speed for a given load and fuel type. With regard to chemical composition, both black carbon (which approximates elemental carbon content) and particle-phase polycyclic aromatic hydrocarbons decreased at all speed and load conditions when using B20 in place of the base fuel. Also, B20 produced less C17-C31 alkanes when compared to the base fuel.

Table of Contents

List of Appendices

Appendix A: Chemical Composition

Appendix B: Fuel Analysis Report

Appendix C: INNOVA Analyzer Calibration Sheets

Appendix D: Thermocouple Calibration Sheets

Appendix E: Mass Flow Controllers Calibration Sheets

Appendix F: Pressure Transducer Calibration Sheets

List of Tables

List of Figures

xi

List of Acronyms

Acronym	Definition
AC	alternating current
AIM	Aerosol Instrument Manager
ANOVA	analysis of variance
APEX	Aircraft Particulate Emissions Experiment
APPCD	Air Pollution Prevention and Control Division
ASAE	American Society of Agricultural Engineers
ASTM	American Society for Testing and Materials
ATI	Advanced Telemetrics International
B&K	Bruell and Kjaer
BC	black carbon
BTU	British thermal units
C	carbon
C_3H_8	propane
CAI	California Analytical Instruments, Inc
CD	compact disc
CEM	continuous emissions monitors
CEMS	continuous emission monitoring systems
CFD	computational fluid dynamics
CFR	Code of Federal Regulations
CO	carbon monoxide
CO_2	carbon dioxide
CPC	Condensation Particle Counter
DAS	Data Acquisition System
DC	direct current
DD60	Detroit Diesel Series 60
DDEC60	Detroit Diesel Series 60 Engine Computer
DEAL	Diesel Emissions Aerosol Laboratory (Previously named Mobile Diesel Laboratory or MDL)
DLS	descriptive level of significance
DMA	Differential Mobility Analyzer

Acronym	Definition
DP	differential pressure
DQI	data quality indicator
DR	dilution ratio
EC	elemental carbon
EC/OC	elemental carbon/organic carbon
EC/PM	(weight) fraction of elemental carbon in particulate matter
EF	emission factor
EF_M	mass emission factor
EF_N	number emission factor
EF_{THC}	total hydrocarbon emission factor
ELPI	Electrical Low Pressure Impactor
EM	distance-specific emission rate
EPA	Environmental Protection Agency
ER	emission rate
ER_{NOx}	emission rate for oxides of nitrogen
ESP	electrostatic precipitator
FIA	Flame Ionization Analyzer
FID	flame ionization detector
FM-200	hydrofluorocarbon tracer gas (1,1,1,2,3,3-heptafluoropropane)
FPCL	Fine Particle Characterization Laboratory
FTP	Federal Test Procedure
GC	gas chromatography
GC/MS	gas chromatography/mass spectroscopy
GHV	gross heat value
GMD	geometric mean diameter
GVW	gross vehicle weight
H	hydrogen
H_2O	water
HL	heated sample line
HP	Hewlett-Packard
HPLC	high performance liquid chromatograph

Acronym	Definition
I/O	input/output
IC	ion chromatography
kW	kilowatt
LPM	liters per minute
MFM	mass flow meter
MnO_2	manganese dioxide
MOP	miscellaneous operating procedure
MPA	magneto pneumatic
MS	mass spectrometer
MSD	mass-selective detection
MW C_3H_8	molecular weight of C_3H_8
MWCO	molecular weight of CO
MWNO	molecular weight of NO
N/A	not applicable
NC	North Carolina
NCDOT	North Carolina Department of Transportation
ND	not determined
NDIR	non dispersive infrared
NH_4^+	ammonium ion
NIOSH	National Institute for Occupational Safety and Health
NO	nitric oxide
NO/NO_X	nitric oxide/oxides of nitrogen
NO_2	nitrogen dioxide
NO_3^-	nitrate ion
NO_X	oxides of nitrogen
NREL	National Renewable Energy Laboratory
NS	non speciated
OAQPS	Office of Air Quality Planning and Standards
OC	organic carbon
OC/EC	organic carbon/elemental carbon
OC/PM	(weight) fraction of organic carbon in particulate matter

Acronym	Definition
PAH	polycyclic aromatic hydrocarbons
PAS	photoelectric aerosol sensor
PM	particulate matter
PM_{10}	particles with an aerodynamic diameter of 10 µm or less
$PM_{2.5}$	particles with an aerodynamic diameter of 2.5 µm or less
PSD	particle size distribution
PTV	programmable temperature vaporizing (inlet)
PUF	polyurethane foam
QAPP	Quality Assurance Project Plan
QCM	quartz crystal microbalance
QF	quartz filter
R&P	Rupprecht & Patashnick
RH	relative humidity
RHC	ratio of hydrogen to carbon
RL	road load
RPD	relative percent difference
RPM	revolutions per minute
RSD	relative standard deviation
SAE	Society of Automotive Engineers
SD	standard deviation
SG	span gas
SMPS	Scanning Mobility Particle Sizer
SO_2	sulfur dioxide
SO_4^{-2}	sulfate ion
SS	sum of squares
TCD	thermal conductivity detector
TD	thermal denuder
TEOM	tapered element oscillating microbalance
TF	Teflon
THC	total hydrocarbons
U.S.	United States

Acronym	Definition
U.S. EPA	United States Environmental Protection Agency
UPS	uninterruptible power supplies
UV	ultraviolet
VV	gross vehicle weight variable used in equations
WT	weight
WVU	West Virginia University
XRF	X Ray fluorescence

Chapter 1
Introduction

1.1   Background

The fine particulate matter (PM) from diesel trucks is of interest to both the U. S. Environmental Protection Agency's (EPA's) Office of Transportation and Air Quality in their regulatory program for on-road vehicles and the Office of Air Quality Planning and Standards for implementation of the PM-2.5 (PM with an aerodynamic diameter equal to or less than 2.5 µm) ambient air quality standard. In prior research conducted by EPA's National Risk Management Research Laboratory, Air Pollution Prevention and Control Division (APPCD), stack dilution sampling was used to characterize the PM emissions from APPCD's Kenworth T-800 tractor equipped with a high mileage Detroit Diesel Series 60 (DD60) engine and associated 14 m (45 ft) Great Dane trailer. However, when stack emissions data were compared to concurrent measurements conducted in the exhaust plume, it was determined that the stack dilution method produced substantially smaller particles than actually exist in the plume (Brown et al., 2000). Therefore, in order to collect data more representative of the "real world," a decision was made to abandon stack dilution sampling in favor of plume measurements for all future on-road experiments.

In order to design a suitable capture/collection system for plume sampling purposes, a significant effort was conducted consisting of a combination of computational fluid dynamics modeling (CFD), tracer gas analyses, and flow visualization experiments using smoke, colored streamers, and oil stain tests (Kinsey et al., 2006a). This effort was conducted in collaboration with an expert in vehicle aerodynamics at the Kenworth Truck Company in Kirkland, WA. The research resulted in a special probe and associated flow tunnel system that was installed in the rear of the Great Dane trailer. The probe position was selected from the results of the tracer gas measurements to incorporate a significant portion of the exhaust plume under varying wind conditions.

In addition, due to the overall age and condition of the original DD60, a new 2000 model year replacement engine was purchased for the Kenworth tractor. Before its installation, however, a series of tests were performed in the engine test cell at West Virginia University (WVU) using a secondary dilution tunnel constructed for this purpose (Kinsey et al., 2006b). The objective of these experiments was to determine the "baseline" emissions from the new engine and, more importantly, to compare the data obtained by various aerosol analyzers, samplers, and sampling media and to assess their usefulness in future on-road plume sampling. The WVU experiments were conducted in two phases with the first phase (June 2001) devoted to evaluation of the new DD60 under different operating conditions and the second phase (January 2003) to the assessment of alternate analyzer operating protocols and sampling media using a smaller Navistar engine operated at steady state. The results of the WVU testing were used in the selection of the various samplers and analyzers described in Section 4.

This report contains a description of the Diesel Emissions Aerosol Laboratory (DEAL), followed by the procedures for and the results from conducting a series of on-road experiments in the fall of 2004 using a low-sulfur base fuel meeting 2005 specifications and a 20% mixture of soy-derived biodiesel and base (B20) fuels. These experiments were conducted on a stretch of US-70 at near zero grade in New Bern, North Carolina and on a stretch of I-77 at ~4% grade that crosses the North Carolina-Virginia border around Fancy Gap, Virginia. Partial funding for this project was provided by the U.S. Department of Energy's (DOE's) National Renewable Energy Laboratory in Golden, CO, through Interagency agreement No. DE-A104-2001AL67139.

1.2   Objectives

The objectives of the on-road experiments were to

- Generate the data necessary to develop predictive emission factors that relate PM emissions to key vehicle operating parameters,

- Develop chemical source profiles of the PM emissions from the APPCD research vehicle under "real world" conditions focusing on the effects of atmospheric dilution on gas-to-particle conversion,

- Compare the emissions generated by the two fuel types, and

- Begin development of a database from which a suitable dilution sampling methodology can be developed for a chassis dynamometer system that emulates the characteristics of the "real world" plume produced by heavy-duty diesel trucks.

1.3   Report Organization

This document reports the results of the on-road testing conducted during the experimental program. Sections 1 and 2 describe the DEAL and its associated instrumentation. Section 4 provides the field test procedures, Section 5 provides the post-test laboratory analyses, and Section 6 provides the data analysis procedures used to produce the experimental results. Sections 7 through 9 present the test results for vehicle operation, gaseous emissions, and PM-2.5 emissions, respectively. Quality Assurance and Quality Control is described in Section 10, and Section 11 compares the results to historical data. Finally, the research findings are provided in Section 12 and the references in Section 13. Due to the generally low reliability of the black carbon and particle surface polycyclic aromatic hydrocarbon instruments as well as the small time-integrated sample set collected, these data are provided in Appendix A. Also appended are the fuel analyses and instrument calibrations for the study.

Chapter 2
Diesel Emissions Aerosol Laboratory (DEAL)

2.1   General Description

The DEAL consists of a Kenworth T-800 diesel-powered tractor and a 14-m (45-ft) Great Dane trailer shown in the photograph in Figure 2-1. The general specifications of the DEAL are outlined in Table 2-1. A unique capability of the DEAL is the ability to capture a sample from a target source using a plume sampling system while simultaneously measuring a combination of the ambient plus vehicular background using a separate system collecting a sample from the tractor-trailer gap (see Kinsey et al., 2006a) . In addition to capturing air samples from a target source and background, the DEAL monitors other vehicle system parameters such as drive shaft torque, exhaust flow, engine RPM, and acceleration.

Figure 2-2 shows the DEAL layout and the locations of the two sampling systems. The sample measurements for the air pollutants and tracer gases measured in the study are summarized in Table 2-2. A detailed description of the construction and operation of the DEAL and the various instruments may be found in the Mobile Diesel Laboratory Fine PM Emissions Support: Steady-State Experiments, Quality Assurance Project Plan (QAPP), U.S. EPA, Research Triangle Park, NC, January 2003, which is included here by reference (U.S. EPA, 2004).

Electric power is supplied to the trailer through two panel boxes from which individual circuits are run to various locations inside the trailer to support the power requirements of all the instruments, pumps, blowers, and other equipment. The panel boxes can receive power from a conventional power source or from two 12 kW diesel-powered generators mounted to the underside of the trailer. The exhaust from the generators are ducted into the flow field beneath the trailer so as not to contaminate the exhaust plume from the main propulsion engine. When the DEAL is in its staging configuration, it can accept external (i.e., utility) power and additional calibration gases. All instruments used are supplied conditioned power via uninterruptible power supplies (UPS). Pumps and other equipment that do not contain delicate electronics do not receive conditioned power.

The facility includes removable weights (large blocks of concrete), which simulate the effects of truck payload on emissions. The weight is removable in 12 discrete increments, limited only by the necessity to distribute the load evenly within the cargo area. The presence or absence of weight, which is undetectable by the Data Acquisition System (DAS), is recorded in the project notebook. The gross vehicle weight of both the loaded and unloaded vehicle is determined prior to a sampling campaign by running the vehicle across a certified scale. Section 3.2.1 discusses further the procedure for transferring the weights, the actual number of weights used and the loaded testing weight for the campaign.

Figure 2-1.   Kenworth T-800 Tractor and Great Dane Trailer, Locations of the Plume and Background Sampling Probes

Table 2-1.   General Specifications for the DEAL

Vehicle Parameter	Specification
SAE Vehicle Classification	3-S2
Gross Vehicle Weight (GVW) classification	8
Service classification	D
Gross train weight or gross vehicle weight	36,280 kg (80,000 lbs)
Tractor wheelbase	6.1 m (20 ft)
Length of trailer	14 m (45 ft)
Tire size/type	Michelin 11R24.5 radial
Engine	2000 Detroit Diesel Series 60
Engine displacement	12.7 liters
Engine power output	373 kW (500 hp) @ 2100 rpm
Engine emission limit (measured at WVU)[a]	0.13 g/kWXhr (0.1 g/bhpXhr)

a. See Kinsey et al. 2006a.
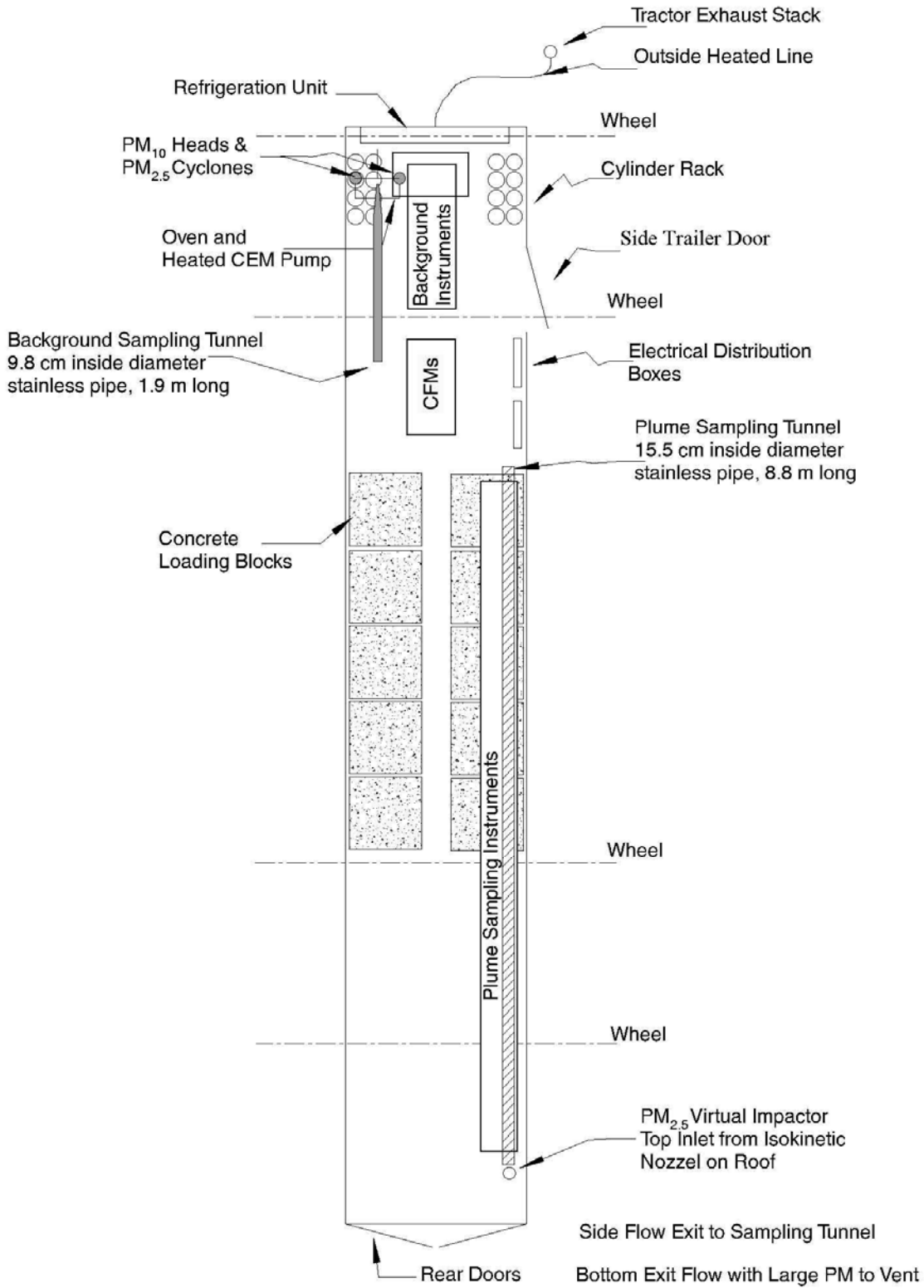
Figure 2-2.   DEAL Trailer Layout

Table 2-2.   Summary of DEAL Vehicle System and Environmental Measurements

Experimental Parameter	Sampling Location [a]	Measurement Technique	Type of Sample Collection	Instrument(s) / Sampling Media	Serial Number(s) [b]
Total PM-2.5 Mass Concentration	Background/Splitter 1	Tapered element microbalance	Continuous	Thermo Electron Series 1400a Tapered Element Oscillating Microbalance (1400 TEOM)	1400AB2314900007
	Background/Splitter 1	Gravimetric analysis	Time-integrated	47-mm Teflon filter in stainless steel holder equipped with double quartz back-up filters for collection of gas-phase "blow-off" [c] (Teflon Filter)	N/A [b]
	Plume/Splitter 1	Microbalance	Continuous	Thermo Electron Series 1105a Tapered Element Oscillating Microbalance (1105a TEOM)	1105A201359902
	Plume/Splitter 1	Microbalance	Continuous	SEMTECH Model RPM-100 Quartz Crystal Microbalance, (QCM)	1
	Plume/Splitter 1	Gravimetric analysis	Time-integrated	47-mm Teflon filter in FTP holder equipped with double quartz back-up filters for collection of gasphase "blow-off" (FTP 1) [c]	N/A
Total PM-2.5 Number Concentration [d]	Background/Splitter 2	Condensation nuclei counter	Condensation nuclei counter	TSI Model 3025a Condensation Particle Counter (CPC)	1236
	Plume/Splitter 2	Condensation nuclei counter	Condensation nuclei counter	TSI Model 3025a Condensation Particle Counter (CPC)	1238

Experimental Parameter	Sampling Location [a]	Measurement Technique	Type of Sample Collection	Instrument(s) / Sampling Media	Serial Number(s) [b]
Particle Size Distribution	Background/Splitter 2	Low-pressure cascade impactor (aerodynamic diameter)	Continuous/Time-integrated [e]	Dekati Electrical Low Pressure Impactor (ELPI)	24139
	Background/Splitter 2	Electrical mobility classifier/condensation nuclei counter (electrical mobility diameter)	Continuous	TSI Model 3934 Scanning Mobility Particle Sizer (SMPS): Model 3071A Classifier and Model 3010 Condensation Particle Counter (CPC) (3934 SMPS	543 (Classifier) 2151 (CPC)
	Plume/Splitter 2	Low-pressure cascade impactor (aerodynamic diameter)	Continuous/time integrated [e]	Dekati Electrical Low Pressure Impactor (ELPI)	24167
	Plume/Splitter 2	Electrical mobility classifier/ condensation nuclei counter (electrical mobility diameter)	Continuous	TSI Model 3936 (long) Scanning Mobility Particle Sizer (SMPS): Model 3080 Classifier, Model 3025a CPC, and Model 3081 DMA [f] (3936 SMPS) TSI Model 3936 (nano) Scanning Mobility Particle Sizer (SMPS): Model 3080 Classifier, Model 3025a CPC, and Model 3085 DMA (Nano SMPS)	8237 (Classifier) 1339 (CPC) 1042 (DMA) 8041 (Classifier) 1239 (CPC) 5125 (DMA)

Experimental Parameter	Sampling Location [a]	Measurement Technique	Type of Sample Collection	Instrument(s) / Sampling Media	Serial Number(s) [b]
Elemental/Organic Carbon (EC/OC)	Background/Splitter 1	Thermo-optical analysis (NIOSH Method 5040)	Time-integrated	Pre-fired 47-mm quartz filter with double quartz back-up filter (Quartz Filter)	N/A
	Plume/Splitter 1	Thermo-optical analysis (NIOSH Method 5040)	Time-integrated	Pre-fired 47-mm quartz filter with double quartz back-up filter (FTP 2)	N/A
	Plume/Splitter 3	Optical attenuation/UV absorption ("black" and "blue" carbon) [g]	Continuous	Magee (Andersen) Model AE-2 Aethalometer (Aethalometer)	181
	Stack	Thermo-optical analysis (NIOSH Method 5040)	Time-integrated	Heated pre-fired 142 mm quartz filter in special holder	N/A
Semivolatile Organic compounds [h]	Background/Splitter 1 (speciated tests)	GC/MS [i]	Time-integrated	Pre-fired 47-mm quartz filter equipped with (4) PUF plugs for collection of gas-phase "blow-off" [c, j] (quartz filter)	N/A
	Plume/Splitter 1(speciated tests)	GC/MS [i]	Time-integrated	Pre-fired 47-mm quartz filter equipped with (4) PUF plugs for collection of gas-phase "blow-off" [c, j] (FTP 2)	N/A
	Plume/Splitter 3	UV analyzer (surface PAHs) [k]	Continuous	EcoChem Model PAS 2000 (PAS 2000)	145
PM volatile organic compounds	Plume/ Splitter 3	Gravimetric/thermo-optical analysis	Time-integrated	Dekati Model EKA-111 thermal denuder with parallel Teflon and double pre-fired quartz filters (Thermal Denuder)	63157

Experimental Parameter	Sampling Location [a]	Measurement Technique	Type of Sample Collection	Instrument(s) / Sampling Media	Serial Number(s) [b]
Tracer Gas [l]	Background	Infrared absorption	Periodic continuous	INNOVA Air Tech Instruments A/S Model 1314A Photoacoustic Analyzer (Gas Tracer)	032-010
	Plume	Infrared absorption	Periodic continuous	INNOVA Air Tech Instruments A/S Model 1314A Photoacoustic Analyzer (Gas Tracer)	032-010
Carbon Monoxide (CO)	Background	Nondispersive infrared	Integrated bag [m]	California Analytical Model 300	1L09016
	Stack	Nondispersive infrared	Continuous	California Analytical Model 300 (low Concentration)	1L09016
Carbon Dioxide (CO_2)	Background	Nondispersive infrared	Integrated bag [m]	California Analytical Model 300	1L09016
	Stack	Nondispersive infrared	Continuous	California Analytical Model 300	1L09016
Oxygen (O_2)	Background	Magneto	Integrated bag [m]	Horiba Model MPA	570762112
	Stack	Magneto	Continuous	Horiba Model MPA	570762112
Nitrogen Oxides (NO_X)	Background	Chemiluminescence	Integrated bag [m]	California Analytical Model 400 HCLD	7L07002
	Stack	Chemiluminescence	Continuous	California Analytical Model 400 HCLD	7L07002
Total Hydrocarbons (THC)	Background	Heated flame ionization	Integrated bag [m]	Horiba Model FIA	8512710101
	Stack	Heated flame ionization	Continuous	Horiba Model FIA	8512710101
Engine Speed	Tractor engine	Rotation sensor	Continuous	DDEC60 [n]	N/A
Vehicle Speed	Tractor chassis	Optical fifth wheel	Continuous	Datron DLS-1 Speed Sensor	03.0488
Fuel Flow	Tractor engine	Injector position	Continuous	DDEC60	N/A
Shaft Torque	Engine Drive Shaft	Strain gages	Continuous	ATI 2000 Series	6-4-7481-1 (module); 750 (electronics)

Experimental Parameter	Sampling Location [a]	Measurement Technique	Type of Sample Collection	Instrument(s) / Sampling Media	Serial Number(s) [b]
Grade and Acceleration [o]	Trailer Chassis	Gyroscope	Continuous	Crossbow Model VG600CA	9913611
Engine Temperature	Various	Thermocouple	Continuous	Omega Engineering	N/A
Exhaust Flow Rate	Exhaust Stack	Multi-orifice pitot tube with differential pressure cell	Continuous	Dieterich Annubar DCR 16S with Validyne P55D Pressure Transmitter	119798 (pressure transducer)
Exhaust Gas Temperature	Exhaust Stack	Thermocouple	Continuous	Omega Engineering	N/A

a. Speciated refers to those tests for which PM chemical composition was determined.

b. N/A = not available.

c. FTP = Federal Test Procedure per 40 CFR, Part 86. "Blow off" are gas-phase semi-volatile species that have been released from the particulate deposited on the primary filter by the airflow passing through the medium. During the "speciated" runs, the double quartz back-up filters are replaced by a series of 4 polyurethane foam (PUF) plugs.

d. These are redundant measurements and were not used in the data analysis.

e. Aluminum foil substrates from ELPI were also analyzed gravimetrically to determine particle size distribution by mass, but not included in the data analysis.

f. DMA (differential mobility analyzer) is part of SMPS and classifies aerosols by electrical mobility.

g. The Aethalometer measures "black" carbon, which approximates elemental carbon content, and "blue" carbon, which is similar to organic carbon.

h. Used during "speciated" runs only, except for EcoChem 2000.

I. GC/MS = gas chromatography/mass spectroscopy.

j. This sampling train replaces the usual quartz/double quartz filter system used in the other tests conducted. The primary quartz filter will also be analyzed for EC/OC by NIOSH 5040.

k. PAHs = polycyclic aromatic hydrocarbons.

l. Tracer gas = 1,1,1,2,3,3,3 heptafluoropropane. Background determined pre-test from engine exhaust gas sampling.

m. Post-test analysis of time integrated Tedlar bag sample collected over the entire test period.

n. Detroit Diesel Series 60 engine computer. Signals will also be obtained for fuel flow and percent rate torque.

o. This instrument was operated but did not provide any useful data. Acceleration was calculated from vehicle speed, and grade was determined using a microbarometer.

2.2　Plume Sample Extraction System

Two fine PM monitoring systems, each consisting of a similar array of particle instruments, are installed in the trailer shown in Figure 2-1. One of the two arrays of particle instruments receives a representative sample through an isokinetic probe positioned in the tractor exhaust plume. As stated previously, the probe design and location were selected from the tracer gas measurements. The plume sample flows through the isokinetic probe into a PM-2.5 "cut-point" (i.e., 50% collection efficiency for unit density spheres $\leq 2.5\ \mu m$) virtual impactor, and then into a 8.8 m, 15.2 cm diameter stainless steel sampling tunnel. (Note: the probe is maintained at isoknetic sampling conditions by manually adjusting the open area to the mean wind velocity based on vehicle speed.) Particle losses to the tunnel walls were not characterized but are expected to be minimal based on well-established aerosol theory. A photograph of the probe and the virtual impactor is shown in Figure 2-3. The right picture in Figure 2-3 was taken from the rear of the trailer with a view toward the front so that the background sampling bench is also visible in the far back between the gas cylinder storage racks.

Figure 2-3.　Plume Sampling System Probe (left) and Virtual Impactor Connected to the Sampling Tunnel (right)

Inside the trailer, the tunnel is supported from the trailer floor by columns integrated into the plume instrument rack. Figure 2-4 shows photographs of the plume tunnel and plume bench. The pictures were taken from the side door looking toward the rear of the trailer. The left picture was taken during initial fabrication and before installing the continuous emission monitor (CEM) bench and any particle instruments or other sensors. Also visible is the plume instrument bench below the tunnel. The right picture was taken after installation of the instruments in the plume sampling bench.

Positioned through ports installed in the tunnel are "buttonhook" probes traditionally used for stack sampling which are staggered in height. The probes extract a sample of the gas inside the tunnel, which is directed to the instruments through four-way splitters and either stainless steel or conductive silicon tubing (Vanguard Products). Figure 2-5 shows a schematic of the plume sampling system with complete organic speciation and Figure 2-6 shows the plume sampling system in the non-speciated configuration. The only difference between the speciated and the non-speciated configurations is that, in the speciated configuration, polyurethane foam (PUF)

plugs are substituted for the quartz back-up filters downstream of FTP 2 on splitter 1. For more information about how the two configurations change the analytical plan refer to Section 2.8. As can be seen in Figures 2-5 and 2-6, all instruments sample the same gas stream with no cross-contamination.

Figure 2-4.   Photographs of the DEAL during Fabrication Showing Sampling Tunnel and Plume Bench (left), and with Instruments Installed (right)
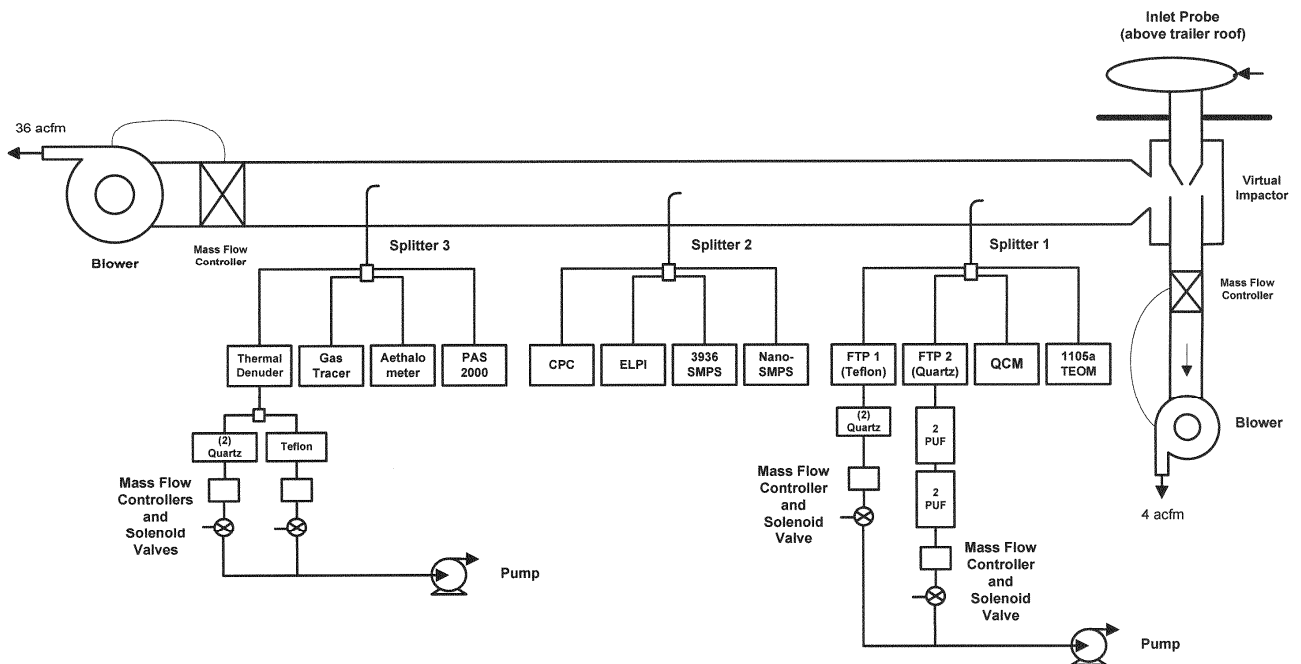
Figure 2-5.   Flow Schematic of Plume Sampling System for Speciated Runs
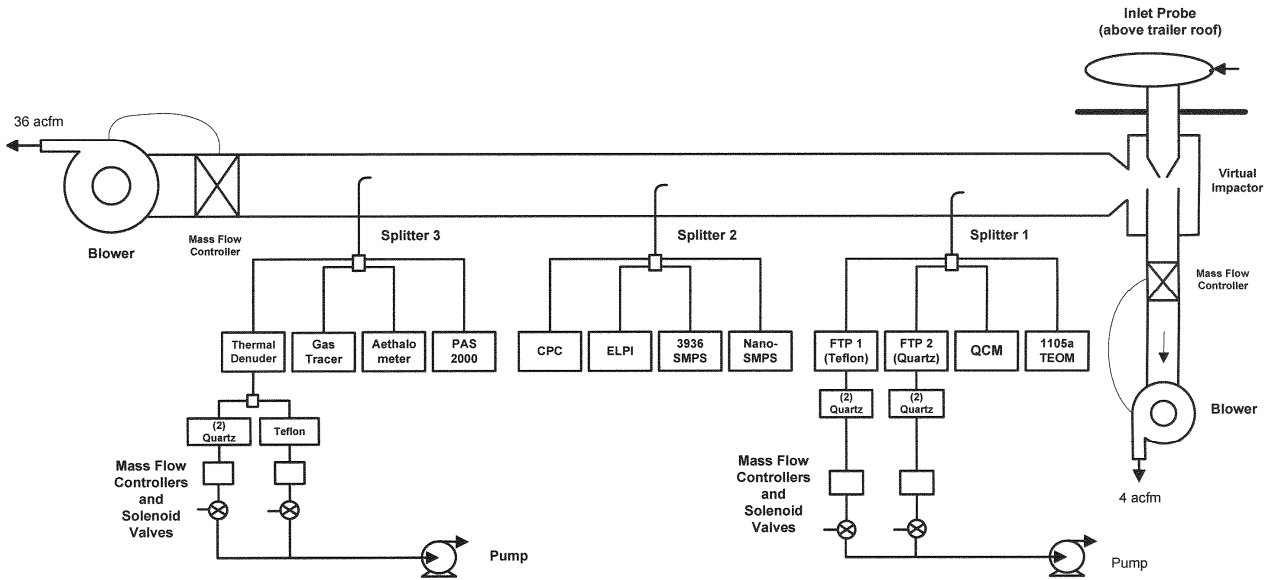
Figure 2-6.   Flow Schematic of Plume Sampling System for Non-Speciated Runs

2.3   Background Sample Extraction System

The background PM instrument array receives a sample external to the tractor exhaust plume, which takes into account both ambient background and the emissions from other vehicles (see Kinsey et al., 2006a). Pictures of the background sampling bench are shown in Figure 2-7. The background sample flows from the probe into two parallel precollectors to remove particles with an aerodynamic diameter greater than PM-2.5 and then flows into a tunnel from which the instruments draw their sample through a series of staggered probes and splitters similar to the plume sampling tunnel. Figure 2-8 shows a schematic of the background sampling system for runs with complete organic speciation, and Figure 2-9 shows the background sampling system in the non-speciated configuration. The only difference between the speciated and the non-speciated configurations is that, in the speciated configuration, PUF plugs are substituted for the quartz back-up filters downstream of the quartz filter on splitter 1. For more information about how the two different configurations change the analytical plan refer to Section 2.8.

Vibration isolators are installed on all particle instruments in both the plume and background sampling systems. The bottoms of the isolators are mounted on aluminum channels cut to fit the depth of the instrument racks, which are fabricated of 10-cm angle iron. These channels with the instruments mounted on top are securely clamped to the instrument rack and the rack base is bolted to the trailer floor.
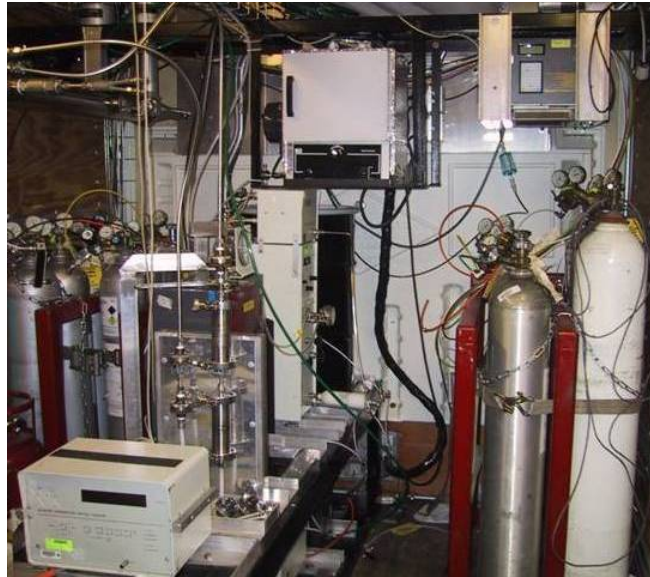
Figure 2-7.   Background Bench Before the Background Tunnel and Instruments were Installed (left), and after Installation (right)
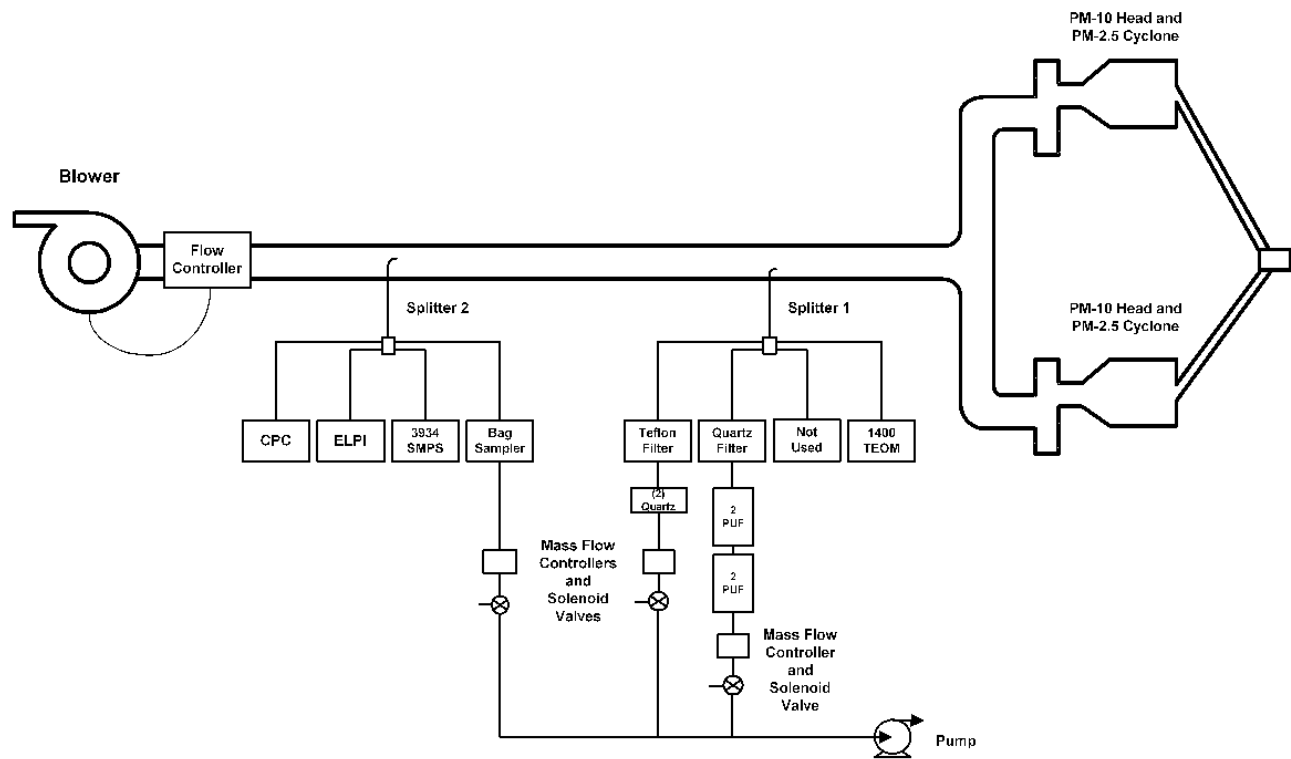
Figure 2-8.   Flow Schematic of the Background Sampling System for Speciated Tests
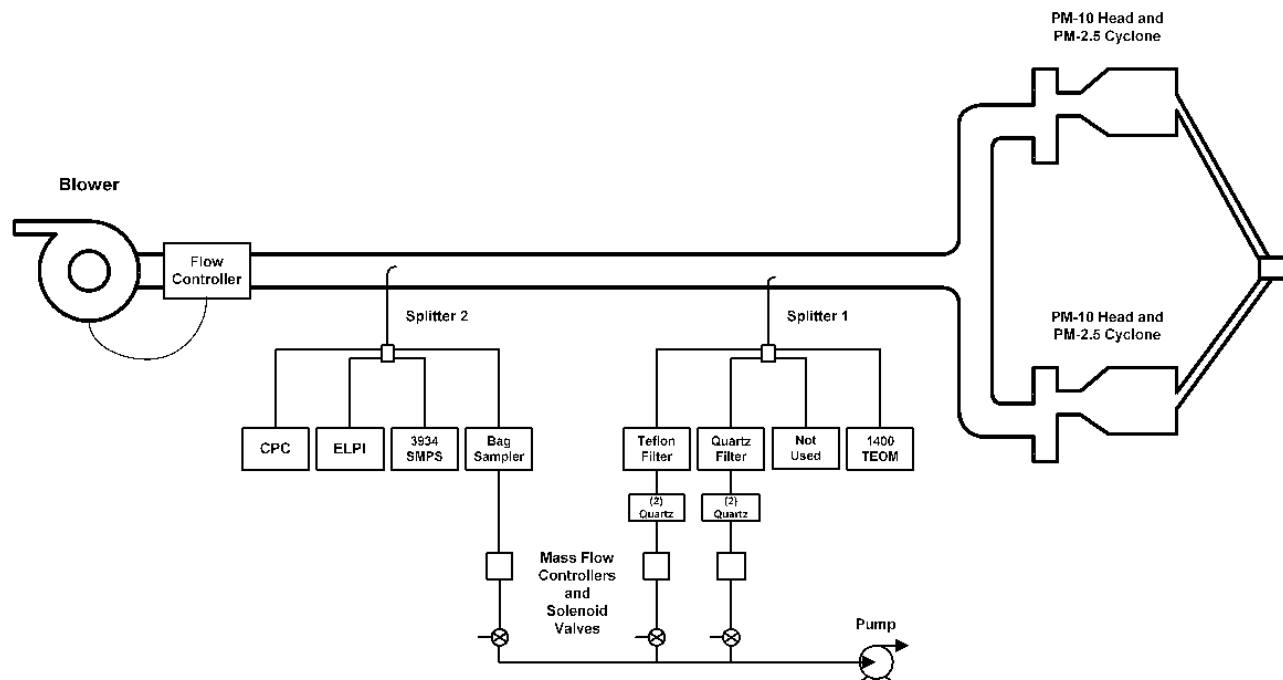
Figure 2-9.   Flow Schematic for the Background Sampling System for Non-Speciated Tests

2.4   Vehicle Operating Parameters

Finally, other instrumentation is also installed in the DEAL to measure key vehicle operating parameters, including parameters that must be determined in order to report emissions in appropriate units and ancillary information that may effect emissions. Monitored vehicle parameters are shown in the schematic illustrated in Figure 2-10.

The data acquisition system (DAS) receives input from sensors that indicate various vehicle operating parameters in real time. Except for the gyroscope and DDEC60 (Detroit Diesel Engine Computer, Series 60), all signals from the vehicle sensors are run through an analog to digital converter and further converted by DASYLAB software to the applicable units of measure.

The DDEC60 engine speed sensor consists of a frequency-to-voltage converter connected to the truck's tachometer input. Other signals logged from the DDEC60 include fuel consumption rate and percent of rated engine torque.

An optical "5th wheel" measurement device (Datron DLS1), attached to the underside of the tractor, measures vehicle speed. This device uses a combination of lenses, a rotating optical grating, photo diodes, and sophisticated analog and digital signal processing to measure the speed of "objects" moving across its illuminated field of vision. For this application, the sensor points straight down toward the pavement and uses irregularities in the roadway surface to detect movement. The raw output consists of a voltage proportional to velocity. A picture representative of this sensor is shown on the bottom of Figure 2-11.
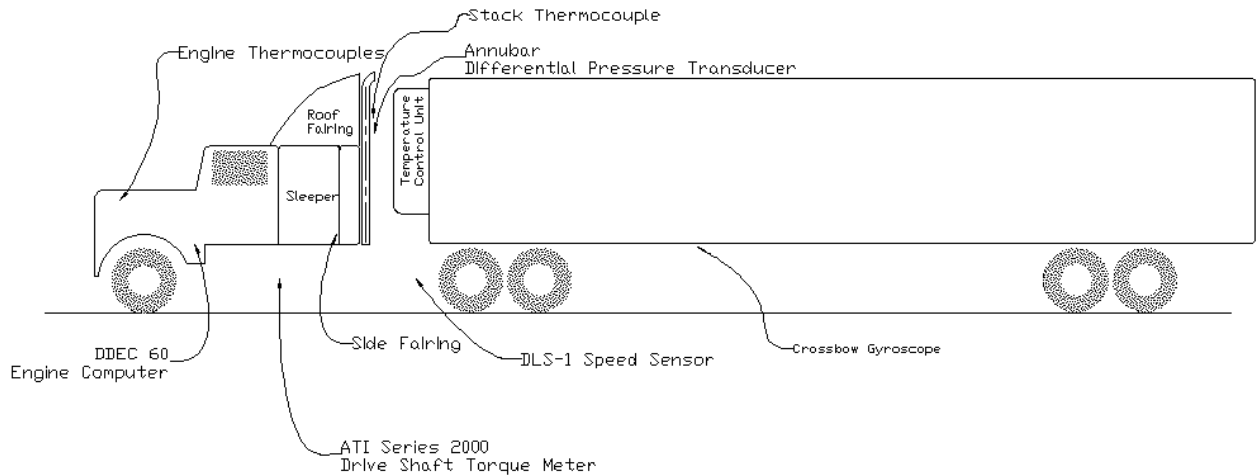
**Figure 2-10.   Schematic of the DEAL Showing the Locations of Sensors that Monitor
Various Vehicle Parameters**

**Figure 2-11.   The ATI Torque Meter Sensor (left) and the Datron Optical Speed Sensor
(right)**

An Advanced Telemetrics International (ATI) Series 2000 torque meter measures drive shaft
torque. The torque meter uses a Wheatstone bridge made up of four resistive strain gauges to
measure the elastic deformation of the drive shaft as torque is applied by the drive train. The
bridge is connected to an electronics module that occupies half of a balanced split-ring housing
clamped around the drive shaft. The electronics module filters and amplifies the signal, which is
transmitted away from the shaft by a frequency modulated transmitter housed in the other half of
the ring. A small antenna mounted nearby picks up the signal for the receiving unit mounted in
the truck cab. Pictures representative of the balanced ring and the receiver are shown in Figure 2-
11.

Exhaust flow is measured by an averaging pitot tube (Annubar), which generates a differential pressure (dP) signal proportional to exhaust gas velocity. A transducer converts the dP to a voltage, which is logged by the DAS. Another dP transducer, along with a thermocouple, provides the static pressure and temperature data necessary to calculate exhaust gas density.

Finally, the Crossbow VG600CA measures vehicle grade and acceleration using three rate sensors oriented in the x, y, and z plane. The sensors consist of a vibrating ceramic plate that utilizes the Coriolis Effect to output the angular rate of change and acceleration. A picture representing the Crossbow gyroscope is shown in Figure 2-12. Table 2-3 lists the various sensors and signal outputs used for the monitoring of vehicle operation.

Figure 2-12.   The Crossbow Gyroscope VG600CA

Table 2-3.   Vehicle Parameters and Sensors

Experimental Parameter	Sampling Location	Measurement Technique	Instrument(s)	Type of Data Collected
Engine speed	Engine	Rotation Sensor	DDEC 60	Digital
Vehicle speed	Under Tractor	Optical Sensor	Datron DLS1 Speed Sensor	0-5 volt analog signal
Fuel flow	Engine	Engine Computer	DDEC 60	Digital
Shaft torque	Drive Shaft	Strain Gage	ATI Strain Gage	0-5 volt analog signal
Exhaust flow rate	Stack	Differential Pressure	Dieterich Standard Annubar + Validyne Pressure Transducer	Analog Transducer Signal
Grade/ Acceleration[a]	Trailer	3-axis gyroscope	Crossbow Model VG600CA	Digital

a. Paroscientific Model 745-16B microbarometer (altimeter) was actually used to determine grade as discussed in Section 4.2.2.

2.5   Data Acquisition System

The DAS used in the DEAL consists of a multicomputer network containing five computers, a monitor, a keyboard, and a mouse installed in the CEM rack plus a sixth computer, two flat screen monitors, a keyboard, and a mouse installed in the tractor sleeper compartment. The computers in the trailer are networked via a wireless router to the computer in the sleeper to allow file access and transfers. A keyboard-video-monitor switch also allows the operator in the

sleeper to access and run instrument operating software on the computers in the trailer. The network is time synchronized by a clock card in the master computer, which is set daily to an atomic clock traceable to a National Institute of Standards and Technology standard. All instrument measurements are recorded on the DAS as digital or analog-to-digital data streams and stored in individual files, which are archived daily on compact disks. All calculated quantities are determined post test from raw data as described in Section 6.

Chapter 3
DEAL Instrumentation

3.1   Continuous Exhaust Gas Monitoring

The continuous emissions monitors (CEM) system design and operation generally follows the requirements of 40 CFR (Code of Federal Regulations) 86 Subpart D §86.309-79 and is shown in Figure 3-1. A heated pump inside the trailer is used to extract the exhaust gas sample from the stack under negative pressure through HL1 (heated sample line 1) to the front of the trailer where it enters the trailer through the bulkhead. At this point, a second heated line, HL2, inside the trailer carries the sample flow to an oven that contains a filter and heated pump. The sample exits the heated pump into a third heated line and flows to a cross that is located inside a heated box ("hot box") mounted in the CEM bench. A backpressure regulator inside the hot box is used to regulate the sample gas pressure in all lines downstream of the cross. One exit of the cross leads to a second filter inside the hot box and then flows through a tee into a Nafion dryer and finally to a manifold that supplies sample flow to the oxygen (O_2), carbon dioxide (CO_2), carbon monoxide (CO) (low range) and CO (high range) analyzers. The other exit from the cross connects to a fourth heated line that allows a portion of the sample flow to be extracted before further filtering and water removal and flows to the sample inlet of the total hydrocarbon (THC) analyzer. Downstream of the second filter, a portion of the flow is extracted from the branch of the tee before water removal and flows through a fifth heated line and into the nitrogen oxides (NO_X) analyzer. All continuous gas analyzers are mounted in the trailer's vibration and shock-resistant instrument rack.

The calibration gas delivery system consists of several toggle valves, two manifolds and a pressure regulator. The cylinder regulators are connected directly to the toggle valves in the span gas (SG) manifold. The calibration gas flows from the SG manifold into a pressure-reducing regulator and into the calibration manifold. Through the calibration manifold, any one of the gas analyzers can be fed any of the calibration gases directly for instrument calibration, or the gas can be fed to a three-way valve at the exhaust stack so a bias check can be performed on the entire system.

The analog signal outputs from the CEMs are connected to the DAS through an analog-to-digital converter. In addition to providing an instantaneous display of analyzer response, the DAS compiles, averages, and saves analyzer data at a user-set frequency. Descriptions of the analyzers used to measure the gaseous emissions from the heavy-duty diesel engine are given below.
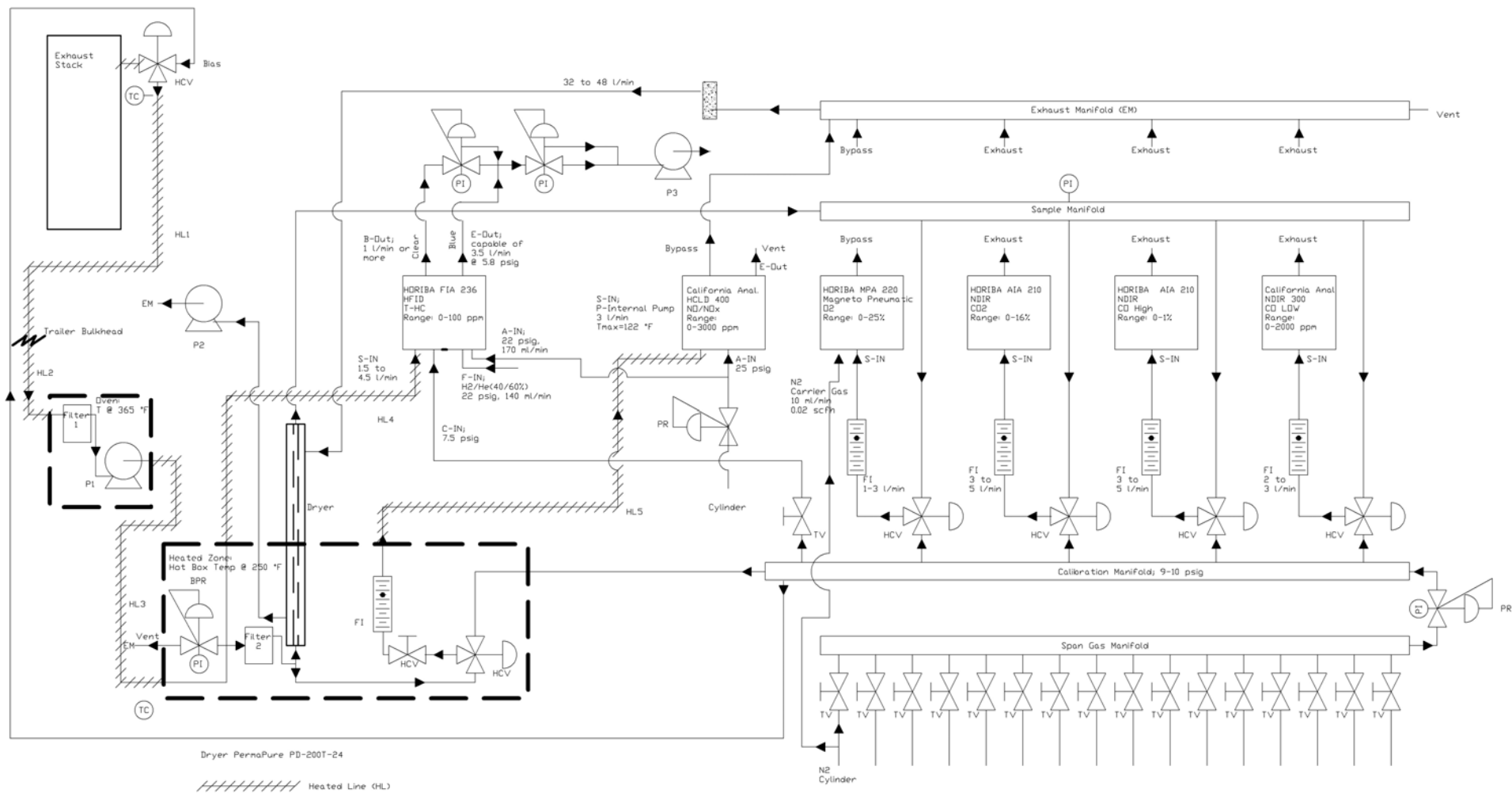
Figure 3-1.   Schematic of the Continuous Emissions Monitoring (CEM) System in the DEAL.

3.1.1 O_2 Analyzer

In the Horiba Instruments Model MPA 220 (Magneto-Pneumatic) O_2 analyzer, an uneven magnetic field is applied to the sample gas. If oxygen, a paramagnetic gas, is present, the gas is drawn to the strongest part of the magnetic field, raising the pressure at that point. A gas that is not paramagnetic (such as nitrogen) can be used to take the pressure rise out of the magnetic field. Two electromagnets are excited alternately and the pressure changes are converted into electrical signals by a condenser microphone. Output is linear in proportion to the oxygen concentration. The O_2 concentration range measured by this instrument is 0–25 percent.

3.1.2 NO_X Analyzer

The California Analytical Instruments, Inc., (CAI) HCLD 400 heated chemiluminescence analyzer automatically and continuously determines the concentration of nitric oxide (NO) or NO_X. Operated under the NO_X mode, the analyzer directs the sample through a reaction chamber where nitrogen dioxide (NO_2) completely dissociates into NO. The NO is completely converted to NO_2 via gas phase oxidation by the molecular ozone generated by the analyzer. In this reaction, the NO_2 molecules are energized to an electronically excited state. Immediate reversion of the excited NO_2 to the non-excited ground state takes place and is accompanied by the emission of photons. The photons impinge on a photomultiplier detector and generate a low-level DC current. The DC current is amplified to drive a front panel meter and data recorder. The NO_X concentration seen by the instrument includes the contributions of both the NO in the sample and the NO resulting from the dissociation of the NO_2 in the sample. The NO_X concentration range measured by this instrument is 0–3000 ppm.

3.1.3 CO/CO_2 Analyzer

A CAI Model 300 Non Dispersive Infrared (NDIR) analyzer has three channels. Two were used in these experiments to continuously measure concentrations of CO (0–2000 ppm) and CO_2 (0–20%) in the sample gas.

The CAI Model 300 analyzer is based on the infrared absorption characteristics of gases. A single infrared light beam is modulated by a chopper system and passed through a sample cell of predetermined length containing the gas sample to be analyzed. As the beam passes through the cell, the sample gas absorbs some of its energy. The attenuated beam (transmittance) emerges from the cell and is introduced to the front chamber of a two-chamber infrared microflow detector. The detector is filled with the gas component of interest and, consequently, the beam experiences further energy absorption. This absorption process increases the pressure in both chambers. The differential pressure between the front and rear chambers of the detector causes a slight gas flow between the two chambers. This flow is detected by a mass-flow sensor and is converted into an alternate current (AC) signal. The AC signal is amplified and rectified into a direct current (DC) voltage signal and ultimately supplied to the output terminal and digital panel meter. The electrical output signal is directly proportional to the concentration of the sample gas. Note that the Quality Assurance Project Plan (QAPP) states that the Horiba Model AIA 210 NDIR CO_2 Analyzer would be used to measure the CO_2 concentrations, but it was removed from the CEM bench to allow room for an additional computer before starting the testing campaign.

3.1.4   THC Analyzer

The Horiba Instruments Model FIA-236 incorporates a flame ionization detector (FID), which adds hydrogen to the column effluent and passes the mixture through a jet where it is mixed with entrained air and burned. The ionized gas (charged particles and electrons produced during combustion) passes through a cylindrical electrode. A voltage applied across the jet and cylindrical electrode sets up a current in the ionized particles. An electrometer monitors this current to derive a measure of the component concentration. The THC concentration range measured by this instrument is 0–100 ppm assuming a one carbon gas is used. The upper range becomes a multiple of the number of carbon atoms in the gas. For example, this research used propane which resulted in an upper range of 300 ppm.

3.2   Tracer Gas Analyzer

Since PM samples are being extracted from the plume and not directly from the DEAL tractor exhaust, a method is needed to convert the average plume concentration to an equivalent stack concentration and, using the exhaust gas volumetric flow rate, to the appropriate PM-2.5 emission rate. To accomplish this, a hydrofluorocarbon tracer gas (1,1,1,2,3,3-heptafluoropropane, or FM-200) was injected into the exhaust stack and measured in the plume sampling system (Figures 2-5 and 2-6) using an INNOVA Model 1314 photoacoustic gas analyzer. FM-200 was metered into the exhaust gas stream from a cylinder using a regulator and calibrated precision rotameter. Using the average flow of tracer gas and measured plume concentration, both the dilution ratio and equivalent PM-2.5 emission rate were calculated as outlined in Section 6.4.

In the INNOVA Model 1314, the pump draws air from the sampling point through two air-filters to flush out the "old" sample in the measurement system and replaces it with a "new" air sample. The "new" sample is hermetically sealed in the analysis cell by closing the inlet and outlet valves. Light from an infrared source is reflected off a mirror and passes first through a mechanical chopper, which pulsates it, and then through one of the optical filters in the filter carousel. The light transmitted by the optical filter is selectively absorbed by the gas being monitored, causing the temperature of the gas to increase. Because the light is pulsating, the gas temperature increases and decreases, causing a corresponding increase and decrease in the pressure of the gas (an acoustic signal) in the closed cell. Two microphones mounted in the cell wall measure this acoustic signal, which is directly proportional to the concentration of the monitored gas present in the cell.

The calibration of this instrument was verified before deployment with a calibration check using certified calibration gas. Checks spanning the instrument range were performed during field testing using the calibration gases specified in Section 10.1.2. Zero checks were also conducted in the field per miscellaneous operating procedure (MOP) 1419 (U.S.EPA, 2004).

3.3   Continuous PM-2.5 Monitoring

Reference the schematics of the plume and background sampling system in Figures 2-5, 2-6, 2-8, and 2-9 for the locations of the instruments described in the following sections.

3.3.1   PM Mass Measurements

Three instruments located in the DEAL are designed to measure the mass of the particulate matter directly. Two of them receive a sample from the plume sampling system and one receives its sample from the background sampling system.

3.3.1.1   Quartz Crystal Microbalance (QCM)

An older instrument, which has recently been re-introduced to automotive engine testing, is the QCM. The harmonic oscillator principle used in the QCM is similar to the Tapered Element Oscillating Microbalance (see TEOM below) except that the collected PM is actually deposited onto the crystal element using an electrostatic precipitator (ESP). Due to its high frequency operation, the QCM exhibits far less instrumental noise than the TEOM but also can overload in a relatively short period. To offset this problem, a dilutor is supplied with the instrument to extend the useful life of the crystal element.

3.3.1.2   Tapered Element Oscillating Microbalance (TEOM)

The TEOM Series 1105 Diesel Particulate Monitor and Series 1400a Ambient Particulate Monitor incorporates a patented inertial balance that directly measures the mass collected on an exchangeable filter cartridge. It monitors the change in the natural oscillating frequency of a tapered element as additional mass collects on the filter. The sample flow passes through the filter, where PM collects and then continues through the hollow tapered element on its way to a dynamic flow control system and vacuum pump.

The TEOM mass transducer does not normally require recalibration because it is specially designed and constructed from nonfatiguing materials. Its mass calibration may be verified however, using an optional mass calibration verification kit that contains a filter of known mass. A flow controller maintains the sample flow rate input by the user. TEOM Series 1105 interfaces with the multicomputer via an I/O (input/output) card, cable and software supplied by the manufacturer. The TEOM Series 1400a monitor uses the same technology as the 1105a but incorporates an internal microprocessor and data storage system.

3.3.2   PM Count Measurements

The DEAL contains a variety of particle counters that cover the range of particle sizes from 2 nm to 10 µm.

3.3.2.1   DEKATI Electrical Low Pressure Impactor (ELPI)

The DEKATI Electrical Low Pressure Impactor (ELPI) is a real-time particle size spectrometer designed for real time monitoring of aerosol particle size distribution. The ELPI measures airborne particle sizes in the range of 0.03 to 10 µm with 12 channels. The principle is based on charging, inertial classification, and electrical detection of the aerosol particles. The instrument consists primarily of a corona charger, low-pressure cascade impactor and multi-channel electrometer. It communicates with the DAS via a serial port using the ELPIVI software provided with the instrument. The software is used for setup and configuration and to view data.

3.3.2.2   TSI Scanning Mobility Particle Sizer (SMPS)

The TSI Model 3934 SMPS is a system that measures the size distribution of aerosols in the size range from 10 to 1000 nm. The particles are classified by their electrical mobility with the Model 3071A Electrostatic Classifier, and their concentration is measured with the Model 3010 Condensation Particle Counter (CPC). The system communicates with the DAS via a serial port. The Aerosol Instrument Manager (AIM) software is used for setup and configuration and to view data.

The TSI Model 3936 Long SMPS is a system that measures the size distribution of aerosols in the size range from ~9 nm to 1000 nm. The particles are classified by their electrical mobility with the Model 3080 Electrostatic Classifier with a Model 3081 Long Differential Mobility Analyzer (DMA), and their concentration is then measured with the Model 3025A CPC. The Long DMA is the traditional length DMA used in the older Model 3071 Electrostatic Classifier. The system communicates with the multicomputer via a serial port. The AIM software package is used for setup and configuration and to view data.

The TSI Model 3936 Nano SMPS is a system that measures the size distribution of aerosols in the size range from 2 nm to 150 nm. The particles are classified with the Model 3080 Electrostatic Classifier together with a Model 3085 Nano DMA, and their concentration is then measured with the Model 3025A CPC. The Nano DMA is optimized for the size range below 20 nm. The system communicates to the multicomputer via a serial port. The AIM software package is used for setup and configuration and to view data.

3.3.2.3   Condensation Particle Counter (CPC)

The Model 3025A CPC detects and counts particles larger than 3 nm in diameter by an optical detector after a supersaturated vapor (n-butyl alcohol) condenses onto the particles, causing them to grow into larger droplets. The range of particle concentration extends from less than 0.01 particle/cm^3 to 9.99 x 10^4 particle/cm^3. The system communicates with the multi-computer via a serial port. The CPC LOG software developed by APPCD is used to log the data.

3.3.3   PM Black Carbon Magee Aethalometer

The Magee (Andersen) Model AE-2 Aethalometer measures real-time "black" (or elemental) carbon. It is designed for fully automatic and unattended operation. The sample is collected as a spot on a roll of quartz fiber tape. An optical method is then used to measure the attenuation of a beam of light transmitted through the sample. The optical attenuation is linearly proportional to the amount of black carbon collected on the quartz fiber tape. The aethalometer communicates with the DAS via an analog output signal with a voltage range of 0–5 volts. Operation of the instrument is checked using an optical test strip.

3.3.4   PM Polycyclic Aromatic Hydrocarbons—Photoelectric Aerosol Sensor (PAS) 2000

PAS 2000 (Photoelectric Aerosol Sensor) works on the principle of photoionization of particle surface-bound Polycyclic Aromatic Hydrocarbons (PAHs). Using an excimer lamp the aerosol flow is exposed to UV radiation. The excimer lamp offers a high intensity, narrow band source

of UV radiation. The wavelength of the light is chosen such that only the PAH coated aerosols are ionized, while gas molecules and noncarbon aerosols remain neutral. The aerosol particles that have PAH molecules adsorbed on the surface emit electrons, which are subsequently removed when an electric field is applied. The remaining positively charged particles are collected on a filter inside an electrometer, where the charge is measured. The resulting electric current establishes a signal that is proportional to the concentration of total particle-bound PAHs.

3.4   Time-Integrated Sampling

As discussed previously, the on-road study encompassed both "speciated" and "non-speciated" tests. The number and types of sampling media used in these tests are different as shown previously in Figures 2-5 and 2-6 for the plume sampling tunnel and Figures 2-8 and 2-9 for the background sampling system.

The filter FTP filter holders and Teflon sampling media used in the time-integrated samplers for plume sampling (Figures 2-5 and 2-6 of Section 2) comply with 40 CFR, Part 86, § 86.1310-2007 (January 18, 2001). Commercially available stainless steel, 47-mm filter holders were used in the remainder of the measurements.

For the speciated runs (Figures 2-5 and 2-8), the specific media used in the program were as follows:

- FTP Sampler 1: Teflon primary filter for total PM-2.5 mass plus two back-to-back pre-fired quartz filters for determination of organic carbon (OC) "blow off". ("Blow-off" refers to the removal of volatiles by the sample gas passing through the collected PM on the filter.)

- FTP Sampler 2: Pre-fired quartz primary filter for elemental/organic carbon (EC/OC) content plus a series of four PUF plugs for determination of gas-phase semi-volatile organic composition.

- Thermal denuder (TD): Parallel filter holders with one containing a Teflon filter collecting non-volatile PM mass and the other incorporating two back-to-back pre-fired quartz filters for EC/OC composition.

- ELPI: Aluminum foil substrates plus pre-fired quartz back-up filter for the determination of PM mass and semi-volatile organic composition.

In the case of the non-speciated runs (Figures 2-6 and 2-9), the following media were used for the on-road testing:

- FTP Sampler 1: Teflon primary filter for total PM-2.5 mass plus two back-to-back pre-fired quartz filters for determination of OC "blow off".

- FTP Sampler 2: Pre-fired quartz primary filter for EC/OC content plus two back-to-back pre-fired quartz filters for determination of OC "blow off".

- TD: Parallel filter holders with one containing a Teflon filter representing non-volatile PM mass and the other incorporating two back-to-back pre-fired quartz filters for EC/OC composition.

- ELPI: Aluminum foil substrates plus Teflon back-up filter for the determination of PM mass.

Table 3-1 lists all time-integrated samples collected during the on-road truck experiments, the media and analytical technique used, and the total number of samples including the blank run. Details of the media preparation procedures and individual analyses performed are contained in the Quality Assurance Project Plan (QAPP) for the EPA's Fine Particle Characterization Laboratory (FPCL), which is included in this document by reference. (U.S. EPA, 2005)

3.5   Fuel

Three different fuels were used in the testing campaign. The first was a locally available pump grade fuel, second was a low sulfur fuel (15 ppm) meeting EPA 2005 standards, and third was a 20% blend of soy-based biodiesel and low sulfur diesel fuels (B20). Both the low sulfur fuel and the biodiesel blend were supplied by DOE. Once received, the fuel was stored in a temperature controlled fuel storage building to prevent its degradation. When time to begin the testing campaign approached, a trailer equipped with a temperature control unit was leased to store the fuel at the test site in New Bern, NC. The photograph in Figure 3-2 shows the temperature controlled trailer on left side of the photograph as positioned at the New Bern staging area.

Diesel fuel samples and engine oil samples were collected during the testing campaign and analyzed using the methods in Table 3-2. The table lists the parameters that were determined for all the fuel and oil analyses, the method used for each analysis, and the minimum volume required for each method. The combined parameters in the shaded area constitute the Ultimate Analysis for the fuel. Fuel and oil analysis procedures were performed by CORE Laboratories in Houston, Texas

Table 3-1.   Analytical Plan for On-Road Truck Experiments

Type of Analysis	Sampling Media	Analytical Method	No. of Samples/Test	No. of Tests[a]	Total Samples Planned	Total Samples Actual
PM mass (PM-2.5)	47-mm Teflon filters (unspeciated runs)[b]	Gravimetric	5	12	60	28
	47-mm Teflon filters (speciated runs)[b]	Gravimetric	3	5	15	18
	Al foil ELPI substrates	Gravimetric	24	17	408	336[c]
Elemental/organic carbon (EC/OC)	47-mm pre-fired quartz filters (unspeciated runs)[d]	NIOSH 5040	12	12	144	114
	47-mm pre-fired quartz filters (speciated runs)[d]	NIOSH 5040	10	5	50	56
Semi-volatile organics[a]	47-mm pre-fired quartz filters (included in total above)	Multi-solvent extraction + GC/MS[e]	4	5	20	32
	PUF plugs[f]	Multi-solvent extraction + GC/MS[e]	8	7	56	56
	Al foil ELPI substrates (included in total above)[g]	Thermal desorption + GC/MS[e]	24	7	168	0[g]
	47-mm pre-fired quartz filters	Thermal desorption + GC/MS[e]	2	7	14	14
Water-soluble ions	47-mm Teflon filters	Ion chromatography	2	7	14	12
Elemental composition	47-mm Teflon filters	X-ray fluorescence spectroscopy	2	7	14	12
				Total Analyses	**963**	**846**

a. Includes shakedown tests and tunnel blank run.

b. Includes all Teflon filters for total PM-2.5 mass, ELPI back-ups, and thermal denuder.

c. Data not used.

d. Totals include primary quartz filters, back-up quartz filters, and filters for thermal denuder train.

e. GC/MS = gas chromatography/mass spectroscopy.

f. Four plugs/test for the background and plume.

g. Thermal desorption analysis of ELPI samples have not been done.

Figure 3-2.   New Bern Staging Area

Table 3-2.   Fuel and Lube Oil Analysis Methods [a]

Fluid	Parameter	Units	(ml)	Method
Fuel	Boiling Point	Degree Fahrenheit (°F)	100	ASTM D-86
	Flash Point	°F	75	ASTM D-93
	Cloud Point	°F	50	ASTM D-2500
	Cetane Number		2000	ASTM D-613
	Lubricity	Mm @ °60	4	ASTM D-6079
	Water	ppm wt		ASTM E-203
	C, H_2, N_2	WT %	10	ASTM D-5291
	N_2, Trace	ppm wt	10	ASTM D-4629
	Sulfur	WT %	5	ASTM D-2622
	Ash	WT %	200	ASTM D-482
	O_2 (diff)	WT %		Calculated Value
	Heating Value	British Thermal Units (BTU)/lb	5	ASTM D-240
	Viscosity	cSt @ 40 °C	50	ASTM D-445
	Specific Gravity	@ 60/60 °F	3	ASTM D-4052
Oil	Sulfur	WT%	30	ASTM D-4294

a. Note that results are generally provided in English units and then converted to SI for the purpose of this report.

Chapter 4
Field Test Sites and Testing Procedures

4.1 Staging Area

The staging area for the New Bern, NC testing campaign was arranged with the cooperation of the North Carolina Department of Transportation (NCDOT), Division 2, District 2 located on 231 S. Glenburnie Rd, New Bern, NC. They shared space inside their maintenance yard for setting up the staging area. A photograph of the staging area at the NCDOT was shown previously in Figure 3-2. The photograph shows the temperature controlled fuel storage trailer on the left, the trailer used to transfer the concrete blocks in and out of the DEAL in the center, and the DEAL on the right. Also located behind the DEAL is a 20 foot office trailer that was used for media storage and as a mobile lab to load and recover media before and after tests. Also located behind the DEAL is the electrical power drop that was used to supply the DEAL with electrical power.

4.2 General Experimental Procedures

The campaign was divided into two stages. From 2 September 2004 to 30 October 2004, 20 tests were conducted on a level stretch of old highway U.S-70 near New Bern, NC. These tests examined the influence of fuel type, vehicle speed, and vehicle load on diesel truck emissions. Two test were conducted during the second stage, one on 16 December 2004 and one on 21 December 2004. These two tests were conducted on a mountainous stretch of I-77 between exits 1 and 8 and investigated the influence road grade has on diesel truck emissions. This stage used only readily available pump fuel.

4.2.1 New Bern Tests

Twenty on-road experiments were performed over 14 days during the New Bern 2004 sampling campaign. On 8 of the 14 days, only 1 test was completed per day; on the remaining 6 days, 2 tests were completed per day. Initially, a full day was required to perform one test, but as the field team established a routine and improved efficiency, two tests per day became feasible. Other factors that affected the number of tests the team was able to conduct were the logistics of recovering and re-loading media, fuel and oil changes for the tractor, changing the payload, etc. Duplicate tests were conducted per the QAPP (U.S. EPA, 2004).

Originally, two sets of on-road experiments were planned. In the first set the DEAL was to be operated on a pump grade diesel fuel (~350 ppm sulfur content), and in the second set, a 20% biodiesel blend. Shortly before testing began, the U.S. DOE requested that 2005 specification low sulfur diesel fuel be used as the baseline fuel. Table 4-1 lists the matrix of tests that were actually completed during the New Bern campaign.

Table 4-1.   Test Matrix for Fuel Type, Vehicle Speed, Speciation, and Vehicle Weight

Test Number[a]	Test Date	Fuel Type[b]	Vehicle Speed, km/h	Speciation [c]	Gross Weight, kg	Road Grade, %
T1	9/02/04	Pump Diesel	105	Y	33,890	0
T2	10/01/04	Pump Diesel	105	Y	33,890	0
T3	10/13/04	Pump Diesel	105	Y	33,890	0
T4	10/14/014	Pump Diesel	105	N	33,890	0
T5	10/19/04	Low Sulfur	105	Y	33,890	0
T6	10/20/04	Low Sulfur	105	Y	33,890	0
T7	10/21/04	Low Sulfur	56	N	33,890	0
T8	10/21/04	Low Sulfur	56	N	33,890	0
T9	10/22/04	Low Sulfur	56	N	21,350	0
T10	10/22/04	Low Sulfur	56	N	21,350	0
T11	10/23/04	Low Sulfur	105	N	21,350	0
T12	10/23/04	Low Sulfur	105	N	21,350	0
T13	10/26/04	Bio Diesel	105	N	21,350	0
T14	10/26/04	Bio Diesel	105	N	21,350	0
T15	10/27/04	Bio Diesel	56	N	21,350	0
T16	10/27/04	Bio Diesel	56	N	21,350	0
T17	10/28/04	Bio Diesel	56	N	33,890	0
T18	10/28/04	Bio Diesel	56	N	33,890	0
T19	10/29/04	Bio Diesel	105	Y	33,890	0
T20	10/30/04	Bio Diesel	105	Y	33,890	0
T21	12/16/04	Pump Diesel	89	N	21,350	3.9
T22	12/21/04	Pump Diesel	73	N	33,890	3.9

a. Duplicate test pairs indicated by shading every other pair beginning with test pair 5&6

b. Low sulfur fuel has a sulfur content ~15 ppm (weight). B20 is a blend of 20% soy biodiesel and low sulfur diesel fuel meeting the requirements of ASTM D6751, ASTM (2007).

c.   "Speciation" indicates those tests where complete chemical characterization is performed.

The test matrix lists the test numbers assigned to each test in the field. Duplicate tests were conducted back to back starting with Test 5 in Table 4-1. Every other duplicate test pair is colored for easier identification. In addition to the 16 tests specified in the QAPP, four tests were performed using a pump diesel fuel, referred to as test numbers 1–4 in this report. These four tests served as shakedown tests.

Testing was performed at two vehicle speeds and load conditions. Also, at the conclusion of the on-road testing, a "tunnel blank" run was performed to determine if any correction to the data collected during the other tests was needed. During each experiment, concurrent plume, background, and exhaust gas sampling was performed using a combination of on-line and time-integrated instruments along with continuous sampling of key vehicle operating parameters.

Details of the specific instruments used and sampling performed are provided in Section 2 of this report.

Before each day's testing, the DEAL was prepared by first activating all analyzers, pumps, sampling tunnels, and the DAS to allow the equipment to warm up. (Note that most instruments were left "hot" overnight to assure stable operation). During this period, the sampling media were installed in each of the time-integrated samplers and the samplers mounted on the respective sampling tunnel flow splitter. In addition, all appropriate quality control checks were performed of the instruments including leaks checks, zero/span/bias checks of the CEM bench, etc. The truck engine was started and allowed to idle. After a sufficient warm up period (~10 min), the truck was driven to the road test section to be used for that day's experiments.

After arriving at the selected route, testing began immediately upon achieving a stable speed for the desired test. For each test, the road section was driven as many times as necessary to obtain adequate sample mass for chemical analysis. Eight passes were required when driving at 105 km/h and four passes when driving at 56 km/h. During each pass (~20 min at 105 km/h or ~38 min at 56 km/h), the time-integrated sampling equipment was activated or deactivated as necessary, with a time log of each test recorded by the system operator (EPA principal investigator) in a bound laboratory notebook. At the completion of the required number of passes, the truck returned to the staging area for sample and data recovery. A map of the test route is shown in Figure 4-1. The eastern end of the test route is defined by the intersection of US-70 and NC-43, and the West end of the route is defined by a break in the median (not shown) just east of Dover. One pass is one trip driving from the eastern end of the route to the western end of the route, or vice versa, a distance of about 35 km.

Figure 4-1.   On-Road Diesel Emissions Test Route on Old US-70

After arriving at the staging area at the completion of each experiment, the time-integrated samplers were removed from the DEAL and returned to the field laboratory for sample recovery and the electronic files recovered from the DAS. During sample recovery, all electronic data files saved on the DAS were organized into the proper hard drive directory, and an archive of each file set was copied to compact disk. At the end of each day's testing, all electronic files were reviewed and any questionable data identified so the test(s) could be repeated if necessary.

4.2.2 Mountainous I-77 Tests

Tests to investigate the effects of road grade on emission rates were conducted on a segment of I-77 near Fancy Gap, VA, a short distance north of the North Carolina border. The route is shown in Figure 4-2. A total of two tests were completed on two different days. The DEAL was operated without a load on the first test day (see Table 4-1) and with a load on the second day Each test day began by driving about 150 miles from the EPA facility in RTP, NC to a rest area in Virginia that is located on I-77 immediately after crossing the border. Prior to departing from EPA, the DEAL's generators were started, and the CEM analyzers were turned on to allow them time to warm-up in-route. The rest stop served as a convenient staging area close to the segment of road on which the emissions from the DEAL would be tested. Once at the rest stop, the DAS computers were started, the CEMs were calibrated, and other instruments used during the tests were activated. A new instrument, the Paroscientific 745-16B Microbarometer, was also added to the DEAL for the purpose of measuring road grade during these tests. All instruments and sensors used during tests in the mountains are listed in Table 4-2.

After completing the pre-test procedures, the driver would leave the rest stop and drive directly onto I-77 North to begin the test, which consisted of four round trip passes between Exit 1 and Exit 8. After completing the test, the driver would return to the rest area for post test calibrations and shut down procedures.

Table 4-2.   Measurements Taken during the Tests on I-77

Parameter	Instrument
CO	California Analytical Model 300
CO_2	California Analytical Model 300
O_2	Horiba MPA 220
NO_X	California Analytical HCLD 400
THC (as Propane)	Horiba FIA 236
Drive Shaft Torque	ATI 2000 Series
Engine Speed	DDEC60
Fuel Flow	DDEC60
Vehicle Speed	Datron DLS-1 speed sensor
Grade and Acceleration	Crossbow Model VG600CA
Engine Temperature	Omega Engineering
Exhaust Gas Temperature	Omega Engineering
Change in Elevation (i.e., grade)	Paroscientific 745-16B
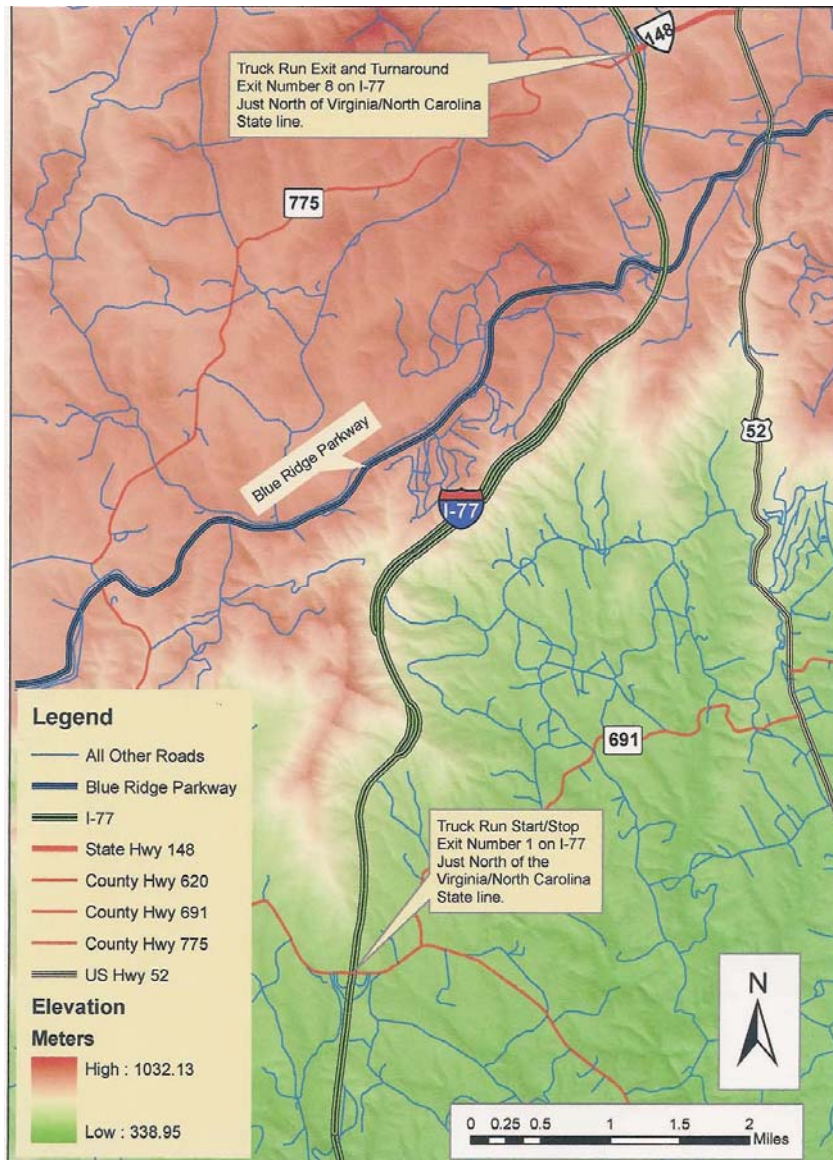
Figure 4-2. **On-Road Diesel Emissions Test Route in the Mountains on I-77**

4.3 Tractor-Trailer Payload

As mentioned in Section 2.1, the facility uses weights to simulate different payloads. These payload weights positioned in the DEAL trailer are blocks of concrete measuring about 1 m³ and weighing about 1360 kg (3000 lbs) each. Table 4-3 lists the certified weights taken of the DEAL for the loaded and unloaded tests for the New Bern testing campaign. The unloaded weight includes the tractor-trailer and all the equipment present in the trailer during testing. The loaded weight is the same as the unloaded weight with the addition of nine of the blocks of concrete that simulate a payload. During the New Bern campaign, the test matrix was configured to minimize the number of times that the blocks of concrete would have to be moved into or out of the trailer.

Table 4-3.   DEAL Loaded and Unloaded Testing Weights

Station on DEAL	Unloaded Weight, kg (Lbs)	Loaded Weight, kg (Lbs)
Steer Axial	4900 (10,800)	5010 (11,040)
Drive Axial	9760 (21,520)	13,940 (30,740)
Trailer Axial	6690 (14,740)	14,940 (32,940)
Gross Weight	21,350 (47,060)	33,890 (74,720)

4.4   Vehicle Operation

As mentioned previously, a test consisted of operating the tractor-trailer at a constant speed for a number of passes either on a 35 km stretch of old US-70 near New Bern, NC that has approximately zero grade or on a section of Virginia I-77 between exits 1 and 8, which is near Fancy Gap, VA. The two target speeds selected for the zero grade tests were 56 and 105 km/h. The driver maintained a constant vehicle speed during the pass while the actual speed used to calculate the emission factors was recorded on DAS by the optical fifth wheel (Section 2.4). The time when the vehicle reached the target speed at the beginning of each pass was recorded by hand, and the time was recorded again at the end of each pass before decelerating and making the turn for the return pass.

Vehicle operation during the tests in the mountains consisted of driving the DEAL from I-77 Exit 1 in VA to I-77 Exit 8, a total distance of about 12 km (7.5 mi). North-bound from Exit 1, the DEAL traveled up a road grade of approximately 3.9% for about 11 km (6.5 mi) before reaching the top of the grade where the Blue Ridge Parkway passes over I-77. The driver continued on I-77 and left the interstate at Exit 8, turned left over the overpass, and re-entered I-77 onto the south-bound lanes. Upon returning to Exit 1, the driver would exit the interstate and reenter I-77 onto the northbound lanes for another round trip pass. One day's test consisted of making four complete round trips.

Table 4-4 lists the test speeds, the gear in which the tractor was driven, and the approximate engine speed. Table 4-1 lists the test numbers and the constant speed for each test along with the vehicle weight for all tests conducted. Precautions were taken for operating a slow moving vehicle on old US-70 by following the DEAL with a chase vehicle during tests at low speed. A photograph of the chase vehicle is shown in Figure 4-3.

Table 4-4.   Vehicle Operating Parameters

Location	Vehicle Speed	Gear	Engine Speed (r/min)
Old US-70	56 km/h (35 mi/h)	8th	1550
	105 km/h (65 mi/h)	10th	1500
I-77	89 km/h (55 mi/h)	variable	
	73 km/h (45 mi/h)	variable	

Figure 4-3.   Chase Vehicle Used during Low Speed Tests

4.5   Coast-Down Testing

A coast-down technique was employed to produce a model of road load force as a function of vehicle speed per SAE Recommended Practice J1236 and J2263 (SAE, 1996a; SAE 1996b). The road load force determined from the results of this model was then used to determine the power specific emission factors. As outlined in Section 6.6, the coast-down tests were performed on the same segment of old US-70 near New Bern, NC as the on-road tests but on a day when no other tests were planned. The coast down procedure required only a few of the DEAL instruments; therefore, the fine PM particle instruments and gas analyzers were not used. Instruments that were employed were the optical fifth wheel to record vehicle speed and the gyroscope. After starting the necessary instruments, the procedure required that the tractor accelerate to approximately 105 or 56 km/h (depending on the test conditions for which road load was required) then, with the transmission in neutral, allow the tractor-trailer to coast down to 8 km/h. Triplicate tests were performed with the trailer loaded and unloaded.

4.6   Test Fuel

In tests 1 through 4, sampling was conducted with the vehicle operated loaded and under steady-state conditions at near zero grade using a pump grade diesel fuel obtained near the staging area. Tests 5 through 12 used the low sulfur fuel, and tests 13 through 20 used the B20. Finally, tests 21 and 22 also used pump grade fuel for the measurements on mountain road grades.

Before switching from the pump grade fuel to the low sulfur fuel, the Kenworth tractor and the fuel storage trailer had to be driven from the New Bern, NC test site to a local truck dealership in Dunn, NC, to remove the pump grade fuel and to refill the tanks with the low sulfur fuel. In addition to changing the fuel and the fuel filter, the oil and oil filter were changed. The one-way trip of 170 km back to the staging area in New Bern was used as a run-in period to re-condition

the engine on the new fuel. The same procedure was followed to switch from the low sulfur fuel to B20. During the fuel changing process, sample containers were on hand to collect fuel and oil samples. Table 4-5 lists the fuel samples collected, and the fuel analysis reports are provided in Appendix B.

Table 4-5.   Fuel and Oil Samples Collected and Analyzed

Sample Type	Sample ID
Pump Diesel Fuel	Pump Diesel Fuel 10/15/04
Low Sulfur Diesel Fuel	Low Sulfur Diesel Fuel 10/15/04
B20	Bio Diesel Fuel 10/25/04
Engine Oil	Pre-Low Sulfur Diesel Fuel Tests 10/15/04
Engine Oil	Post-Low Sulfur Diesel Fuel Tests 10/25/04
Engine Oil	Pre-Bio-Diesel Fuel Tests 10/25/04
Engine Oil	Post-Bio-Diesel Fuel Tests 10/30/04

4.7   CEM Operation

Neither of the two Horiba Instruments Model AIA 210 NDIR Analyzers mentioned in Section 4 of the QAPP were used during the tests. The CAI Model NDIR 300 Analyzer, also mentioned in Section 4 of the QAPP, was determined to be sufficient to measure the expected concentrations of carbon monoxide and carbon dioxide. It was necessary to remove the Horiba analyzers to make room for additional computers.

The pre- and post-test procedures for the operation of the CEMs in the New Bern campaign followed Section 4.3 of the QAPP. These procedures are briefly outlined below.

Pre-test CEM procedures:

- Filters were changed on a daily basis in the "Hot Box" and the "Oven".

- The heated sample lines were turned on first thing allowing them to warm-up before calibrations.

- The instruments were allowed to remain on 24 hours a day during the campaign.

- Bias checks were performed before every test to check for leaks.

- The set points for the heated sample line controllers were checked daily. Table 4-6 lists the controller setpoints.

- Gas analyzer flows were checked and monitored using the rotameters installed in the CEM bench.

- The zero and span gases were introduced under the same flow and pressure conditions that were used during the multipoint calibrations.

Immediately upon returning to the staging area after completing the final test of the day, zero and span responses were checked as soon as practically possible.

Table 4-6.   Temperature Controller Setpoints for CEM System

Component [a]	Controller Setpoint [b]
Outside Heated Sample Line (HL1)	360 °F (182 °C)
Inside Heated Sample Lines (HL2, HL3, HL4)	360 °F (182 °C)
NO_X Heated Sample Line (HL5)	266 °F (130 °C)
Oven	365 °F (185 °C)
Hot Box	160 °F (71 °C)

a. See CEM description in Section 3.1.
b. Based on 40 CFR, Part 86 requirements

4.8   Tracer Gas Analysis

A general description of the tracer gas analyzer is provided in section 3.2 along with the general description of the DEAL. A more detailed schematic of the tracer gas injection system and the tracer gas analyzer system is shown in Figure 4-4.
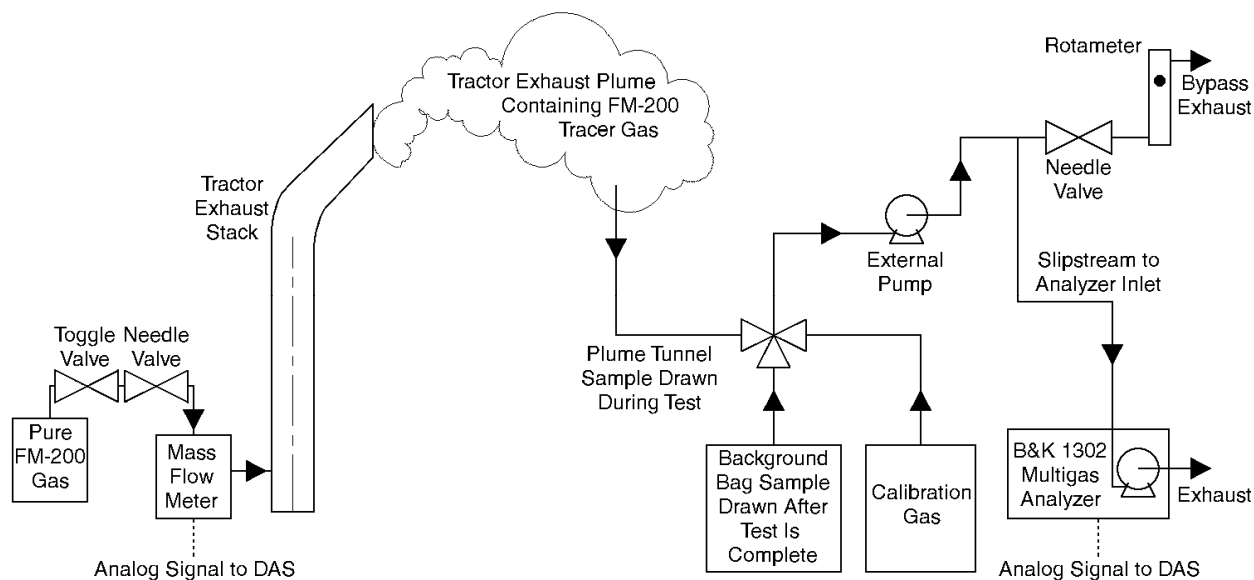
Figure 4-4.   Tracer Gas Injection System and Tracer Gas Analyzer System

After completion of the pretest multigas analyzer calibration checks, the analyzer was allowed to sample continuously from the plume sample tunnel until time to perform the post-test calibration checks. When the DEAL reached the desired constant operating test speed at the beginning of

each pass, the toggle valve was switched open to allow flow of the FM-200 gas to enter the tractor exhaust stack, and the time was recorded on a log sheet. A real-time reading of the concentration of the FM-200 gas was observed during on-road testing using the remote operator's station located in the tractor sleeper. A concentration of approximately 2 ppm was expected based on previous shake-down runs and the position of the needle valve upstream of the flow meter. If a concentration close to that expected was observed, then no adjustments were made to the valve position.

The analog signal from the flow meter recorded the real time flow of the tracer gas being injected into the stack while the multi-gas analyzer recorded the real time concentrations of the FM-200 gas in the exhaust plume sample. At the end of each pass, the toggle valve was closed to conserve FM-200 and the "Off" time recorded on a log sheet. The sample data readings from the multi-gas analyzer were stored in the instrument's internal memory and were downloaded at the end of the test day via an RS-232 serial port.

Table 4-7 lists the FM-200 consumption rate that was necessary to achieve a concentration of about 2 ppm of FM-200 in the plume sample at two different speeds.

Table 4-7.   FM-200 Consumption Rates

FM-200	56 km/h	105 km/h
Volumetric Flow, Measured	1.81 L/min	1.36 L/min
Mass Flow, Calculated (Gas Density of 0.032 g/L)	3.50 kg/h	2.63 kg/h

4.9   PM-2.5 Instrument Operation

Since there are no standard techniques for on-road determination of diesel PM or monitoring of vehicle operating parameters, the various instrumentation methods used in the study were developed from the applicable operating manual and the experience gained during the experiments conducted at WVU described earlier (Kinsey et al., 2006b). Miscellaneous operating procedures (MOPs) were developed for each instrument type as provided in the approved QAPP (U.S. EPA, 2004). Table 4-8 lists the specific MOP applicable to each instrument previously described in Section 2.

A situation worthy of mention relevant to the operation of the fine PM instruments is need for frequent cleaning of the QCM crystal. Early in the campaign, the instrument would go offline in the middle of a pass, invalidating that pass. Therefore, the procedures were modified in the field to include cleaning the QCM crystal at the end of every pass during a 56 km/h test and at the end of every other pass during a 105 km/h test. Also, a spare crystal holder was available in the event the crystal failed completely during a particular experiment.

Table 4-8.   Miscellaneous Operating Procedures

General Category	MOP Title	MOP Number
Vehicle Operation	DEAL Facility Setup: Staging Configuration	1400
	Load Shifting for the DEAL	1401
	Preparations for DEAL On-Road Testing	1402
	Return from On-Road Testing for the DEAL	1403
	DEAL Shutdown Procedures	1404
Gaseous Pollutant Monitoring	CEMS Startup	1405
	CEMS Multi-Point Calibration	1406
	CEMS 2-Point Calibration Check	1407
	CEMS System Bias Check	1408
	CEMS Response Time Check	1409
	CEMS Overnight/Standby Mode	1410
	Operation of CAI Model 300 CO_2 Analyzer	1420
	Operation of Horiba MPA 220 O_2 Analyzer	1421
	Operation of CAI Model 400 NO/NO_X Analyzer	1422
	Operation of Horiba AIA 210 CO Analyzer	1423
	Operation of Horiba FIA 236 THC Analyzer	1424
PM Monitoring	Operation of TSI SMPS Model 3934	1411
	Operation of TSI SMPS Model 3936	1412
	Basic Operation and Maintenance of Dekati ELPI	1413
	Operation of Series 1105a TEOM	1414
	Operation of Series 1400a TEOM	1415
	Operation of Magee (Andersen) AE-2 Aethalometer	1416
	Operation of Eco-Chem PAS 2000 Real Time PAH Monitor	1417
Tracer Gas Monitoring	Operation of B&K 1302 Gas Analyzer for Tracer Gas Measurements	1418
	Performing Zero Check of the B&K 1302 Analyzer	1419

4.10 Time Integrated Sampling

The pre-fired quartz filters installed in both sampling arrays were prepared and analyzed according to NIOSH Method 5040, Elemental Carbon (Diesel Particulate). The PUF plugs used in the speciated tests were prepared and analyzed per the applicable MOPs outlined in the Facility Manual for the FPCL appended to the QAPP (U.S. EPA, 2004).

All sampling media were prepared in the FPCL before leaving for the field. Prior to and after sampling, the quartz filters and ELPI substrates listed in Table 3-1 were stored in aluminum foil-lined, plastic Petri dishes inside a laboratory freezer maintained at –50 °C. The Teflon filters were also stored inside plastic Petri dishes in the –50E freezer. Finally, the PUF plugs were stored and transported in glass jars with Teflon twist caps. During transport and in the field laboratory, all sampling media were stored in a small portable freezer operated at a temperature

of approximately –20 °C. This portable freezer was also used as the primary shipping container for the sampling media to and from the sampling site and was operated on generator power en-route.

Chapter 5
Post-Test Laboratory Analysis

The samples of fine PM collected during testing by integrated sampling media were taken to the laboratory for chemical analysis. The samples were stored in a freezer during transportation to minimize sample losses. Upon arrival at the laboratory, the sampling information (such as the sampling location of individual media and the test date, ID, and conditions) was collected and recorded in the sample log system. The samples were stored in a freezer at temperatures below -20 °C until analysis. By keeping in a sealed container in a frozen state, samples could safely be stored without degradation for a long period of time. The instruments and procedures for the analyses conducted in the laboratory are described below, with the applicable MOPs listed in Table 5-1.

Table 5-1.   Analytical MOPs

Procedure	MOP
Gravimetric analysis	2503
Elemental analysis	EPA Method IO-3.3
Analysis of water-soluble inorganic ions	2512 & 2513
OC/EC analysis	2511
Analysis of organic PM:	
Compositing and spiking	504
Sample extraction and concentration	2504
Extract methylation	2505
GC/MS analysis	2507
Analysis of PUFs	2509

5.1   PM-2.5 Gravimetric Analysis

The PM-2.5 gravimetric analysis was performed by weighing the individual Teflon filters before and after sampling on a Sartorius microbalance having a detection limit of 1 µg. The filter weighing was done in accordance with the standard procedure for PM-2.5 samples (MOP 2503). The method requires that the filter samples be conditioned before weighing by equilibration for a minimum of 24 hours in an environmental chamber which is maintained at 20–23 °C and a relative humidity of 30% to 40%. To eliminate the possible electrical charge accumulating on the surface, both sides of each Teflon filter were exposed to Polonium strips for at least 20 seconds before placing the filter on the balance. Before sampling, the blank Teflon filters were tare weighed and placed in Analyslide dishes that were purchased from Pall Gelman and had

individual IDs. The weight change in the same filter after sampling was then used for PM mass emission calculation.

5.2   Elemental Analysis

After post-test weighing, the Teflon filters were analyzed by EPA's National Exposure Research Laboratory using X-Ray Fluorescence (XRF) and EPA Method IO-3.3 to quantitatively determine elements in the PM collected on the filters (U.S. EPA, 1999). In the XRF analysis, a Kevek Model EDX-171 energy dispersive spectrometer with a 200 watt rhodium target tube as an excitation source was used.

5.3   Analysis of Water-Soluble Inorganic Ions

After non-destructive analyses (weighing and XRF), the Teflon membrane filter samples were analyzed using a Dionex DX-120 ion chromatograph (IC) for isocratic ion analysis including potassium (K^+), ammonia (NH_4^+), magnesium (Mg^{+2}), calcium (Ca^{+2}), nitrate (NO_3^{-1}), sulfate (SO_4^{-2}), nitrite (NO_2^{-1}), and chloride (Cl^{-1}). During this analysis, PM on each Teflon filter was extracted by placing the filter in a vial with 10 mL HPLC (high performance liquid chromatograph) grade (low conductivity) water (H_2O). The extract was then sonicated for 30 min and introduced at the head of an ion-exchange resin column of the ion chromatograph (IC). The ions in the sample were detected by the conductivity detector and quantified through the use of external standards. The concentrations of the ions found in the water solution were then converted to the mass on the filter by multiplying the concentrations with the volume of the extraction water, 10 mL.

5.4   Analysis of Organic and Elemental Carbon

The quartz fiber filter samples were analyzed by a thermal/optical carbon analyzer provided by Sunset laboratory Inc. for determination of EC/OC before undergoing solvent extraction. The OC and EC were determined based on the two-stage thermal-optical method outlined in NIOSH Method 5040 (NIOSH, 2003). The method proceeds in two stages. First, organic and carbonate carbon are evolved in a helium atmosphere as the temperature is stepped to about 850 °C. The evolved carbon is catalytically oxidized to CO_2 in a bed of granular manganese dioxide (MnO_2), and then reduced to methane in an N/firebrick methanator. Methane is subsequently quantified by FID. In the second stage, the oven temperature is reduced, an oxygen-helium mix is introduced, and the temperature is stepped to about 940 °C. As oxygen enters the oven, pyrolytically generated carbon is oxidized, and a concurrent increase in filter transmittance occurs. The point at which the filter transmittance reaches its initial value is defined as the split between OC and EC. Carbon evolved prior to the split is considered OC (including carbonate), and carbon volatilized after the split is considered EC. The instrument has a lower detection limit on the order of 0.2 µg/cm^2 filter for both OC and EC.

It has been found that new quartz fiber filters usually have an OC background of 2 to 5 µg/cm^2. For this reason, the purchased quartz filters were pre-fired in a kiln at 550 °C for 12 hours before use. The clean quartz filters were stored in petri dishes lined with cleaned aluminum foil. Aluminum foil liners were cut to cover the inside surfaces of the Petri dishes so that the filters did not directly touch the dish when placed inside the lined dishes. The aluminum liners were

also baked at 550 °C for 12 hours and then compressed into the Petri dishes using a cleaned Lucite plug machined to fit snugly into the dishes. The filters and liners were handled with Teflon forceps to avoid any contamination.

Only a portion of quartz filter sample was used for OC and EC analysis, which was obtained using a punch tool specially provided by Sunset Lab. The 1.45 cm^2 filter punch was then placed on the sample holder of the instrument for analysis. The analyzer reports the OC and EC contents in µg per cm^2. Since the actual exposure area of quartz filter was 13.45 cm^2, the OC and EC mass on the filter were calculated by multiplying the reported OC or EC content (µg/cm^2) by 13.45 cm^2 to obtain a mass value in µg.

5.5 Analysis of Particle Phase Organic Compounds

After OC/EC analysis, the semi-volatile organic com-pounds in the PM collected on quartz filters were solvent extracted and quantified with gas chromatography/mass spectroscopy (GC/MS). The PM speciation included (1) sample compositing; (2) solvent extraction and concentration; (3) extract methlation; and (4) GC/MS analysis as described in the following sections.

5.5.1 Sample Compositing and Spiking

For better GC/MS results, ideally a filter sample should contain approximately 1.0 mg of OC as measured by the OC/EC analyzer. However, the OC on each of the quartz filter collected from the on-road tests was much less. As a result, the filters at the same sampling positions for the same types of fuel but different tests were composited as described in Table 5-2. The composited filters were placed in a jar and were spiked with internal standard solution. The exact volume of spike solution is recorded since this value is used in the quantification calculations.

Table 5-2.   Composites of Quartz Filter Samples

Composite[a]	QF ID	OC (mg)	# of Punches
T5&6 Plume Front	Q100704H	1.341	1
	Q100103C	1.039	1
	Total	**2.380**	**2**
T5&6 Plume Backup	Q100704E	0.154	1
	Q100704G	0.110	1
	Q100103A	0.219	1
	Q100103B	0.083	1
	Total	**0.567**	**4**
T5&6 Thermal Denuder Backup	Q100704C	0.033	1
	Q100704D	0.013	1
	Q100103D	0.044	1
	Q100103E	0.015	1
	Total	**0.105**	**4**

Composite[a]	QF ID	OC (mg)	# of Punches
	Q100704K	0.030	1
T5&6 BKG Front	Q100103H	0.047	1
	Total	**0.077**	**2**
	Q100704A	0.033	2
	Q100704B	0.020	1
T5&6 BKG Backup	Q100103F	0.023	2
	Q100103G	0.018	1
	Total	**0.095**	**6**
	Q093004X	0.242	1
T19&20 Plume Front	Q100103L	0.244	1
	Total	**0.486**	**2**
	Q093004V	0.102	1
	Q093004W	0.097	1
T19&20 Plume Backup	Q100103J	0.099	1
	Q100103K	0.064	2
	Total	**0.362**	**5**
	Q100103I	0.081	1
	Q093004Y	0.013	1
T19&20 Thermal Denuder Backup	Q100103M	0.058	1
	Q100103N	0.015	1
	Total	**0.167**	**4**
	Q092904T	0.051	1
T19&20 BKG Front	Q100103Y	0.044	2
	Total	**0.095**	**3**
	Q100604H	0.048	1
	Q100604E	0.025	1
T19&20 BKG Backup	Q100103O	0.024	1
	Q100103P	0.021	1
	Total	**0.117**	**4**

a. Front = first filter(s) in a series; BKup = backup filter(s); BKG = background

5.5.2 Sample Extraction and Concentration

Spiked filter composites were extracted with five successive 10-minute sonication steps. The first two extractions were performed with hexane and then were followed by three extractions with a 2:1 mixture of benzene and isopropyl alcohol. Filters were sonicated for 10 minutes at ambient temperature. The water temperature in the sonicator was monitored and maintained below 32 °C.

Following sonication, the extract was transferred to the flask of the in-line transfer and filtration apparatus. The transfer apparatus was thoroughly cleaned before extract transfer. The glass parts, including the quartz wool-packed Pasteur pipette, were solvent rinsed and then baked in aluminum foil at 550 °C for at least 12 hours. Teflon parts were cleaned by sonication with dichloromethane and then air dried. The assembled in-line transfer apparatus was rinsed by transferring high purity distilled benzene up through the Teflon transfer line and the quartz packed pipette into the flask by use of a vacuum system. The rinse benzene was discarded, and the flask was then re-rinsed and then reinstalled. The extract was transferred to the flask by connecting a vacuum of approximately 10 cm of mercury via corrugated Teflon tubing connected to the side arm. All five extracts were collected together in the same flask.

The composited extract was then transferred and concentrated in the test tube of a Zymark Model TurboVap II Concentration Workstation. In the Zymark, the extract was concentrated by passing a gentle stream of pure nitrogen over the surface of the liquid to evaporate the solvent to a total liquid volume of 0.5–0.75 mL. The water bath temperature of the concentrator was kept at 35–40 °C. After concentration, the extract was completely transferred to a clean amber vial and further concentrated by nitrogen blow-down to approximately 250 μL. Concentrated extract was stored in the vial with a Teflon-lined cap in a freezer until derivatization and analysis.

5.5.3   Extract Methylation

Each concentrated extract was split into two fractions: neutral and methylated. The sample was split by first measuring the total volume of the concentrated extract with a thoroughly cleaned gas-tight volumetric syringe. The total volume of sample was recorded. Half of it was returned to the original vial, and the other half was placed in a second cleaned vial and labeled for methylation.

Methylation was performed to yield methyl esters of fatty acids that would otherwise not be eluted from the GC column. The sample was methylated by adding approximately 10 μL of high purity methanol and 100 μL of diazomethane solution to the methylation fraction of extract. After the reaction was complete, the methyled extract was reconcentrated by nitrogen blowdown to the original volume of aliquot before methylation. The methylated extract was stored in the freezer until analysis.

5.5.4   GC/MS Analysis

The extracts were analyzed with an HP 6890/5973 GC/MS equipped with thermal conductivity detector (TCD) model HP-G1530A, autoinjector model HP-G1513A, programmable Temperature Vaporizing (PTV) inlet, mass selective detection (MSD) interface, and FID model HP-G1526A. An HP-5ms GC column was used to separate the various organic compounds in the sample. Ultra pure helium was used as the carrier gas. The GC/MS operating conditions are summarized in Table 5-3. Positive identification of a compound via GC/MS was confirmed when the GC retention time and mass spectrum of the unknown compound match those of an authentic standard compound under identical instrumental conditions.

Table 5-3.   GC/MS Operating Conditions

Operating Parameters	Instrument Setting
Injector Temperature (°C)	300
GC/MS Interface Temperature (°C)	300
Initial Oven Temperature (°C)	65
Initial Oven Hold Time (min)	10
Oven Temperature Ramp Rate (°C/min)	10
Final Oven Temperature (°C)	300
Final Oven Temperature Hold Time (min)	41.5
Carrier Gas	Helium
Carrier Gas Flowrate (mL/min)	1.0
Injection	Splitless
Purge Flow to Split Vent (mL/min)	30
Gas Saver (mL/min)	20
Mass Spectrometer Conditions:	
Solvent Delay (min)	3.5
Data Collection Mode	Scan
Scan Range (amu)	50-500
Source Temperature (°C)	230
Quad Temperature (°C)	150

For quantification of the target marker compounds by GC/MS, known quantities of deuterated internal standards were included in each quantification standard and spiked onto each sample. Each compound that was quantified by GC/MS is referenced to one of more internal standards such that the response of each compound relative to the appropriate internal standard(s) is fixed with only minor variation in MS detector response, MS tune parameters, GC injection conditions, and GC column conditions. Detail operating procedure for GC/MS analysis can be found in MOP 2507 (U.S. EPA, 2005).

Chapter 6
Experimental Data Analysis

The post-test data analysis involved four primary steps: raw data gathering, emission factor calculation, power demand calculation, and data correlation. The methods and procedures used in each step of data reduction are discussed below.

6.1   Raw Data Analysis

All electronic data recorded in the test field were stored on six CDs: (1) New Bern Test (base fuel plus shakedown), (2) New Bern Test (B20 runs), (3) Roll Down, (4) Tunnel Blank, (5) I-77 Road Grade Test (12/16/04), and (6) I-77 Road Grade Test (12/21/04). The first step of data analysis was to gather all useful data from these raw data CDs for emission and power demand calculation. The analog files recorded the vehicle operating parameters, flow rates, exhaust gas compositions, as well as fuel feed rates. The concentrations of CO_2, CO, O_2, NO_X, and THC in the raw exhaust gas were recorded every second and stored in the files titled "Analog mm-dd-yy F1". These files also stored the sampling flow rates for all the plume and background filters. However, the flow rates for the filters behind the TDs were recorded in the files "Analog mm-dd-yy F2". The vehicle speed was stored in the files "Analog mm-dd-yy". The fuel feed rate was recorded in "DD60 mm-dd-yy". The change in atmospheric pressure monitored by the micro-barometer and used to determine road grade was stored in "MB mm-dd-yy". Table 6-1 summarizes these parameters and their raw data file sources. The electronic data recorded by various PM monitoring instruments were stored in the corresponding raw data files.

In addition to the above electronic data, the information required for emission evaluation includes weather reports and fuel analytical reports. The field weather reports, which were obtained from State Climate Office of North Carolina, provided data needed for calculation of the ambient air moisture content as a function of test time. The fuel compositions (Appendix B) were used in emission factor calculation.

There were 20 tests (T1 to T20) conducted on a level segment of US-70 near New Bern, NC in October 2004. T1 to T4 were shakedown tests using available pump grade diesel fuel. For tests T5 to T12, a low-sulfur diesel fuel, called "base fuel" in this study, was used. To investigate the effects of fuel type on emissions, B20 was used in tests T13 to T20. Since the data recorded from the shakedown tests (T1 to T4) were not adequate for comparing of pump grade diesel with the other two diesel fuels, only the results for base fuel and B20 are discussed in this report. The effects of road grade on emissions were investigated in two preliminary grade tests (T21 and T22). These additional tests were conducted again using available pump fuel in December 2004 between I-77 Exits 1 and 8 that had a road grade of approximately 4%. During these tests, only gaseous emissions were measured.

Table 6-1.   Measurement Parameters Analyzed and their Source Files

Measurement Parameter	Unit	File Name	Column Title
Vehicle Speed	km/h	Analog mm-dd-yy	5TH_WHEEL [kmh]
Anubar Reading	in H_2O	Analog mm-dd-yy	ANUBAR ["H_2O]
Stack Temperature	^oC	Analog mm-dd-yy	STACK [-C]
Trace Injection Rate	L/min	Analog mm-dd-yy	MFM [a] [LPM][b]
Plume Front TF[c] Flow Rate	L/min	Analog mm-dd-yy F1	FTP1 [LPM]
Plume Front QF[d] Flow Rate	L/min	Analog mm-dd-yy F1	FTP2 [LPM]
Background TF Flow Rate	L/min	Analog mm-dd-yy F1	Back Teflon [LPM]
Background QF Flow Rate	L/min	Analog mm-dd-yy F1	Back Quartz [LPM]
TF after Denuder Flow Rate	L/min	Analog mm-dd-yy F2	TD[e]. QUARTZ [LPM]
QF after Denuder Flow Rate	L/min	Analog mm-dd-yy F2	TD. TEF[f]. [LPM]
Exhaust CO Concentration	ppm	Analog mm-dd-yy F1	CO Low [ppm]
Exhaust CO_2 Concentration	%	Analog mm-dd-yy F1	CO_2 [%]
Exhaust NO_X Concentration	ppm	Analog mm-dd-yy F1	NO_X [ppm]
Exhaust O_2 Concentration	%	Analog mm-dd-yy F1	O_2 [%]
Exhaust THC Concentration	Ppm	Analog mm-dd-yy F1	THC [ppm]
Fuel Feed Rate	gal/h	DD60 mm-dd-yy	Fuel Rate(gal/hr)
Micro-Barometer Reading	Psi	MB mm-dd-yy	CHANNEL1
Exhaust Black carbon	ng/m^3	Analog mm-dd-yy F2	MAGEE [ng/m^3]
Exhaust PAH concentration	ng/m^3	Analog mm-dd-yy F2	PAH [ng/m^3]
ELPI background PM concentration	#/cm^3	ELPI C Test # mm-dd-yy	
ELPI plume PM concentration	#/cm^3	ELPI D Test # mm-dd-yy	
SMPS background PM concentration	#/cm^3	Old SMPS mm-dd-yy	
SMPS plume PM concentration	#/cm^3	Long mm-dd-yy	
Nano-SMPS plume PM concentration	#/cm^3	Nano mm-dd-yy	
TEOM background PM concentration	µ/cm^3	1400 mm-dd-yy	30-min MC & 1-hr MC
TEOM plume PM concentration	mg/cm^3	RPyyyymmddxxxxxxR	Mass Conc 5 & Mass Conc 8
QCM plume PM concentration	mg/cm^3	QCM mm-dd-yy	Conc (mg/m^3)

a. MFM = mass flow meter
b. LPM = liters per minute
c. TF = Teflon filter
d. QF = quartz filter
e. TD = thermal denuder
f. TEF = Teflon

In addition to fuel type and road grade, the effects of vehicle weight and vehicle speed on emissions were investigated. In these steady-state, constant speed tests, the tractor-trailer was operated either unloaded at a gross vehicle weight (GVW) of 21,350 kg or loaded with large blocks of concrete to a GVW of 33,890 kg. The GVW was measured by running the vehicle across a certified scale. The effect of vehicle speed on emissions was also investigated by operating the vehicle at either 105 or 56 km/h. It should be pointed out that, due to operating difficulty, the two speeds maintained in the 4% grade road tests in Virginia were different from those used in the level road tests. The test conditions were summarized previously in Table 4-1.

The raw data recorded from the measurements of emissions and vehicle parameters were smoothed using the "medsmooth" function in MathCad, version 2001 Professional. The measurements that were smoothed in this study include CO_2, CO, NO_X, THC, vehicle speed, fuel feed rate, and microbarometer pressure.

Because different instruments were used in monitoring vehicle emissions, it is important to synchronize them with clock time so that the emission and vehicle operating data for each individual pass can be extracted and analyzed. Many of the instruments used in this study recorded data every second. However, there were two notable exceptions. The atmospheric pressure was recorded every 1.6 s by the micro-barometer, while the weather data were reported every hour. These two raw data parameters had to be interpolated to obtain their values at each second. An Excel macro based on the Lagrange interpolation technique was developed for this analysis.

Due to the inherent difference in response time of different instruments as well as the transport time required in the sample collection system, it was expected that, in the emission evaluation, the emissions measurement would always lag the power measurement. A cross-correlation technique was used to determine the measurement delay time for emissions of each gas species. In the cross-correlation, two sets of time-series data—emissions measurements and power measurements—were correlated and the correlation coefficient was calculated. The time delay was determined by adjusting how the times of the two data sets are aligned with respect to one another until the correlation coefficient between emissions and power measurements was maximized. The on-road steady-state tests were conducted by running the vehicle back and forth on the same segment of highway, and the data when the vehicle reached a specified constant speed were collected for emission calculation.

Each individual test consists of a number of repeated passes with the identical vehicle driving condition. To characterize the steady-state emissions, the gathered data for each test were broken down to groups according to the time period of each individual pass in which the truck was operated under the same steady-state condition. The emission data in each pass recorded by an instrument were averaged to obtain an average for that pass and that measurement. The standard deviation in the recorded data was also estimated for each pass and used as a measure of uncertainty in the pass-average obtained. The pass-average obtained was then used to calculate the emission factor and power demand for that pass. The uncertainty in pass-average emission factor was estimated from the uncertainties in the primary measurements involved in the calculation and is given as

$$u_R = \left[\left(\frac{\partial R}{\partial x_1} u_1 \right)^2 + \left(\frac{\partial R}{\partial x_2} u_2 \right)^2 + \cdots + \left(\frac{\partial R}{\partial x_n} u_n \right)^2 \right]^{1/2}$$ (6-1)

where

u_R = uncertainty in R,

R = a function of individual variables, $R = R(x_1, x_2, X\,X\,X, x_n)$,

$u_1, u_2, X\,X\,X, u_n$ = uncertainties in independent variables $x_1, x_2, X\,X\,X, u_n$, and

n = number of independent variables.

The test-average is the average of all the pass averages in the same test. The uncertainty in a test-average was calculated from the uncertainties of all the passes in the test by

$$w_t = \frac{\sqrt{\sum_{i=1}^{n} \left(w_i^2 \right)}}{n}$$ (6-2)

where

w_t = uncertainty in test average,

w_i = uncertainty in pass-average of the Ith pass, and

n = number of passes in the test.

6.2   Emission Factors for Gaseous Pollutants

The gaseous emission factors were calculated using the method recommended by the Society of Automotive Engineers (SAE), ARP 1533 (SAE, 2004). The method calculates the emission factors by means of a comprehensive material balance between the inputs of fuel and combustion air and the outputs of exhaust gas compositions. The method provides advantages in emission factor calculation in two respects: first, it makes it possible to calculate instant emission factors from the continuous CEM measurements, which is particularly useful if unsteady-state test data are to be analyzed; second, it calculates the emission factor without the use of exhaust gas flow rate, which requires the measurement of local velocities in the stack. Since the exhaust gas velocity varies with time and measurement location in the stack, the SAE method eliminates the uncertainty attributed by the anubar meter measurement. This will be demonstrated later in Section 7.6.

According to the SAE method, a matrix equation as described by Equation (6-3) was established from the material balances of C, H, O, N, and S over the combustion process:

$$Y = A^T B$$ (6-3)

The matrices Y, A, and B are

$$
Y = \begin{bmatrix} Y_1 \\ Y_2 \\ Y_3 \\ Y_4 \\ Y_5 \\ Y_6 \\ Y_7 \\ Y_8 \\ Y_9 \\ Y_{10} \end{bmatrix}, \quad
A = \begin{bmatrix}
0 & 1 & 0 & 0 & 0 & 1 & 3 & 0 & 0 & -(T+U) \\
0 & 0 & 0 & 0 & 2 & 0 & 8 & 0 & 0 & -(2h+4U) \\
0 & 2 & 0 & 2 & 1 & 1 & 0 & 1 & 2 & (2R+2T+h) \\
0 & 0 & 2 & 0 & 0 & 0 & 0 & 1 & 0 & -2S \\
0 & 0 & 0 & 0 & 0 & 0 & 0 & 0 & 1 & 0 \\
[CO_2]_d & -1 & 0 & 0 & -[CO_2]_d & 0 & 0 & 0 & 0 & 0 \\
[CO]_d & 0 & 0 & 0 & [CO]_d & -1 & 0 & 0 & 0 & 0 \\
[THC]_w & 0 & 0 & 0 & 0 & 0 & -1 & 0 & 0 & 0 \\
[NO_X]_w & 0 & 0 & 0 & 0 & 0 & 0 & -1 & 0 & 0 \\
-1 & 1 & 1 & 1 & 1 & 1 & 1 & 1 & 1 & 0
\end{bmatrix}, \quad
B = \begin{bmatrix} m \\ n \\ p \\ q \\ r \\ 0 \\ 0 \\ 0 \\ 0 \\ 0 \end{bmatrix}
$$

where

$[CO_2]_d$ = CO₂ mole fraction concentration on dry basis measured by CEM, %,

$[CO]_d$ = CO mole fraction concentration of dry basis measured by CEM, ppm,

$[THC]_w$ = mole fraction concentration of total hydrocarbon, expressed as C_3H_8, on wet basis measured by CEM, ppm,

$[NO_X]_w$ = oxides of nitrogen mole fraction concentration, expressed as NO, on wet basis measured by CEM, ppm,

m = weight percentage of carbon in fuel,

n = weight percentage of hydrogen in fuel,

p = weight percentage of oxygen in fuel,

q = weight percentage of nitrogen in fuel,

r = weight percentage of sulfur in fuel,

T = mole fraction of CO_2 in dry air = 0.00034,

U = mole fraction of methane in dry air = 0,

R = mole fraction of O_2 in dry air = 0.20948,

S = mole fraction of N_2 and Ar in dry air = 0.79018,

h = moisture content in ambient air, mole of moisture per mole of dry air,

Y_1 = total g-mol of exhaust produced per 100 g of fuel burned,

Y_2 = g-mol of CO_2 produced per 100 g of fuel burned,

Y_3 = g-mol of N_2 in exhaust gas per 100 g of fuel burned,

Y_4 = g-mol of O_2 in exhaust gas per 100 g of fuel burned,

Y_5 = g-mol of moisture in exhaust gas per 100 g of fuel burned,

Y_6 = g-mol of CO produced per 100 g of fuel burned,

Y_7 = g-mol of THC produced per 100 g of fuel burned,

Y_8 = g-mol of NO_X produced per 100 g of fuel burned,

Y_9 = g-mol of SO_2 produced per 100 g of fuel burned, and

Y_{10} = g-mol of air for burning 100 g of fuel.

Thus, the vector Y was solved at every second from the corresponding CEM measurement results and ambient moisture data. The fuel-specific emission factors of gaseous pollutants were then calculated by Eq. 6-4 through 6-6.

For CO

$$EF_{CO} = 10 \cdot Y_6 \cdot MW_{CO} \text{ (g/kg fuel burned)}$$ (6-4)

For THC

$$EF_{THC} = 10 \cdot Y_7 \cdot MW_{C3H8} \text{ (g/kg fuel burned)}$$ (6-5)

For NO$_X$

(g/kg fuel burned) (6-6)

where

MW_{CO} = molecular weight of CO,

MW_{C3H8} = molecular weight of C$_3$H$_8$, and

MW_{NO} = molecular weight of NO.

In order to solve Eq. 6-3, the moisture content in ambient air on a dry basis, h, must be known. This was obtained from the weather reports provided by the State Climate Office. The reports provided the data of air temperature (°F), relative humidity (percent), atmospheric pressure (Mbar), and wind speed (mi/h) monitored in every hour. In order to calculate the ambient moisture content as a function of test time, the reported temperature T_a, relative humidity RH, and pressure P_a were first interpolated to obtain the data in every second. The moisture fraction in ambient air, B_{wa}, was then calculated by Eq. 6-7.

$$B_{wa}(mol/mol) = \frac{RH}{100} \cdot \frac{P_v}{P_a}$$ (6-7)

where

RH = relative moisture, %,

P_v = water vapor pressure at temperature (T_a), Mbar, and

P_a = atmospheric pressure, mbar.

The ambient air moisture on dry basis, h, was calculated from the above moisture fraction by

$$h = \frac{B_{wa}}{(1 - B_{wa})}$$ (6-8)

6.3 Estimate of Exhaust Flow Rate

The Y_1 obtained from solving the SAE matrix equation can be used to estimate the exhaust flow rate by

$$Q_{SAE} = Y_1 \cdot 0.024055 \cdot F_{fuel} \cdot \frac{1}{60} \qquad (6\text{-}9)$$

where

Q_{SAE} = exhaust gas flow rate at standard condition (20 °C and 1 atm), m^3/min,

0.024055 = volume per mole at standard condition (20 °C and 1 atm), m^3/g-mol, and

F_{fuel} = fuel flow rate, 10^2 g/h.

As mentioned previously, the exhaust gas flow rate in this study can also be estimated from the annubar meter measurement. The annubar meter records the pressure difference, which can be used to calculate the exhaust gas velocity in the stack by

$$V_s = K_p C_p (\sqrt{\Delta P})_{avg} \sqrt{\frac{(T_s)_{avg}}{P_s M_s}} \qquad (6\text{-}10)$$

where

V_s = exhaust gas velocity (m/sec),

K_p = Pitot tube constant:

$$K_p = 34.96 \left[\frac{m}{sec} \sqrt{\frac{g/gmole \times (mmHg)}{°K \times mmH_2O}} \right]$$

C_p = manufacturer specified pitot tube coefficient = 0.6168,

ΔP = pressure drop reading from pressure transducer (mmH$_2$O),

T_s = average exhaust gas temperature from thermocouple (K),

P_s = absolute exhaust gas pressure from pressure transducer (mmHg), and

M_s = molecular weight of wet exhaust gas (g/g-mole).

The molecular weight of wet exhaust (M_s) in Eq. 6-10 is calculated from the dry exhaust molecular weight (M_d) and the moisture fraction (B_{ws}) by

$$M_s = M_d (1 - B_{ws}) + 18 B_{ws} \qquad (6\text{-}11)$$

The M_d in the Eq. 6-11 is estimated from the exhaust gas composition obtained from the monitoring instruments by

$$M_s = 0.44 \cdot CO_2(\%) + 0.32 \cdot O_2(\%)$$
$$+ 0.28 \cdot \left[N_2(\%) + CO(\%) \right]$$

(6-12)

The B_{ws} in the Eq. 6-11 is estimated from the exhaust gas composition and ambient air moisture fraction (B_{wa}) as

$$B_{ws} = 1 - \left\{ \left[158 \left(1 - B_{wa} \right) \right] / \left[0.79 \left(1 - B_{wa} \right) F + \right. \right.$$
$$\left. \left. 2 B_{wa} \left(100 - O_2(\%) - CO(\%) - CO_2(\%) \right) \right] \right\}$$

(6-13)

where

$F = 200 + R_{HC}[CO(\%) + CO_2(\%)]$ and the molar ratio of hydrogen to carbon, R_{HC}, in the fuel is obtained from fuel analysis.

Once the average velocity of exhaust gas in the stack is calculated by the Eq. 6-10 to 6-13, the exhaust flow rate under standard conditions can be determined using

$$Q_{annubar} = 60 \cdot V_s \cdot A \cdot \left(\frac{293 \cdot P_s}{T_s \cdot 760} \right)$$

(6-14)

where

$Q_{annubar}$ = exhaust flow rate at 293 °K and 760 mm Hg (m^3/min),

V_s = exhaust gas velocity from Eq. 6-10 (m/s),

A = cross section area of exhaust stack (m^2),

T_s = exhaust gas temperature (°K), and

P_s = absolute exhaust gas pressure (mmHg).

6.4   PM Emission Factors

Various instruments were used in this study to measure PM-2.5 concentrations, either in mass or as particle counts. These measurements were implemented in both plume and background sampling systems. Since the plume sampling was diluted with ambient air, the dilution ratio in the plume system must be determined before the emissions can be estimated. In this study, a known amount of trace FM-200 was injected into the exhaust stack, and its concentration in the plume system was then measured. The dilution ratio was consequently calculated by dividing the trace concentration in the stack with the concentration in the plume by

$$DR = \frac{\dfrac{R_{tr}}{Q_{SAE}} \cdot 1000}{C_{tr}}$$

(6-15)

where

DR = dilution ratio in the plume

R_{tr} = injection rate of FM-200 tracer into the exhaust stack (L/min),

Q_{SAE} = stack exhaust flow rate determined by the SAE method (m^3/min), and

C_{tr} = FM-200 tracer concentration measured in plume (ppmv).

The fuel-specific emission factor for PM particle counts, EF_N, was calculated from the particle number concentration in the plume recorded through a PM monitoring instrument, such as the ELPI, SMPS, or nano SMPS, using

$$EF_N = \frac{200.3 \cdot 10^6 \cdot C_N \cdot f_C \cdot DR}{C_{CO2} + \dfrac{C_{CO}}{10000} + \dfrac{3 \cdot C_{THC}}{10000}} \quad \text{(particles/kg fuel)}$$

(6-16)

where

C_N = particle count concentration in plume recorded by the PM instrument (1/cm^3),

f_C = mass fraction of carbon in diesel fuel (g/g),

DR = plume dilution ratio,

C_{CO2} = wet basis carbon dioxide concentration in exhaust (%) ,

C_{CO} = wet basis carbon monoxide concentration in exhaust (ppmv), and

C_{THC} = wet basis hydrocarbon concentration in exhaust (ppmv).

The fuel-specific emission factor for PM mass, EF_M, was calculated from the particle mass concentration recorded by the PM instrument, such as the TEOM or QCM, using

$$EF_M = \frac{200.3 \cdot C_M \cdot f_C \cdot DR}{C_{CO2} + \dfrac{C_{CO}}{10000} + \dfrac{3 \cdot C_{THC}}{10000}} \quad \text{(mg/kg fuel)}$$

(6-17)

where

C_M = particle mass concentration in plume recorded by the PM instrument, mg/m^3.

Because the CO and THC concentration in the exhaust were usually negligible compared to CO_2 for diesel engine combustion, the second and third terms in the denominator of the Equations. 6-16 and 6-17 were neglected in the calculation in this study. Since the CEM measured CO_2 concentration on a dry basis, the wet basis CO_2 concentration in this study was obtained from the solution of Y_1 and Y_2 in the Equation. 6-3 as

$$C_{CO2} = \frac{Y_2 \times 100}{Y_1} \quad (\%)$$

(6-18)

6.5 Conversion of Emission Measures

There are many ways to quantify emissions. As discussed previously, the fuel-specific emission factor is expressed based on one kg of fuel burned. The emissions can also be expressed as a distance-specific emission factor based on one kilometer of vehicle travel. In addition, the emission rate expressed in milligrams per second is also used as a measure of the emissions. The emission rate was calculated from the fuel-specific emission factor through

$$ER = EF \cdot \frac{F_{fuel}}{3600}$$

(6-19)

where

ER = emission rate (particles/s or mg/s),

EF = fuel-specific emission factor (particles/kg fuel or mg/kg fuel), and

F_{fuel} = fuel feed rate (kg/h).

The emission rate was then used to calculate the distance-specific emission factor by

$$EM = 5782.4 \cdot \frac{ER}{U_V}$$

(6-20)

where

EM = distance-specific emission factor (particles/km or mg/km),

ER = emission rate (particles/s or mg/s), and

U_V = vehicle speed (km/h).

Use of fuel-specific emission factors for estimating light-duty vehicle emissions has been reported by Singer and Harley (1996). Recently, this approach has been utilized by Dreher and Harley (1998) for establishing emission inventory for heavy-duty diesel trucks. In this method, emission factors are normalized to fuel consumption, and vehicle activity is measured by the amount of diesel fuel consumed. Its advantages over the travel based approach are (1) the diesel fuel consumption data are readily available from the tax records, and (2) the fuel based emission

factors fluctuate much less than travel based emission factors as driving conditions change (Pierson et al., 1996).

6.6 Particle Size Distribution

The ELPI, SMPS, and nano SMPS were used in this study to determine the particle size distributions of truck PM emissions under various test conditions. Although the ELPI is a powerful monitoring tool for fast measurement of particle number concentration, it was operated primarily to collect size-classified samples for organic speciation. Therefore, in this report, only the particle size distributions monitored by SMPS and nano SMPS are discussed. To obtain an average particle size distribution for a specific test, the dN/dlogDp data recorded in all the run passes of the test for each size bin were averaged to generate the dN/dlogDp for that size bin. The dN/dlogDp data of all size bins were then smoothed against the particle size by using the supsmooth function in MathCad Version 2001 Professional. The test average particle size distribution was then obtained by multiplying the smoothed dN/dlogDp data by the plume dilution ratio.

After the particle size distribution was determined, the total particle number concentration and particle geometric mean diameter were calculated for the test by

$$N = \sum_{i=1}^{M} \left(dN / d \log D_p \right)_i \times \left(d \log D_P \right)_i$$

(6-21)

and

$$GMD = 10^{\left(\dfrac{\sum_{i=1}^{M} \left(dN / d \log D_p \right)_i \times \left(d \log D_p \right)_i \times \log D_{Pi}}{N} \right)}$$

(6-22)

where

N = particle number concentration (particles/cm^3),

D_P = particle size (nm),

M = total number of size bins, and

GMD = geometric mean diameter, nm

6.7 Vehicle Power Demand

In this report, the gaseous and PM emissions were studied to investigate their correlations with vehicle power demand. In general, the total power demand for a vehicle consists of road load power, P_{RL}, and acceleration power, P_{accel}, as expressed by

$$P = P_{RL} + P_{accel} \tag{6-23}$$

Under steady-state conditions, the total power demand is determined only by the road load power. Thus, the road load power is the power required for a vehicle to maintain a constant speed. The road load depends on rolling resistance of the tires with road, aerodynamic drag, and road grade resistance and is expressed as

$$RL = K_0 W \cos\theta + K_1 V_V + K_2 V_V^2 + W \sin\theta \tag{6-24}$$

where

RL = Road load (N)

K_0 = rolling resistance coefficient (dimensionless),

W = Gross vehicle weight (N),

θ = grade angle determined from micro-barometer readings,

K_1 = first degree drag coefficient (N-s/m),

K_2 = second degree drag coefficient (N-s^2/m^2), and

V_V = vehicle speed (m/s).

In this study, the coefficients, K_0, K_1, and K_2, in the above equation (6-24) were determined from the coast-down testing as described in Sec. 4.5. The coast-down tests were conducted at the segment of US-70 where the emissions tests were performed. During the coast down tests, the truck was initially brought to a speed of approximately 105 or 56 km/h, and then the transmission was switched to neutral and the variation in vehicle speed with time as the vehicle slowed down was recorded every second. From N readings of vehicle speed ($\mathbf{V}_1$, …, V_N from 105 to 10 km/h), a system of linear equations (6-25) can be established based on finite differences

$$\frac{W}{9.81} \frac{(-V_1 + V_3)}{2} = K_0 W + K_1 V_2 + K_2 V_2^2 \tag{6-25a}$$

$$\frac{W}{9.81} \cdot \frac{(-3V_1 + 4V_2 - V_3)}{2} = K_0 W + K_1 V_1 + K_2 V_1^2 \tag{6-25b}$$

X

X

X

$$\frac{W}{9.81} \frac{(-V_{N-2} + V_N)}{2} = K_0 W + K_1 V_{N-1} + K_2 V_{N-1}^2 \tag{6-25n-1}$$

$$\frac{W}{9.81} \frac{(-3V_N + 4V_{N-1} - V_{N-2})}{2} = K_0W + K_1V_N + K_2V_N^2 \qquad (6\text{-}25\text{n})$$

where "9.81" is the acceleration due to gravity (m/s^2) and the gross vehicle weight (W) of the truck is known. These equations are of the form

$$ma = K_0W + K_1V_n + K_2V_n^2$$

where

m = vehicle mass = $W/9.81$, kg and

$a = (V_x \ldots V_y)/2$

The term a is the finite difference expression of the truck deceleration during coast-down tests. The parameters K_0, K_1, and K_2 were estimated from the multipoint data equations 6-25a to 6-25n.

After the coefficients—K_0, K_1, and K_2—were determined, the road load, RL, was then calculated by the Eq. 6-24, and then the road load power, P_{RL}, was given by

$$P_{RL} = \frac{RL \times U_V}{3600} \qquad (6\text{-}26)$$

where

P_{RL} = road load power demand (kW),

RL = road load (N), and

U_V = truck speed (km/h).

The road grade in Eq. 6-24 was determined by the microbarometer, which monitored the pressure changes at every second caused by the change in road altitude as the truck was traveling along the road. The road grade was calculated from the measured pressure change and the corresponding truck travel distance by

$$Grade = \frac{70310 \cdot dP}{dL \cdot \rho_a} \qquad (6\text{-}27)$$

where

$Grade$ = road grade (%),

dP = pressure change measured by the micro-barometer as the truck moves for dL distance along the road (psi),

dL = road distance (m), and

ρ_a = density of air (1.2 kg/m^3).

The road grade angle θ in Eq.6-24 was then given as

$$\theta = \arctan\left(\frac{Grade}{100}\right) \tag{6-28}$$

Eqs. 6-24 and 6-26 indicate that, under steady-state conditions, the three primary factors—vehicle speed, weight, and road grade—affect the truck power demand.

Chapter 7
Analysis of Vehicle Operating Parameters

7.1   Coast-Down Test Results

Coast-down testing was performed with the truck at both an unloaded GVW of 21,350 kg and a loaded GVW of 33,890 kg. Figure 7-1 presents the vehicle speed as a function of time recorded for each coast-down test. In the figure, there are two replicate tests for each truck weight condition. The curves for the loaded truck are on the top, which is believed to be due to its higher momentum. The figure also shows that the curves obtained from the replicate tests are almost identical one to another, indicating good repeatability.
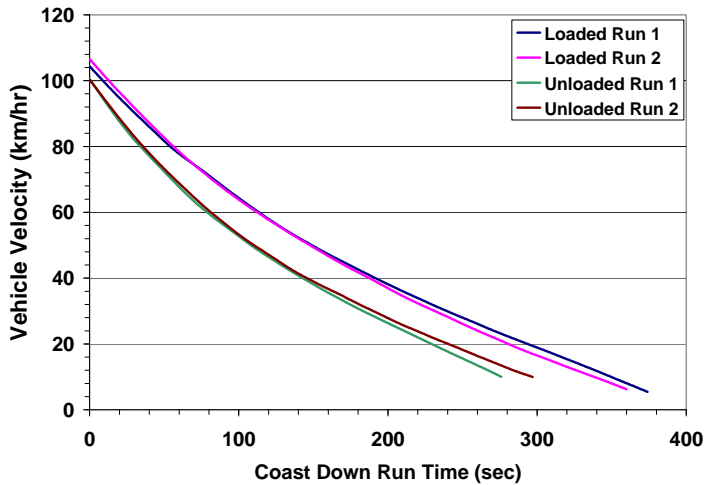
Figure 7-1.   Truck Speed Recorded as a Function of Time in the Coast-Down Tests

From the coast-down test results, the system of linear equations (6-25a to 6-25d) was used to calculate the three coefficients—K_0, K_1, and K_2—which are shown in Table 7-1. The correlation coefficients (r^2) obtained from the data regression for individual tests range from 0.945 to 0.971. By averaging each of the three coefficients for all the four tests, the overall average coefficients were estimated, which are provided at the bottom of the table.

To verify the calculated results, the above three average coefficients were substituted into the right side of Equations 6-25a to 6-25N to calculate the value of $WK_0 + V_VK_1 + V_V^2K_2$ as a function of the truck speed. The results were then compared to the values calculated from the left side of Equations 6-25a to 6-25N at the same truck speed. Figure 7-2 shows the comparison, in which the results calculated from both sides of Equations 6-25a to 6-25n agree well, having a correlation coefficient of $r^2 = 0.979$. As expected, the coefficients are independent of vehicle

weight and can be used in Equation 6-24 for road load power calculation under different truck conditions.

Table 7-1.   Road Load Equation Coefficients Determined From the Coast-Down Tests

Test	Run	K_0	K_1	K_2	r^2
		-	**N×s/m**	**N×s²/m²**	
Loaded	1	0.00466	21.919	3.421	0.945
	2	0.00426	55.532	2.566	0.962
Unloaded	1	0.00542	3.793	3.945	0.956
	2	0.00348	57.000	2.129	0.971
Overall Average		**0.00445**	**34.561**	**3.015**	**0.979**
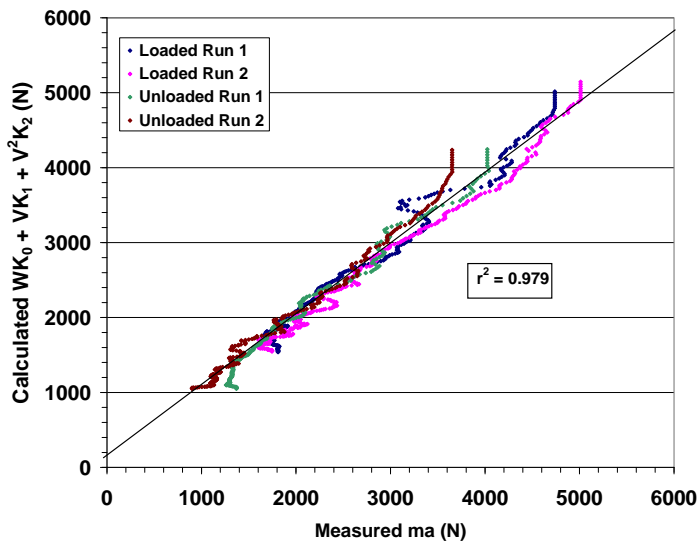
Figure 7-2.   Comparison between the Coast-Down Experimental Data and the Calculation Results from the Three Coefficients

7.2   Road Grade Determination

The road grade in this study was determined from the microbarometer measurements. Table 7-2 presents the results of the road grade and angle θ obtained from Equations 6-27 and 6-28 for each run pass of Test 4 (T4) during the New Bern phase of this study. The table also includes the average truck speed for each pass and the ensemble average of the ten passes for T4, which was 106.8 km/h with a standard deviation (SD) of 0.3 km/h. The test average road grade was 0% with a SD of 0.02%, which indicates the road grade angle was 0E. The 0% road grade determined during T4 indicates that tests T1 to T20 conducted on the segment of US-70 near New Bern, NC were conducted at near-zero grade.

Table 7-2.   Road Grade Determined during Test 4 for the Segment of US-70

Pass	Speed	Road Grade	
		Grade	θ
	km/h	%	Degree
1	105.18	0.01	0.00
2	106.86	-0.01	0.00
3	106.86	0.03	0.00
4	162.45	-0.03	0.00
5	106.21	-0.01	0.00
6	106.92	-0.03	0.00
7	106.91	0.03	0.00
8	106.92	0.00	0.00
9	106.93	0.02	0.00
10	106.97	-0.02	0.00
Average	106.8	0.00	0.00
SD	0.3	0.02	0.00

For the segment of I-77 near Fancy Gap, VA where 4% road grade tests T21 and T22 were conducted, the response of the microbarometer measurement with the variation in road grade variation was monitored. Figure 7-3(a) presents the recorded microbarometer readings as the truck traveled on I-77 north from Exit 1 to Exit 8, showing a 10 km constant uphill grade of approximately 3.93% from Exit 1 and then a downhill grade of 1.16% to Exit 8. The road grade test data in this study were mostly collected in the 10 km uphill section of 3.93% road grade. I-77 southbound from Exit 8 to Exit 1, as shown in Figure 7-3(b), consists approximately of four sections that begin with 1.6 km of 0.98% uphill grade followed by another 1.6 km of 3.81% downhill grade. The downhill grade is then reduced to 1.4% for the next 1.2 km, and finally, the road goes downhill at a constant grade of 4.4% in the last section. These results demonstrate the great potential of the microbarometer in road grade measurement for on-road diesel truck emissions testing.

7.3   Plume Dilution Ratio

The plume dilution ratio and its uncertainty for each pass were determined from the tracer gas measurement data. From the pass-average plume dilution ratios and uncertainties, the test average dilution ratio and uncertainty were then calculated. Table 7-3 is a summary of the calculation results.

(a) I-77 North Bound
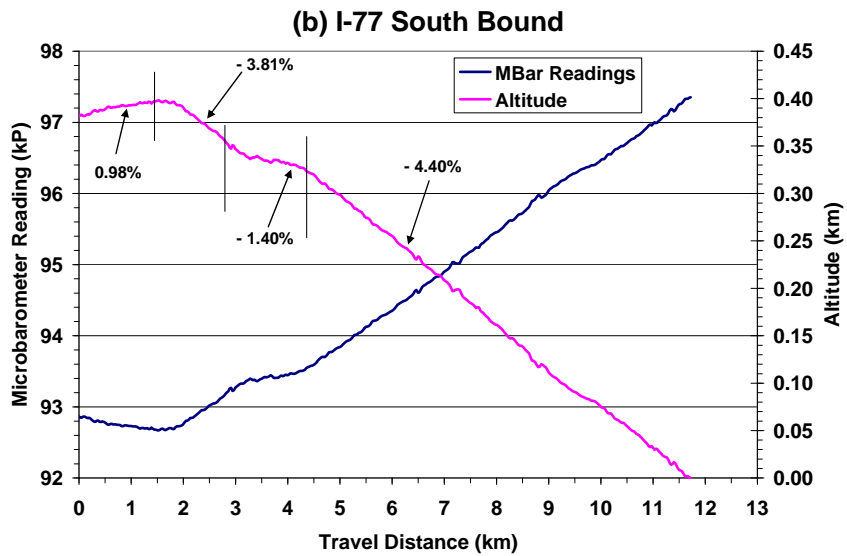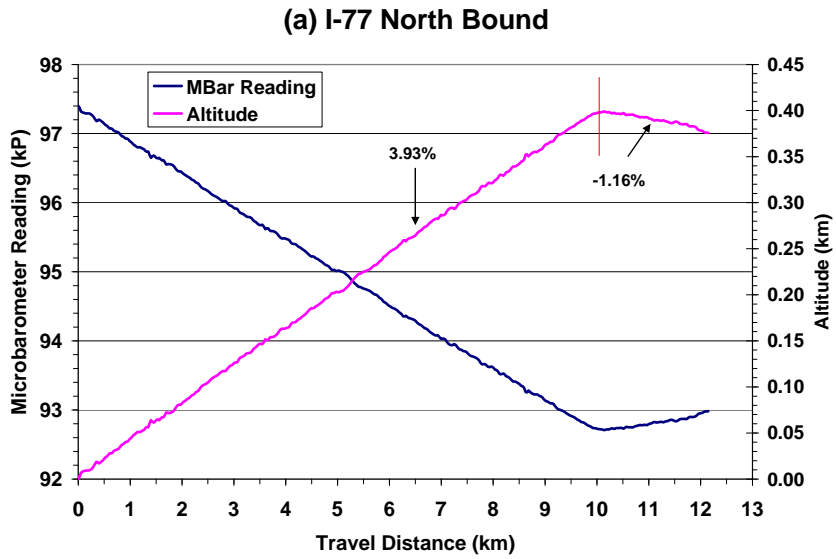
(b) I-77 South Bound

Figure 7-3.   Road Grade of Highway I-77 Measured by the Microbarometer (Mbar) Northbound (a) and Southbound (b)

Table 7-3.   Dilution Ratios and Their Uncertainties for Individual Tests

Test No.	Date	Test			Condition	
		Average	SD[a]	RSD[b]	Average	SD
5	10/19/04	69.81	4.89	7.0	63.74	3.01
6	10/20/04	57.68	3.51	6.1		
7	10/21/04	73.00	12.81	17.6	72.68	8.04
8	10/21/04	72.36	9.72	13.4		
9	10/22/04	99.35	19.95	20.1	95.89	12.96
10	10/22/04	92.43	16.55	17.9		
11	11/23/04	75.21	8.58	11.4	75.21	8.58
12	11/23/04	75.21	8.58	11.4		
13	11/26/04	88.76	18.43	20.8	88.76	18.43
14	11/26/04	88.76	18.43	20.8		
15	10/27/04	78.31	13.06	16.7	80.30	9.22
16	10/27/04	82.28	13.03	15.8		
17	10/28/04	101.66	15.36	15.1	86.32	9.82
18	10/28/04	70.98	12.22	17.2		
19	10/29/04	68.70	3.31	4.8	74.28	3.11
20	10/30/04	79.86	5.26	6.6		

a. SD = standard deviation.

b. RSD = relative standard deviation.

In this study, the tracer concentration was not successfully monitored under all circumstances. For those run passes that failed to properly collect the tracer concentration, the corresponding test-average dilution ratio and its uncertainty calculated from the correct run passes was used for the missing pass-average dilution ratios. For T12 and T14, the tracer measurements failed in all the run passes, and their dilution ratios were assumed to be equal to the test averages of T11 and T13, respectively (see the numbers in the shaded cells in the table).

The relative standard deviations (RSD) in the table indicate that, because of the difficulty in tracer gas measurements, a relative error up to 20% in dilution ratio determination was observed for most of the tests in this study. The large uncertainty in the plume dilution ratio determination had a substantial inverse impact on the results of the PM emission factor and rate calculations. Therefore, CO_2 in the plume should be measured directly in the future on-road studies.

Dilution ratio control was reported to have great influence on the particle size distribution. In their diesel engine tests, Abdul-Khalek et al. (1998) found that, for dilution ratios below 60, the entire size distribution changed with dilution ratio. The dilution ratio had more influence on the particles smaller than 30 nm. Increasing the primary dilution ratio from 4 to 60 resulted in significant decrease in number concentrations. In our study, the dilution ratio was controlled to be greater than 60 for most of the tests. Only T6 had a slightly lower dilution ratio of 57.7.

Therefore, the plume dilution ratios used for this study are considered appropriate for PM emissions measurement.

7.4   Truck Driving Conditions

The effects of truck driving conditions on emissions were investigated in this study by varying truck GVW and driving speed as previously discussed.

The actual average truck speed for each pass of a test was determined from the Datron optical speed sensor data recorded in the field as a function of time. The test-average speed was then calculated from the pass-average speeds of all the passes in the same test. Table 4-1 summarized the test-average truck speed and its uncertainty for each test. The same color bars represent the replicate tests under the same experimental conditions. The very small uncertainties for the level road tests, T5 to T20, indicate that the truck was operated at constant speeds and a steady-state condition was well established. However, the fluctuation in truck speed increased during the two uphill tests, T21 and T22, because it was difficult to maintain a constant speed on the steeper grade The average truck speeds for T21 and T22 were calculated from the data collected when the truck was maintained at nearly constant speed while going uphill with a constant road grade.

7.5   Fuel Types and Compositions

There were three types of diesel fuel used in this study. Pump diesel was obtained locally and was used in the shake-down tests (T1 to T4) and the 4% road grade tests (T21 and T22). The base fuel (a low-sulfur diesel) and a 20% soy-based biodiesel blend (B20) were used in the level road tests (T5 to T20) to investigate the effects of fuel type on truck emissions. Table 7-4 provides the compositions and other important properties of the fuels used. The value of g-moles for each element was estimated based on 100 grams of fuel and is included in the table. The composition in the table shows that both base fuel and B20 have sulfur contents less than 15 ppm in weight as compared with the pump diesel (394 ppm). The three fuels have essentially the same hydrogen content. In comparison to the other two fuels, B20 contains about 3.4% oxygen and has the lowest carbon content, resulting in its slightly lower gross heat value (GHV). Among three fuels, the cetance number is highest for B20. The impact of fuel type on truck emissions will be discussed later in this report.

7.6   Effects on Fuel Consumption and Exhaust Flow

The fuel flow rate is known to closely relate to the truck driving conditions. The monitored fuel feed rates under the different experimental conditions were processed from engine computer data to obtain the pass-average and test average fuel flow rates.

The effects of experimental conditions on fuel flow rate are illustrated as a bar chart by Figure 7-4. The figure shows that fuel type had little impact on fuel consumption. The increase in truck GVW from 21,350 kg to 33,890 kg only increased the fuel flow rate by 10 percent and 15 percent for the base fuel and B20, respectively, at zero grade. However, truck speed and road grade had strong effects on fuel consumption. In the level road tests, the fuel consumption increased by 2.5 times when the truck speed increased from 56 to 105 km/h. The results also show much greater fuel consumption for the truck driving upgrade than on the level road. If the

finding of fuel type having little impact on fuel consumption can also be applied to the pump fuel, approximately twice as much fuel was required for the unloaded truck driving on the 4% grade at about 99 km/h as compared to zero grade. The comparison of the results for the two road grade tests seem to indicate that, unlike what was seen in the level road tests, GVW had more influence than truck speed on the fuel feed rate when traveling uphill.

Table 7-4.   Fuel Compositions and Properties

Element	Pump Diesel		Base Fuel (Low-Sulfur Diesel		Bio-Diesel (B20)	
	wt%	g•mole/ 100 g fuel	wt%	g•mole/ 100 g fuel	wt%	g•mole/ 100 g fuel
C	86.794	7.23	86.238	7.18	83.378	6.94
H	13.153	13.05	13.760	13.65	13.200	13.09
O	0	0	0	0	3.420	0.449
N	0.014	0.0010	0.0009	0.0001	0.0007	0.0001
S	0.0394	0.0012	0.0015	0.0000	0.0012	0.0000
H/C (mol/mol)	1.806		1.901		1.886	
Density (g/cm^3)	0.854		0.857		0.846	
Flash Point (EC)	64.4		64.4		67.8	
Cetane Number	45.1		50.2		51.1	
GHV (kcal/g)	10.80		10.93		10.61	
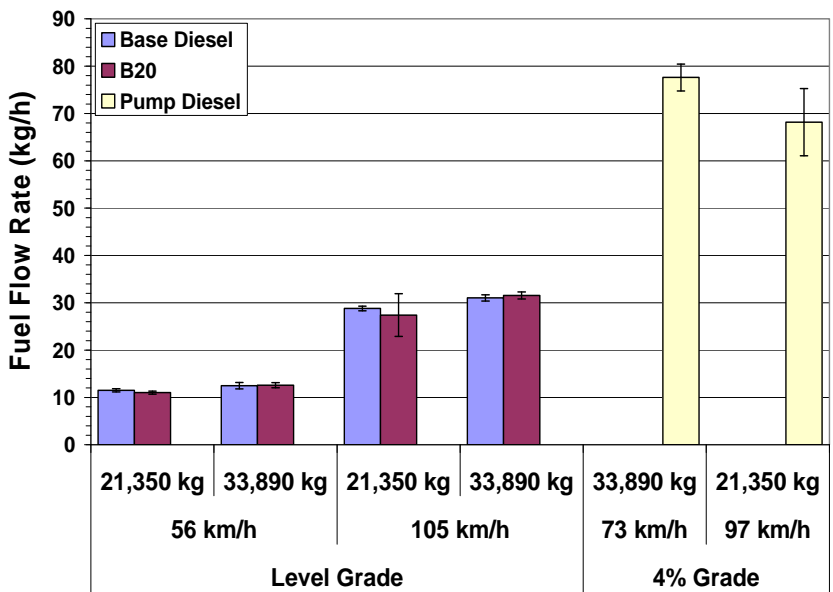
Figure 7-4.   Effects of Driving Condition and Fuel Type on Fuel Consumption

The correlation between fuel consumption and truck power demand was investigated as shown in Figure 7-5. When the fuel flow rates obtained from various experimental conditions were plotted against truck power demand, a second order polynomial equation (7-1) with a correlation coefficient greater than 0.998 was obtained. It demonstrated that the fuel feed rate was closely correlated to the truck power demand regardless of fuel type.
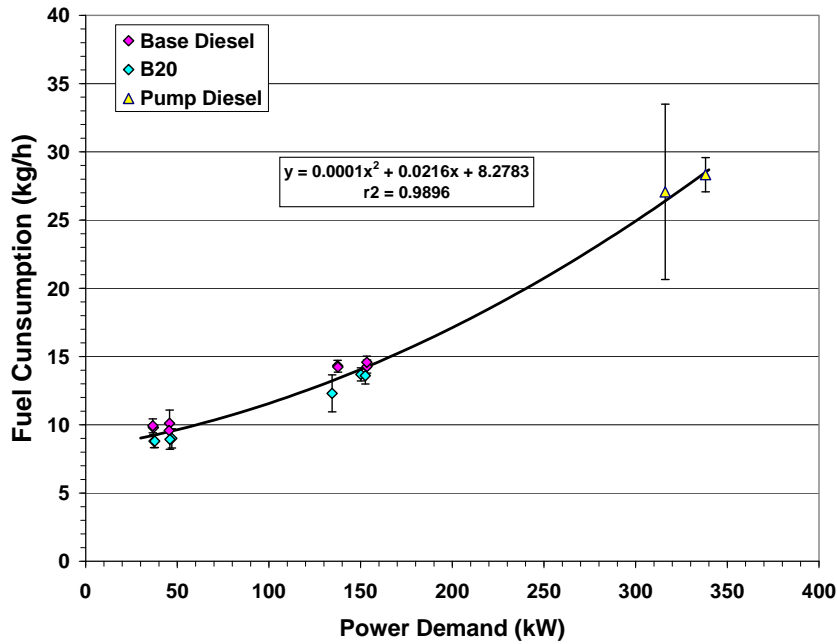
Figure 7-5.   Relationship of Fuel Consumption with Truck Power Demand

$$F_{fuel} = 6.0791 + 0.1311 P_{RL} + 0.0002 P_{RL}^{\,2} \tag{7-1}$$

where

F_{fuel} = fuel consumption, kg/h, and

P_{RL} = truck road load power, kW.

The intercept of 6.0791 kg/h in the equation (7-1) might be attributable to the fuel consumption by truck idle and ancillary loads, such as the air conditioner, etc. (Brodrick et al. 2004)

The close correlation between the observed fuel consumption and power demand explains why the truck speed had a substantial impact on fuel consumption. This is because road load power is dominated by truck speed as described previously in Equations 6-24 and 6-26.

Similar effects were also observed for the exhaust flow rate. Figure 7-6 presents the exhaust flow rate data under different experimental conditions as calculated by Equation 6-9 from the results of the SAE equation (Equation 6-3). The figure again shows that, as expected, the exhaust flow rate was directly related to truck speed and road grade. It is expected that the experimental

conditions should also have a similar relationship to exhaust flow as was the case for fuel consumption because more fuel requires more volume of combustion air which, in turn, produces more volume of exhaust.
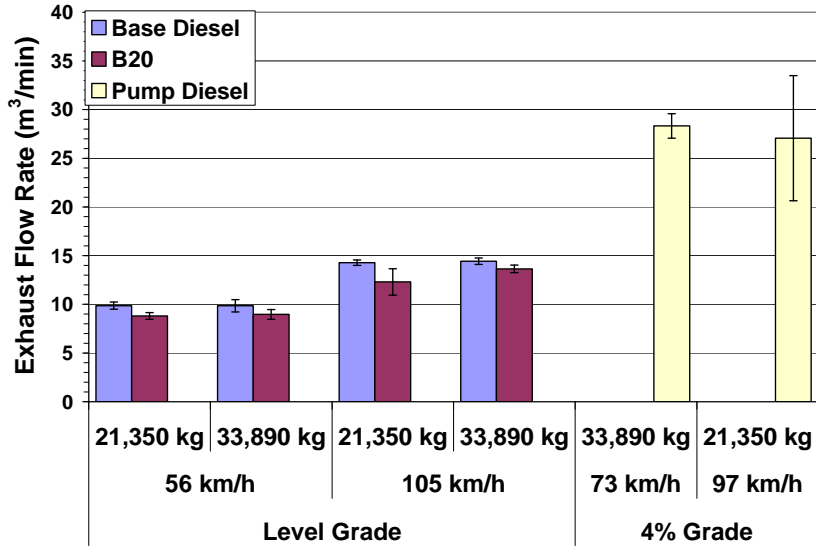
Figure 7-6.   Effects of Test Conditions on Exhaust Flow Rate

As with fuel consumption, the exhaust flow rate was found to be only slightly affected by fuel type. The B20 produced relatively less exhaust flow than the base fuel. For the unloaded truck, the exhaust flow rate from the base fuel was 10% to 15% higher than that of the B20. When the GVW increased to 33,890 kg, the impact of fuel type lessened, and the base fuel produced only about 5% to 10% more exhaust. The relatively lower exhaust flow rate from the use of B20 is probably caused by slight differences in fuel properties affecting engine operation. If the relatively small influence of fuel type is neglected, the exhaust flow rate can be plotted as a function of truck power demand as demonstrated in Figure 7-7.
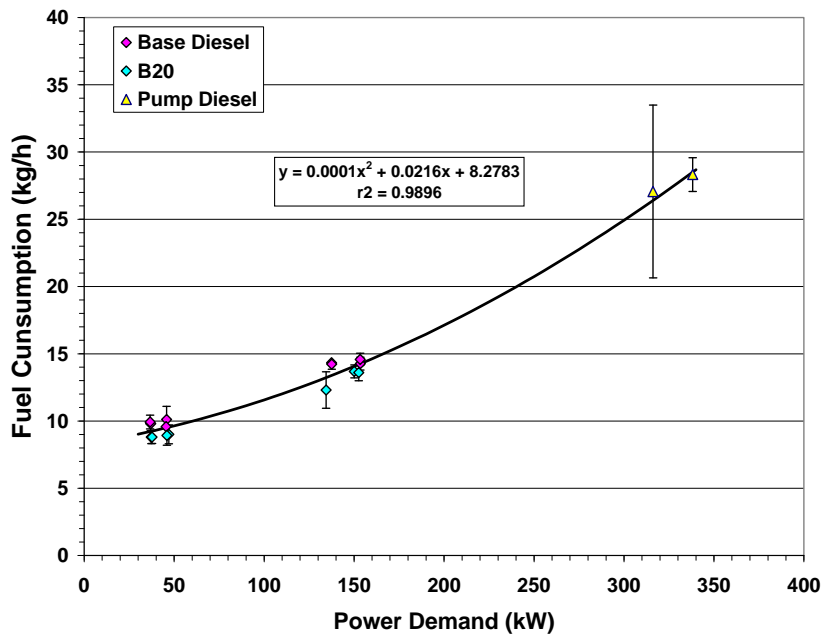
Figure 7-7.   Correlation of Exhaust Flow Rate with Truck Power Demand

This figure shows that the exhaust flow rate under the steady state experimental conditions can be approximated from the power demand by Equation 7-2.

$$Q = 8.2783 + 0.0216 P_{RL} + 0.0001 P_{RL}{}^2 \tag{7-2}$$

where

Q = exhaust flow rate, m^3/min, and

P_{RL} = road load power, kW.

The exhaust flow rate data calculated from the annubar measurements were compared to the data obtained from the SAE calculation as shown in Figure 7-8. The plot of the results shows a correlation coefficient of $r^2 = 0.931$ between the results obtained by the two methods. The intercept of 2.4747 in the correlation equation probably represents a systematic error existing in the annubar measurement. It seems that the annubar overestimated the exhaust flow rate for all the tests. As discussed previously, the exhaust gas velocity fluctuated with run time. In addition, the radial distribution of gas velocity across the exhaust pipe makes it difficult to accurately determine the flow rate from the velocity measurement. Thus, the annubar measurement for exhaust flow rate has relatively greater uncertainty than the method recommended by SAE.
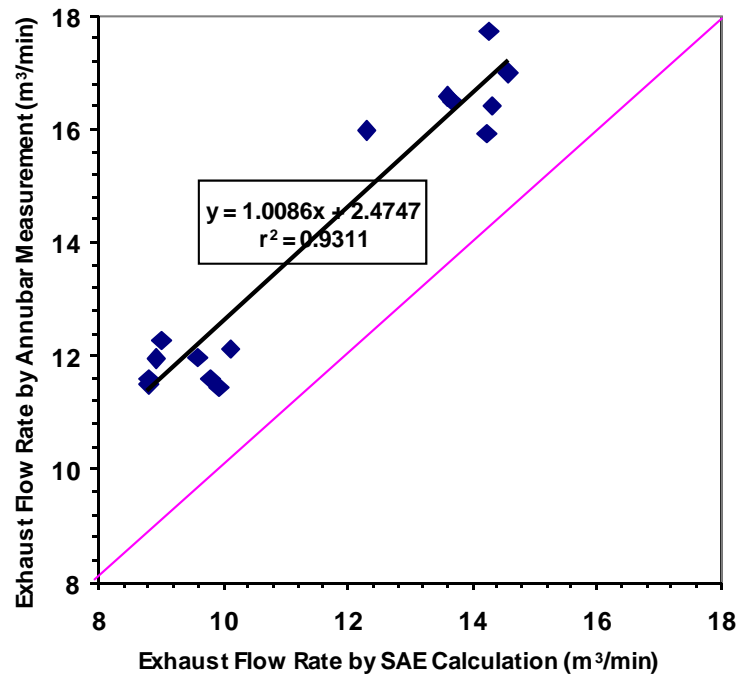
Figure 7-8.   Comparison between Annubar Meter Measurement and SAE ARP 1533 Calculation

Chapter 8
Gaseous Emissions

The gaseous emissions monitored in the truck exhaust include NO_X, CO, and THC. To characterize the emission behavior under different experimental conditions, the fuel-specific emission factor for each pollutant was calculated every second from the gaseous pollutant concentrations using Equations 6-3 to 6-6 and the emission rate and distance-specific emission factor were calculated using Equations 6-19 and 6-20. The pass-averaged and test-averaged fuel-specific emission factor, distance-specific emission factor, and emission rate and their uncertainties were then calculated for individual passes and tests. The results are used in the following discussions of the effects of experimental conditions on these gaseous emissions.

8.1 NO_X Emissions

The test-average NO_X fuel-specific emission factors, emission rates, and distance-specific emission factors and their corresponding standard deviations (SDs) obtained in this study are summarized in Table 8-1. The relative standard deviation (RSD) of the fuel-specific emission factor for each test is also included as a measure of the data quality, indicating that the measurement of NO_X emission data for this study are generally satisfied with an average RSD of 2.79%. For the level road test results, the RSDs are all below 0.1%. The road grade tests has a RSD ranging from 1% to 2.5%.

The effects of the experimental conditions on NO_X fuel emission factor, emission rate, and distance-specific emission factor observed in this study are illustrated in Figure 8-1. The figure shows that all three measures of NO_X emissions increase significantly with truck speed and road grade. However, the changes in truck gross weight and fuel type were found to have less impact on NO_X emissions.

Figure 8-1 shows that fuel type did not have a major effect on the NO_X fuel-specific emission factor when the truck was loaded (33,890 kg) and ran at higher speed (105 km/h). However, using B20 reduced the fuel-specific emission factor by about 9% from the base fuel condition when the loaded truck was running at 56 km/h. For the unloaded truck (21,350 kg) at low speed (56 km/h), the switch from base fuel to B20 reduced the fuel-specific NO_X emission factor by about 12%; whereas a 5% decrease in NO_X was observed when the unloaded truck was traveling at 105 km/h.

The NO_X emissions were strongly affected by truck speed. For the unloaded truck (GVW = 21,350 kg), the fuel-specific emission factor increased by 40% for the base fuel and by 44% for B20 when the truck speed was increased from 56 km/h to 105 km/h. For the loaded truck (GVW = 33,890 kg), the increase in fuel-specific emission factor at higher truck speeds was found to be about 48% for the base fuel and 53% for the B20 as the truck speed increased from 56 to 105 km/h.

Table 8-1.   Test Average Emission Factors and Rates for NO$_X$

Test No.	EF[a] (g/kg fuel)			ER[b] (g/s)		EM[c] (g/km)[d]		P$_{RL}$[e]
	Ave	SD	RSD (%)	Ave	SD	Ave	SD	kW
T5	21.99	0.19	0.87	0.189	0.006	6.35	0.20	153.50
T6	21.48	0.19	0.90	0.186	0.006	6.23	0.20	153.37
T7	12.30	0.61	4.92	0.044	0.004	2.72	0.27	45.76
T8	10.26	0.25	2.45	0.034	0.002	2.13	0.14	45.54
T9	13.97	0.50	3.59	0.045	0.002	2.77	0.15	36.95
T10	13.56	0.51	3.75	0.043	0.002	2.66	0.14	36.65
T11	22.60	0.14	0.63	0.183	0.005	6.13	0.16	137.46
T12	22.96	0.14	0.62	0.182	0.004	6.11	0.15	137.59
T13	21.72	0.16	0.73	0.166	0.018	5.92	0.61	134.42
T14	21.74	0.22	1.01					135.49
T15	13.57	0.44	3.27	0.042	0.002	2.57	0.14	37.27
T16	10.71	0.23	2.16	0.033	0.001	1.98	0.09	37.73
T17	10.27	0.47	4.61	0.037	0.003	2.22	0.17	47.04
T18	10.29	0.42	4.04	0.035	0.003	2.17	0.16	45.99
T19	21.67	0.15	0.68	0.186	0.006	6.31	0.21	150.13
T20	22.47	0.16	0.73	0.201	0.007	6.78	0.24	152.55
T21	22.54	2.44	10.81	0.435	0.066	16.24	2.60	316.15
T22	23.98	1.07	4.47	0.514	0.029	25.45	1.79	338.12
Average[f]			2.79					

a. EF = fuel-specific emission factor.

b. ER = emission rate.

c. EM = distance-specific emission factor.

d. 1 g/mi = 0.621 g/km.

e. P$_{RL}$ = road load power.

f. arithmetic average.
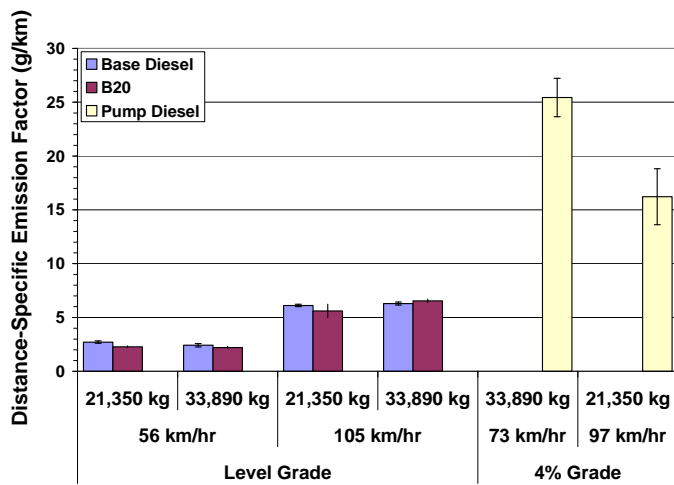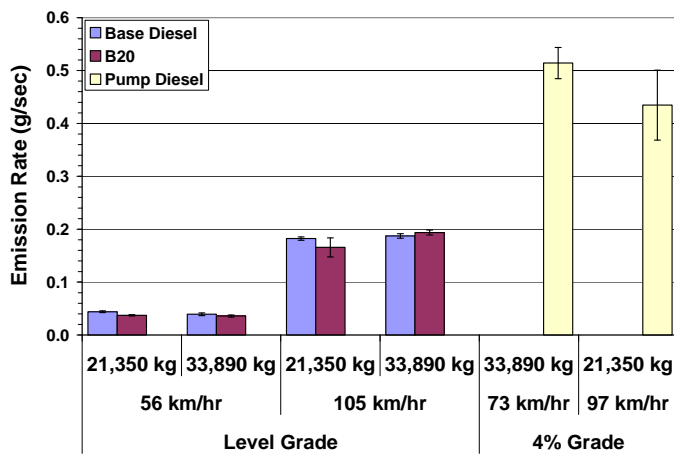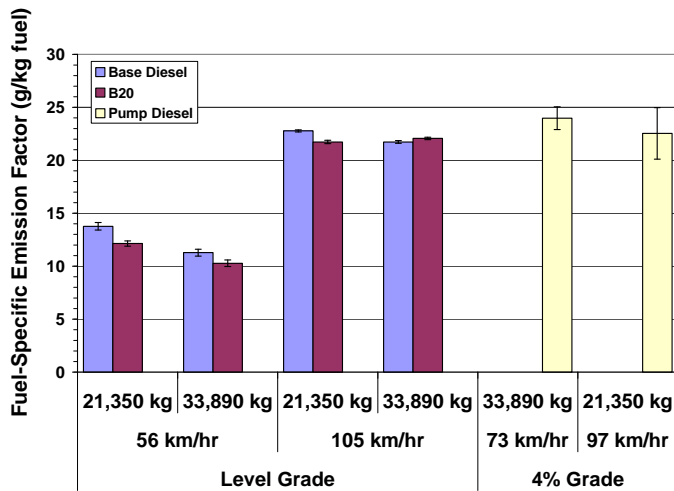
Figure 8-1.   Effects of Experimental Conditions on NO$_X$: Fuel-Specific Emission Factor (top); Emission Rate (center); and Distance-Specific Emission Factor (bottom)

The truck GVW had less effect on NO_X emissions at the same speed. Compared to the unloaded condition, increasing GVW from 21,350 to 33,890 kg reduced the NO_X fuel-specific emission factor at 56 km/h by 18% for the base fuel and by 15% for B20. At 105 km/h, the truck load had no significant impact on the emission factor.

Determination of the road grade effect on NO_X emissions in this study is difficult because tests were conducted with different fuels, on only two road grades, and the truck speeds on the steeper grade did not match those on the level road. However, as expected, a general trend shows that the truck always produces more NO_X emissions when running on a road with a higher grade than on a level road.

By comparing Figure 8-1 with Figures 7-5 and 7-7, quite similar trends were found on how the experimental conditions affected the NO_X emission rate, fuel consumption, and exhaust flow rate. This implies that, just like fuel consumption and exhaust flow, a correlation between the NO_X emission rate and truck power demand may exist regardless of the type of fuel used, as shown by Figure 8-2. Figure 8-2 is a plot of NO_X emission rate with truck power demand, showing that, within the experimental conditions of this study, the NO_X emission rate can be correlated (with a correlation coefficient of 0.991) to truck power demand by linear Equation 8-1.
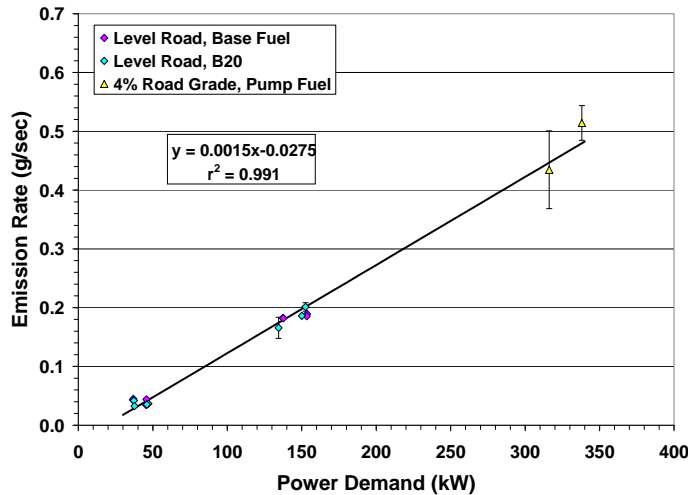
Figure 8-2.   Correlation between NO_X Emission Rate and Power Demand

$$ER_{NOx} = -0.0275 + 0.0015 P_{RL}$$

(8-1)

where

ER_{NOx} = NO_X emission rate (g/sec), and

P_{RL} = road load power, kW

The linear correlation of NO_X with power demand is consistent with that found by a number of previous investigations (Yanowitz et al., 2000; Ramamurthy et al., 1998; Brown et al., 2002).

A three-way analysis of variance (ANOVA) with two replicate tests for each factor was used to further analyze the effects of three parameters (fuel type, vehicle speed, and GVW) and their interactions in the level road tests on the NO_X fuel-specific emission factor. Table 8-2 is a summary of the analysis results, indicating that, within the range of experimental conditions, truck speed is the parameter most affecting the NO_X emission factor, with a descriptive level of significance (DLS) less than 0.0001. The second important factor is GVW with a DLS of 0.0251, which is followed by the interaction between speed and GVW at DLS = 0.0834, and then fuel type at DLS of 0.1075. The other parameters have little impact on the NO_X emission factor, and their impacts are considered to be within experimental error.

Table 8-2.   Three-Way ANOVA Results for NO_X Fuel-Specific Emission Factor

Source	SS^a	df^b	MS^c	F^d	$Pr > F^e$
Fuel	2.7781	1	2.778	3.285	0.1075
Speed	417.1940	1	417.194	493.284	0.0000
GVW	6.3892	1	6.389	7.554	0.0251
Fuel × Speed	0.9213	1	0.921	1.089	0.3271
Speed × GVW	3.3058	1	3.306	3.909	0.0834
Fuel × GVW	1.0139	1	1.014	1.199	0.3054
Fuel × Speed × GVW	0.1443	1	0.144	0.171	0.6904
Error	6.7660	8	0.846		
Total	**438.5126**	**15**			

a. SS = sum of squared measurement deviations from the overall mean..

b. df = degrees of freedom (for each source, number of parameters considered –1).

c. MS = SS/dt.

d. F = ratio of MS of the source to MS of the error.

e. Pr = probability of obtaining an F value equal to or greater than the calculated F (= DLS).

8.2   CO Emissions

The results of emission factors and emission rate obtained in this study for CO emissions are presented in Table 8-3. The table shows that the RSD for the test average CO fuel-specific emission factor was in the range of 5% to 11% for the level road tests and 30% to 80% for the tests at 4% road grade, indicating that the CO emission measurement had greater uncertainty than the NO_X measurement.

The effects of test conditions on the truck CO emissions are summarized in Figure 8-3. The error bars in the figure are the uncertainties in the results observed from the tests, indicating that the uncertainties in the CO emissions results are generally greater than in the NO_X emissions measurements.

Table 8-3.   Test Average Emission Factors and Emission Rates for CO

| Test No.	EF[a] (g/kg fuel)			ER[b] (g/s)		EM[c] (g/km)[d]		P_{RL}[e]
	Ave	SD	RSD (%)	Ave	SD	Ave	SD	kW
T5	1.54	0.11	7.1	0.013	0.001	0.44	0.03	153.50
T6	1.39	0.11	7.7	0.012	0.001	0.40	0.03	153.37
T7	6.62	0.74	11.3	0.024	0.003	1.46	0.20	45.76
T8	7.35	0.80	10.9	0.025	0.003	1.52	0.19	45.54
T9	8.11	0.67	8.3	0.026	0.002	1.60	0.15	36.95
T10	8.92	0.74	8.3	0.028	0.003	1.75	0.16	36.65
T11	2.32	0.12	5.3	0.019	0.001	0.63	0.04	137.46
T12	2.25	0.13	5.6	0.018	0.001	0.60	0.04	137.59
T13	2.05	0.12	5.7	0.014	0.002	0.46	0.06	134.42
T14	1.94	0.16	8.1					135.49
T15	7.27	0.58	7.9	0.022	0.002	1.37	0.12	37.27
T16	8.06	0.62	7.7	0.024	0.002	1.49	0.13	37.73
T17	6.28	0.59	9.5	0.022	0.003	1.36	0.16	47.04
T18	6.50	0.67	10.3	0.022	0.003	1.37	0.17	45.99
T19	1.70	0.10	5.9	0.015	0.001	0.49	0.03	150.13
T20	1.34	0.11	8.5	0.012	0.001	0.40	0.04	152.55
T21	4.52	3.60	79.7	0.082	0.066	0.77	0.20	316.15
T22	2.13	0.63	29.5	0.046	0.013	2.27	0.68	338.12
Average[f]			**13.2**					

a. EF = fuel-specific emission factor.

b. ER = emission rate.

c. EM = distance-specific emission factor.

d. 1 g/mi = 0.621 g/km.

e. P_{RL} = road load power.

f. arithmetic average.
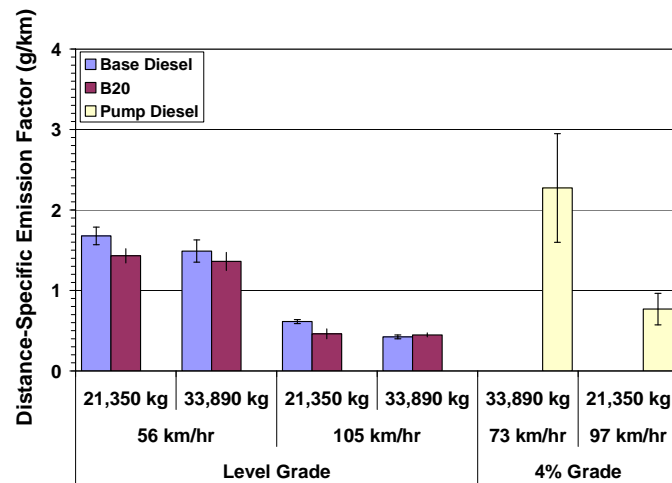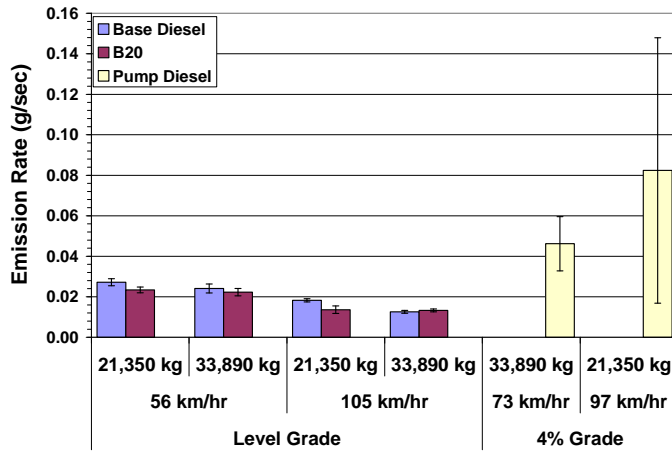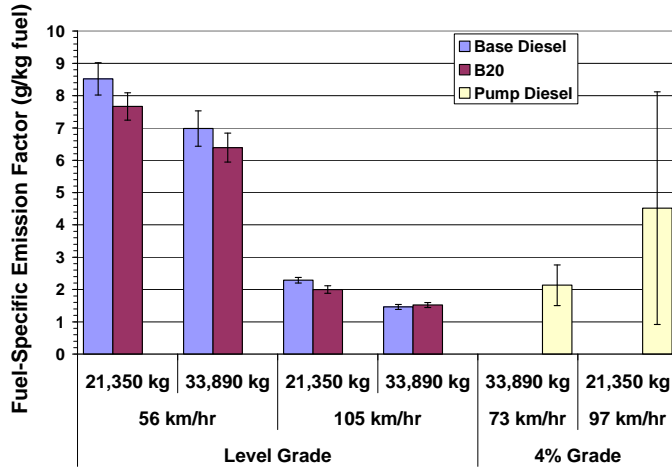
Figure 8-3. Effects of Experimental Conditions on CO: Fuel-Specific Emission Factor (top); Emission Rate (center); and Distance-Specific Emission Factor (bottom)

It can be seen from Figure 8-3 that the CO emissions were inversely related to truck speed. The CO fuel-specific emission factor decreased as the truck speed increased. For the unloaded truck, the CO fuel-specific emission factor was reduced by 73% for the base fuel and 74% for the B20 when the truck speed was increased from 56 to 105 km/h. A similar trend in the CO emission factor was found for the loaded truck as well. The increase in the truck speed from 56 to 105 km/h reduced the CO fuel-specific emission factor by 79% for the base fuel and by 76% for the B20. Since CO is formed by incomplete combustion, the reduction in CO emissions indicates that more compete fuel combustion was reached when the truck operated at the higher speed.

In comparison to the truck speed, the GVW appeared to have relatively less, but still notable, influence on the CO emissions. At the lower truck speed (56 km/h), the CO fuel-specific emission factor was reduced by 17–18% for both fuels as the truck GVW increased from 21,350 to 33,890 kg. When the DEAL was running at the higher speed (105 km/h), the CO reduction was higher for increased GVW: 36% reduction for the base fuel and 24% reduction for the B20.

The effect of fuel type on the CO emission factor was small. About a 10% reduction in the CO emission factor was observed when using B20 and the truck was unloaded. For the loaded truck, the fuel type showed little effect on the CO emissions.

When the CO fuel-specific emission factor is plotted against the power demand, as shown in Figure 8-4, it is seen that, unlike NO_X emission rate vs. power in Figure 8-2, the emission factors for the 4% road grade tests can be more than twice those seen at level grade for the same power demand and thus cannot be included in the level road regression. The figure shows that, for the level road tests, the relationship between the CO fuel-specific emission factor and the truck power demand can be expressed by linear correlation Equations 8-3 and 8-4 for the base fuel and B20, respectively.
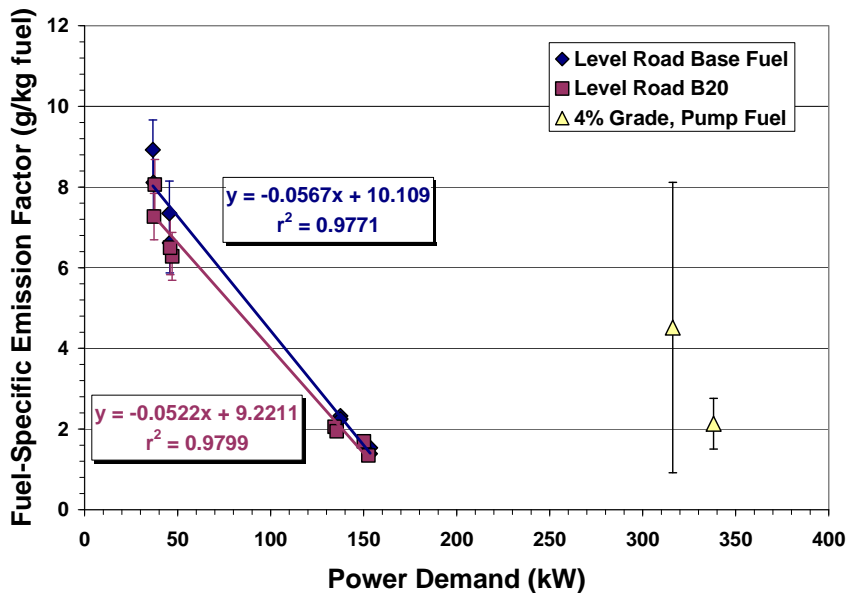
Figure 8-4.   Correlation between CO Fuel-Specific Emission Factor and Power Demand

For base fuel:

$$EF_{CO} = 10.109 - 0.0567P_{RL} \qquad (8\text{-}3)$$

For B20:

$$EF_{CO} = 9.2211 - 0.0522P_{RL} \qquad (8\text{-}4)$$

where

EF_{CO} = CO Fuel specific emission factor, g/kg fuel, and

P_{RL} = road load power, kW.

The correlation coefficients for the above two equations are 0.977 and 0.978, respectively. The comparison of the above two equations indicates that the truck will emit less CO if it switches from base fuel to B20 while the other test conditions remain unchanged. However, driving conditions and road grade will have greater impact on the CO emissions. It should be noted that Equations 8-3 and 8-4 are only valid within the experimental conditions of this study. Because of the limited number of test conditions, caution must be exercised when extrapolation of the results is needed. The data under the 4% road grade conditions are not correlated because of limited number of available data points.

As with NO_X, the level road test data for CO were analyzed by three-way ANOVA to investigate the importance of the test parameters on the CO fuel-specific emission factor. The results are summarized in Table 8-4. It can be seen from the table that both truck speed and GVW play very important roles in affecting the CO emissions. The DLS is less than 0.0001 for the truck speed and is 0.0004 for the GVW. The next important parameter is fuel type, which has a DLS of 0.0469. The interaction between speed and GVW also affects the CO emissions with DLS = 0.0679. The rest of factors in the table have DLS greater than 0.1 and, therefore, are considered that their contributions to the CO emissions are within the experimental errors.

Table 8-4.   Three-way ANOVA Results for CO Fuel-specific Emission Factor

Source	SS[a]	df[b]	MS[c]	F[d]	Pr > F[e]
Fuel	0.701332	1	0.701	5.508	0.0469
Speed	124.21187	1	124.212	975.584	0.0000
GVW	4.2331298	1	4.233	33.248	0.0004
Fuel x Speed	0.3708697	1	0.371	2.913	0.1263
Speed x GVW	0.5666887	1	0.567	4.451	0.0679
Fuel x GVW	0.0920397	1	0.092	0.723	0.4199
Fuel x Speed x GVW	0.0017843	1	0.002	0.014	0.9087
Error	1.0185646	8	0.127		
Total	**131.19628**	**15**			

a. SS = sum of squared measurement deviations from the overall mean.
b. df = degrees of freedom (for each source, number of parameters considered –1).
c. MS = SS/dt.
d. F = ratio of MS of the source to MS of the error.
e. Pr = probability of obtaining an F value equal to or greater than the calculated F (= DLS).

8.3   THC Emissions

All the test-average THC emission factors and emission rates determined in this study are summarized in Table 8-5. The RSD values in this table for all the test-average THC fuel-specific emission factors range from 2% to 11%, with an overall average of 6.1%, indicating that the THC measurements in this study were better than the CO measurements, though not as good as the NO_X monitoring.

Table 8-5.   Test Average Emission Factors and Emission Rates for THC

Test No.	EF[a] (g/kg fuel)			ER[b] (g/s)		EM[c] (g/km)[d]		P$_{RL}$[e]
	Ave	SD	RSD (%)	Ave	SD	Ave	SD	kW
T5	1.11	0.04	3.20	0.0096	0.0004	0.32	0.01	153.50
T6	1.13	0.03	3.05	0.0098	0.0004	0.33	0.01	153.37
T7	5.20	0.58	11.17	0.0186	0.0025	1.15	0.16	45.76
T8	5.65	0.60	10.59	0.0189	0.0023	1.17	0.14	45.54
T9	5.56	0.43	7.78	0.0178	0.0016	1.10	0.10	36.95
T10	6.53	0.48	7.32	0.0207	0.0017	1.28	0.11	36.65
T11	1.35	0.03	2.08	0.0109	0.0004	0.37	0.01	137.46
T12	1.42	0.03	2.18	0.0113	0.0004	0.38	0.01	137.59
T13	1.13	0.02	2.15	0.0083	0.0009	0.28	0.03	134.42
T14	1.15	0.06	5.12					135.49
T15	4.18	0.29	7.04	0.0128	0.0010	0.79	0.06	37.27
T16	5.77	0.44	7.63	0.0175	0.0015	1.06	0.09	37.73
T17	3.74	0.35	9.32	0.0133	0.0015	0.81	0.09	47.04
T18	4.99	0.49	9.80	0.0170	0.0020	1.05	0.12	45.99
T19	1.08	0.03	2.65	0.0093	0.0004	0.32	0.01	150.13
T20	1.00	0.05	4.98	0.0089	0.0005	0.30	0.02	152.55
T21	1.01	0.06	6.31	0.0201	0.0033	0.74	0.13	316.15
T22	0.87	0.07	7.65	0.0186	0.0016	0.92	0.09	338.12
Average[f]			6.11					

a. EF = fuel-specific emission factor.
b. ER = emission rate.
c. EM = distance-specific emission factor.
d. 1 g/mi = 0.621 g/km.
e. P$_{RL}$ = road load power.
f. arithmetic average.

In this study, the test conditions showed similar effects on THC emissions, shown in Figure 8-5, as was the case for CO emissions, which can be seen by comparing Figure 8-5 with Figure 8-3. It was found that truck speed exhibited significant impact on THC emissions. As the truck speed increased from 56 to 105 km/h, the THC fuel-specific emission factor for the unloaded truck was reduced by 77% when using either base fuel or B20.
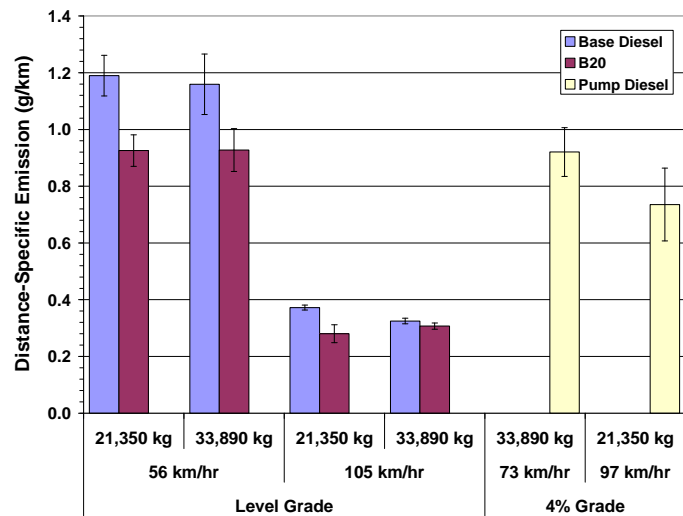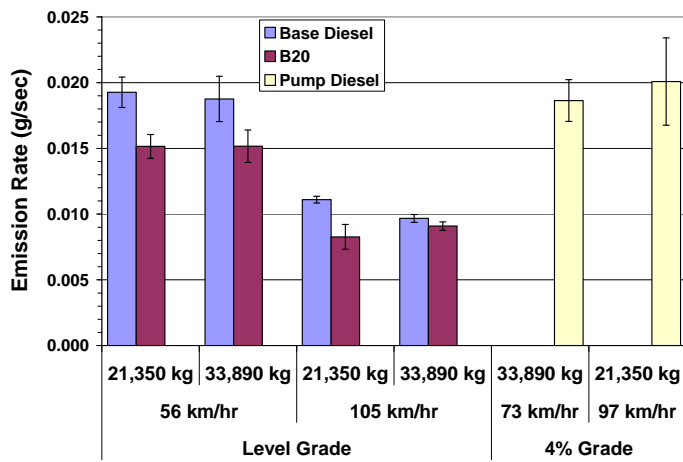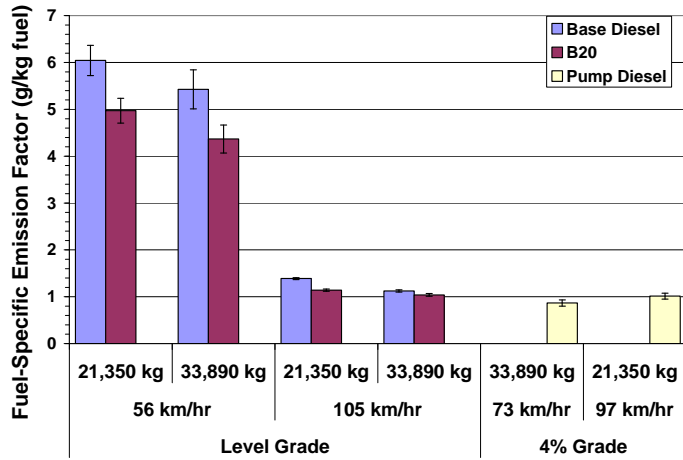
Figure 8-5.   Effects of Test Conditions on THC: Fuel-specific Emission Factor (top); Emission Rate (center); Distance-Specific Emission Factor (bottom)

When the truck was loaded (GVW = 33,890 kg), the reduction in the THC emission factor by increasing truck speed was 79% for the base fuel and 76% for B20.

Truck load was found to have less impact than speed on THC emissions. Under the base fuel condition, the THC fuel-specific emission factor was reduced by only 10% at a speed of 56 km/h when the truck GVW was increased from 21,350 to 33,890 kg. At 105 km/h, this reduction increased to 19%. For the B20, the reduction in THC emission factor by the GVW increase was 12% at 56 km/h and 9% at 105 km/h.

The benefit of using B20 as truck fuel in reducing THC emissions was also observed. A reduction of 18% in the THC fuel-specific emission factor was achieved by switching fuel from base diesel to B20 for the unloaded truck regardless the truck speed. For the loaded truck, the THC emission factor reduction by use of B20 was 20% at 56 km/h but dropped to a 7% decrease in THC emissions at 105 km/h. Figure 8-5 also indicates that the road grade has little influence on the THC fuel-specific emission factor.

Figure 8-6 shows that, when the THC fuel-specific emission factor data obtained from the level road tests were plotted against the truck power demand, straight lines were obtained separately for base fuel and B20 as presented by the Equations 8-5 and 8-6.
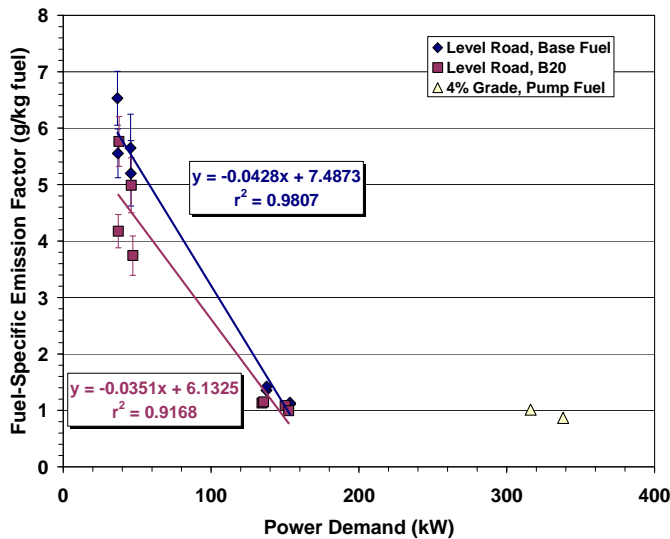
Figure 8-6.   Correlation between THC Fuel-Specific Emission Factor and Power Demand

For the base fuel:

$$EF_{THC} = 7.4873 - 0.0428 P_{RL} \qquad\qquad (8\text{-}5)$$

For B20:

$$EF_{THC} = 6.1325 - 0.0351 P_{RL} \qquad\qquad (8\text{-}6)$$

where

EF_{THC} = THC fuel specific emission factor, g/kg fuel, and

P_{RL} = road load power demand, kW.

The above correlation equations indicate that THC emissions will reduce as the truck power demand is increased, and B20 produces about 20% less THC emissions in comparison to the base fuel. However, the effectiveness in reducing THC emissions by using B20 is gradually reduced as the truck power demand is increased.

The three-way ANOVA was again used to investigate the importance of the test parameters on the THC fuel-specific emission factor based the level road test results. Table 8-6 presents the analysis results. The DLS for the truck speed in the table is below 0.0001, indicating that the truck speed has the greatest effect on the THC emission factor. The second important parameter that influences the THC emission factor is fuel type, which has a DLS value of 0.0638. All the other factors have the values of DLS greater than 0.1, indicating that their impacts on THC emissions are insignificant.

Table 8-6.   Three-way ANOVA Results for THC Fuel-specific Emission Factor

Source	SS[a]	df[b]	MS[c]	F[d]	Pr > F[e]
Fuel	1.516662	1	1.517	4.623	0.0638
Speed	64.928542	1	64.929	197.926	0.0000
GVW	0.629788	1	0.630	1.920	0.2033
Fuel x Speed	0.8111505	1	0.811	2.473	0.1545
Speed x GVW	0.1835844	1	0.184	0.560	0.4758
Fuel x GVW	0.0077604	1	0.008	0.024	0.8816
Fuel x Speed x GVW	0.0057069	1	0.006	0.017	0.8983
Error	2.6243531	8	0.328		
Total	**70.707547**	**15**			

a. SS = sum of squared measurement deviations from the overall mean..

b. df = degrees of freedom (for each source, number of parameters considered –1).

c. MS = SS/dt.

d. F = ratio of MS of the source to MS of the error.

e. Pr = probability of obtaining an F value equal to or greater than the calculated F (= DLS).

Chapter 9
PM-2.5 Emissions

9.1   PM Mass Emissions

The PM mass emissions from the truck in this study were characterized based on the measurement results by Teflon filter sampling, TEOM, and QCM measurements. Teflon filters were installed to collect both plume and background PM, so the PM emission factors and emission rate calculated are background corrected. For the TEOM monitoring, both the plume and background were also measured so that the background correction was made in the estimates of their emission factors and emission rates. In contrast, only the plume was monitored by the QCM, and, therefore, the emission factors calculated from the QCM data were not background corrected.

The Teflon filter gravimetric analysis data were used to calculate the fuel-specific PM mass emission factors under various test conditions. The results are presented in Table 9-1 and compared by different experimental conditions in Figure 9-1. It is interesting to see from the figure that the high emission factors obtained from Teflon filter sampling were also very high for T5 and T6, making these tests questionable. These emission factors are, however, consistent with the PM number measurement results from the ELPI discussed in the next section. Besides T5 and T6, a clear trend regarding how the test conditions affect PM mass emissions can be seen for the rest of tests. The figure shows that, by replacing the base fuel with the B20, about a 58% reduction in fuel-specific PM mass emission factor was achieved when the truck was unloaded and ran at 56 km/h. For the loaded truck, the reduction in PM emissions by switching from the base fuel to B20 was 68% at 56 km/h and 91% at 105 km/h.

As will be seen for PM number emissions in the next section, the truck speed had a major impact on the PM mass emissions. For the unloaded truck, the fuel-specific PM mass emission factor was reduced by 78% for the base fuel and 58% for B20 when the truck speed increased from 56 to 105 km/h. For the loaded truck using B20, as the truck speed increased the PM mass emission factor dropped by 76%.

The truck GVW showed less influence than vehicle speed on PM mass emissions. At 56 km/h, the loaded truck (33,390 kg) emitted 12% less PM than the unloaded truck (21,350 kg) in terms of fuel-specific mass emission factor for the base fuel and 34% less for B20.

Table 9-1.   Results of PM Mass Emissions by Teflon Filters

Test No.	EF[a] (mg/kg)			ER[b] (mg/s)			EM[c] (mg/km)		
	Total PM	Volatile	Non-Vol[d]	Total PM	Volatile	Non-Vol[d]	Total PM	Volatile	Non-Vol[d]
5	1036.5	990.4	46.1	8.91	8.52	0.40	299.4	286.0	13.3
6	707.8	628.5	79.3	6.11	5.43	0.68	205.3	182.3	23.0
7									
8	1008.9	861.0	147.9	3.38	2.89	0.50	209.0	178.4	30.7
9	1445.7	1191.0	254.7	4.65	3.83	0.82	286.4	235.9	50.4
10	852.4	615.4	236.9	2.71	1.95	0.75	167.4	120.9	46.5
11	283.3	178.5	104.8	2.29	1.44	0.85	76.8	48.4	28.4
12	219.9	117.5	102.4	1.74	0.93	0.81	58.5	31.2	27.2
13	220.7	98.9	121.9	1.68	0.75	0.93	56.9	25.5	31.4
14	188.6	70.7	117.9						
15	460.3	244.0	216.3	1.42	0.75	0.67	87.0	46.1	40.9
16	508.2	276.1	232.1	1.54	0.84	0.71	94.1	51.1	43.0
17	365.1	113.5	251.6	1.30	0.40	0.90	78.9	24.5	54.4
18	278.0	95.4	182.6	0.95	0.33	0.63	58.6	20.1	38.5
19	74.3	6.3	68.1	0.64	0.05	0.58	21.6	1.8	19.8
20	81.9	38.1	43.7	0.73	0.34	0.39	24.7	11.5	13.2

a. EF = fuel-specific emission factor.

b. ER = emission rate.

c. EM = distance-specific emission factor; 1 g/mi = 0.621 g/km.

d. Non-Vol = nonvolatile PM determined downstream of thermal denuders.
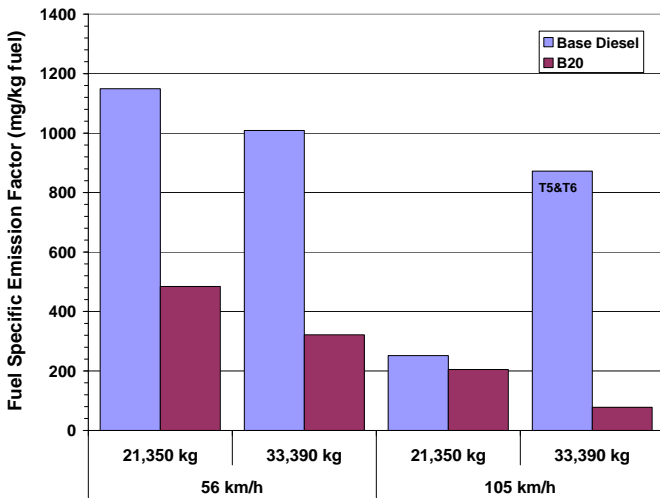
Figure 9-1.   Effects of Test Condition on Fuel-Specific Mass Emission Factor Results Based on Teflon Filter Gravimetric Analysis Data

The fuel-specific PM mass emission factor from the Teflon filter measurements are plotted as a function of truck power demand in Figure 9-2. The point identified by the red square in the figure represents the average emission factor for T5 and T6. Without accounting for T5 and T6, two straight lines were obtained from the data points of the rest of tests for base fuel and B20, respectively. Because of the unusually high Teflon emission factors obtained in T5 and T6, these tests should have been repeated but, unfortunately, this not possible due to time and resource constraints.

The three-way ANOVA was used again to further analyze the Teflon filter data for the importance of the experiment parameters used on affecting the PM mass emissions. Table 9-2 is the ANOVA results. The factors fuel type, truck speed, the interaction between speed and GVW, the interaction between fuel and GVW, and the interaction of fuel, speed and GVW all had a DLS value less than 0.1, indicating that they have significant impact on the fuel-specific PM mass emission factor.

Thermal denuders (TDs) were used in the tests to remove volatile materials in the PM emitted. As a result, the nonvolatile PM was collected on Teflon filters installed down-stream of the TDs. By comparing the gravimetric analysis results obtained from the Teflon filters with and without TDs in front, the fraction of volatile PM was calculated for individual tests. Figure 9-3 presents the percentage of volatile PM under different test conditions. It is seen that, for the base fuel, the PM emitted by the unloaded truck at 56 km/h contained 77% volatiles. As the unloaded truck speed increased to 105 km/h, the fraction of volatile PM dropped to 58%, a 25% reduction. At 56 km/h, the unloaded truck burning B20 produced 53% volatile PM, whereas the volatile content dropped to 41% when the unloaded truck was operated at 105 km/h. Both fuels show a 25% decrease in the volatile PM when the unloaded-truck speed was increased from 56 to 105 km/h. For the loaded truck, the PM volatile content actually increased slightly when the base was used whereas a small decrease was observed for B20.
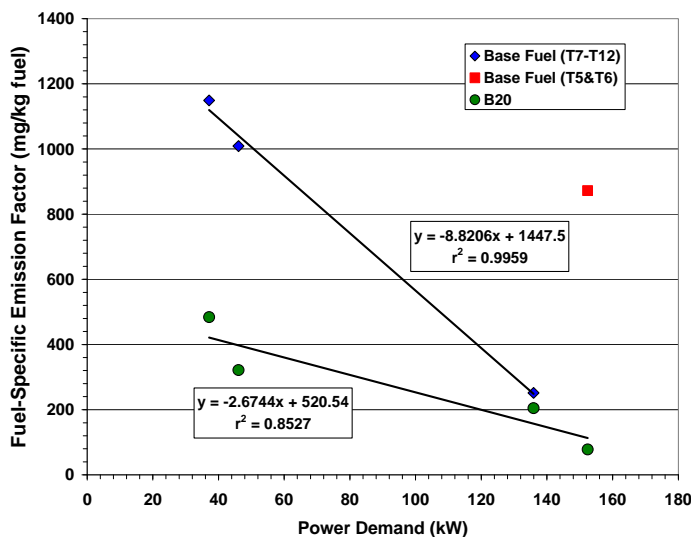
Figure 9-2.   Plot of Fuel-Specific PM Mass Emission Factor Obtained by Teflon Filters as a Function of Power Demand

Table 9-2.   Three-Way ANOVA Results for Teflon Filter PM Mass Measurements.

Source	SS[a]	df[b]	MS[c]	F[d]	Pr > F[e]
Fuel	1202530.1	1	1202530.1	40.500	0.0002
Speed	606238.4	1	606238.4	20.417	0.0020
GVW	9135.4	1	9135.4	0.308	0.5943
Fuel x Speed	65310.1	1	65310.1	2.200	0.1763
Speed x GVW	158727.6	1	158727.6	5.346	0.0495
Fuel x GVW	148115.9	1	148115.9	4.988	0.0560
Fuel x Speed x GVW	131226.9	1	131226.9	4.420	0.0687
Error	237538.5	8	29692.3		
Total	**2558822.7**	**15**			

a. SS = sum of squared measurement deviations from the overall mean.

b. df = degrees of freedom (for each source, number of parameters considered –1).

c. MS = SS/dt.

d. F = ratio of MS of the source to MS of the error.

e. Pr = probability of obtaining an F value equal to or greater than the calculated F (= DLS).
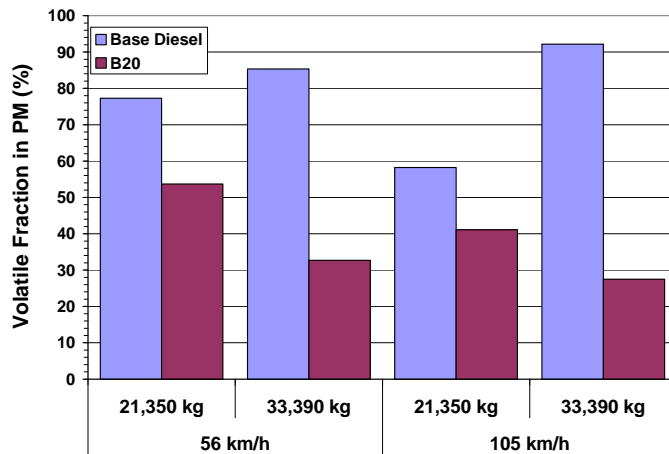
Figure 9-3.   Effects of Test Conditions on Volatile Fraction in PM Based on the Teflon Filter and Thermal Denuder Results

It was also observed that the B20 produced less volatile PM than the base fuel for all conditions. For the unloaded truck traveling at 56 km/h, the volatile PM produced by B20 was about 30% lower than that produced by the base fuel. At 105 km/h, this difference increased to more than 60%. The effects of truck GVW on the fraction of volatile PM were mixed. As the GVW increased, the base fuel showed an increase in volatile PM percentage, but the volatile PM produced by B20 decreased.

Table 9-3 summarizes the results obtained from the TEOM measurements, which, as can be seen, are much lower than the Teflon filter data presented earlier. RSD was not calculated because of the nature of fluctuation in the TEOM measurements as evidenced by the high SDs. The fuel-specific PM mass emission factors obtained from the TEOM measurement data under various test conditions are compared in Figure 9-4. The TEOM results show, as was seen from the Teflon filter data, the PM mass reduction when the truck speed was increased from 56 to 105 km/h was in the 70–80% range. The PM mass emissions also dropped as the truck gross weight increased, though it had less effect than truck speed. It should be pointed out here that the TEOM results in the figure do not show significant emissions improvement by switching from the base fuel to B20. This conflicts with the filter measurements. Since the B20 fueled truck emitted smaller sized and fewer particles as will be discussed in Section 9-2, it can be expected that there should be less PM mass emissions than the base fuel. Therefore, the TEOM results on the effect of fuel type are questionable.

Table 9-3.   Results of PM Mass Emissions by TEOM

Test No.	EF^a (mg/kg fuel)		ER^b (mg/s)		EM^c (mg/km)^d		$P_{RL}{}^e$
	Ave	SD	Ave	SD	Ave	SD	kW
T5	55.83	60.59	0.48	0.52	16.10	17.37	153.50
T6	45.59	47.01	0.39	0.40	13.14	13.49	153.37
T7	263.31	104.35	0.94	0.38	58.03	23.32	45.76
T8	190.06	89.48	0.64	0.30	39.11	18.69	45.54
T9	246.27	180.92	0.79	0.57	48.58	35.56	36.95
T10	271.82	165.09	0.86	0.52	53.23	32.32	36.65
T11	80.54	75.43	0.64	0.60	21.59	20.30	137.46
T12	68.87	72.86	0.53	0.57	17.83	19.32	137.59
T13	84.33	46.10	0.64	0.36	21.64	12.25	134.42
T14							135.49
T15	206.62	113.39	0.65	0.35	39.64	21.80	37.27
T16	347.82	104.85	1.05	0.32	64.28	19.65	37.73
T17	197.89	239.65	0.72	0.87	43.50	52.71	47.04
T18	229.61	5474.31	0.78	18.77	48.17	1159.36	45.99
T19	43.99	1459.49	0.37	12.69	12.62	431.13	150.13
T20	39.14	2299.39	0.35	19.22	11.73	647.62	152.55

a. EF = fuel-specific emission factor.

b. ER = emission rate.

c. EM = distance-specific emission factor.

d. 1 g/mi = 0.621 g/km.

e. PRL = road load power.
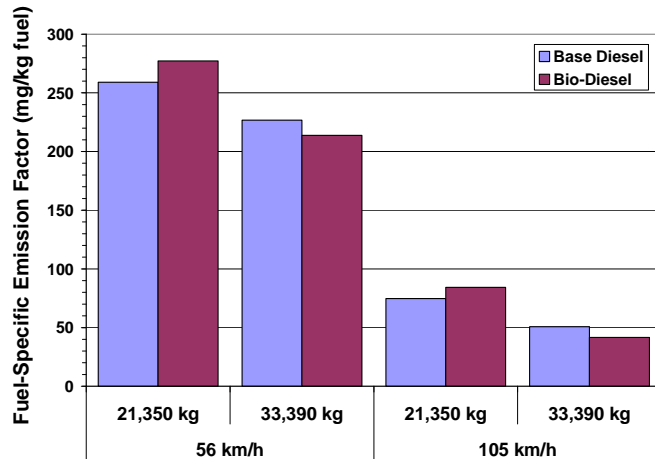
Figure 9-4. **Effects of Test Conditions on Fuel-Specific PM Mass Emission Factor Based on TEOM Measurements**

The three-way ANOVA results of the TEOM data are presented in Table 9-4. The table shows that, among all the factors considered, truck speed and GVW had the DLS less than 0.1 and played important roles in determining the PM mass emissions. This is consistent with the above quantitative discussion.

Table 9-4. **Three-Way ANOVA Results for TEOM PM Mass Measurements**

Source	SS[a]	df[b]	MS[c]	F[d]	Pr > F[e]
Fuel	8.2	1	8.2	0.005	0.9464
Speed	131547.9	1	131547.9	77.305	0.0000
GVW	6609.7	1	6609.7	3.884	0.0842
Fuel x Speed	5.7	1	5.7	0.003	0.9554
Speed x GVW	211.3	1	211.3	0.124	0.7337
Fuel x GVW	622.2	1	622.2	0.366	0.5622
Fuel x Speed x GVW	38.0	1	38.0	0.022	0.8849
Error	13613.4	8	1701.7		
Total	**152656.3**	**15**			

a. SS = sum of squared measurement deviations from the overall mean.

b. df = degrees of freedom (for each source, number of parameters considered –1).

c. MS = SS/dt.

d. F = ratio of MS of the source to MS of the error.

e. Pr = probability of obtaining an F value equal to or greater than the calculated F (= DLS).

The fuel-specific PM mass emission factors obtained by the TEOM measurement were plotted against the truck power demand as illustrated in Figure 9-5, showing the linear correlation of the PM mass emissions measured by the TEOM with the truck power demand. The fuel-specific

emission factor can be predicted approximately from the truck power demand under the steady-state experimental conditions specified in this study by the Equations 9-1 and 9-2.

For base fuel:

$$EF_M = 314.49 - 1.7322P_{RL} \tag{9-1}$$

for B20:

$$EF_M = 324.82 - 1.858P_{RL} \tag{9-2}$$

where

EF_M = fuel specific PM mass emission factor, mg/kg fuel, and

P_{RL} = road load power demand, kW.

Great uncertainty in the QCM measurements was found in this study, though the observed trends of the test conditions effecting the PM mass emissions were generally similar. The PM mass emission data measured by the TEOM were compared with those obtained by Teflon filter sampling and QCM measurements as shown in Figure 9-6. Due to the large errors in the measurements, the fuel-specific PM mass emission factors obtained from the three different sampling instruments were poorly correlated to each other for no immediately apparent reason. This is in contrast to test cell measurements conducted by Kinsey et al. (2006b) at West Virginia University, which showed a correlation coefficient of 0.93 between the TEOM and the Teflon filter results.
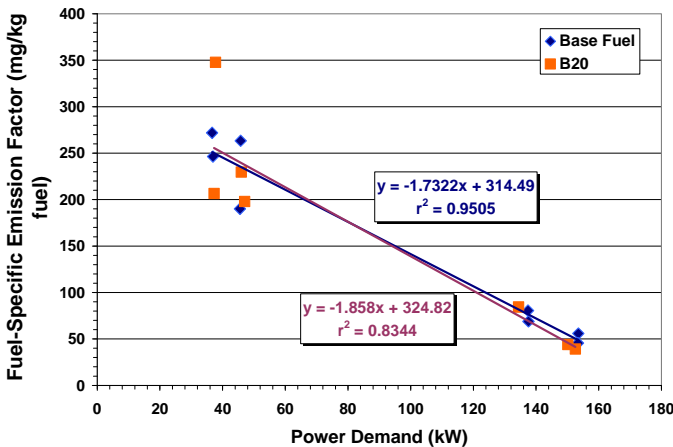
Figure 9-5. **Correlation between the TEOM Fuel-Specific PM Mass Emission Factor and the Truck Power Demand**
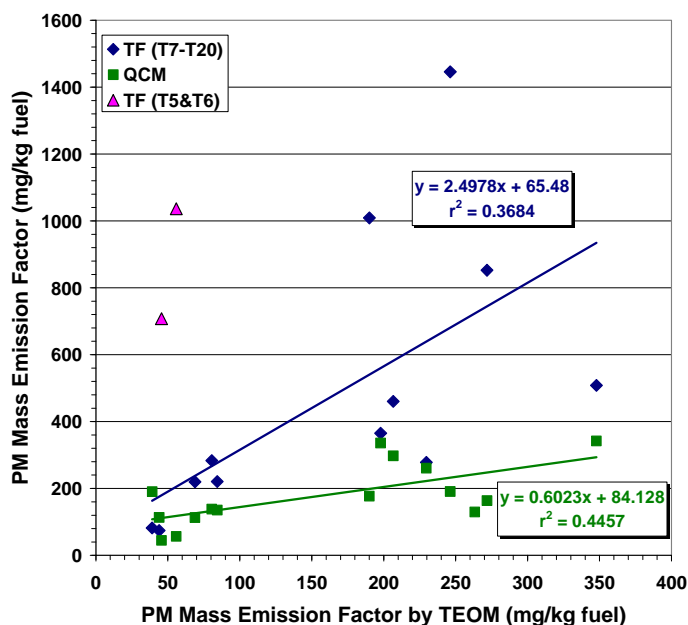
Figure 9-6. **Comparison of PM Emission Factor Results Obtained by Different Instruments**

9.2 PM Number Emissions

The fuel-specific emission factors, emission rates, and distance-specific emission factors in terms of the number of particles were calculated from the SMPS, and ELPI measurement data under different experimental conditions. PM number emissions measured by the nano SMPS are not included here because of the limited particle size range of this instrument. Since both the plume and background were monitored by both the SMPS and ELPI, their fuel-specific emission factors were calculated with background correction. Tables 9-5 and 9-6 summarize the results for SMPS and ELPI, respectively. From the tables it can be seen that the average RSD is 20% for the SMPS and 22% for the ELPI. This indicates: (1) the uncertainty in the particle number measurements was generally greater than that for the gaseous emissions measurements, and (2) the SMPS appeared to have smallest uncertainty in the results among the two PM monitoring instruments. Therefore, the discussion of the effects of test condition on PM count emissions will begin with the SMPS results followed by its comparison with the other two instruments.

The SMPS results are compared in Figure 9-7. Similar trends of the effect of experimental conditions are seen from these plots for all the three emission measures. A large emission reduction in PM number emissions was observed by increasing the truck speed regardless of whether the truck was loaded or unloaded. A reduction of about 98% in fuel-specific PM number emission factor was found for the base fuel and about 95% reduction for the B20 when the truck speed was increased from 56 to 105 km/h.

Table 9-5.   Test Average PM Particle Number Results Obtained from the SMPS

| Test No.	EF[a] (count/kg fuel)			ER[b] (count/s)		EM[c] (g/km)[d]		P$_{RL}$[e]
	Ave.	SD	RSD (%)	Ave.	SD	Ave	SD	kW
T5	5.44E+13	8.98E+12	16.5	4.68E+11	7.84E+10	1.57E+13	2.64E+12	153.50
T6	4.11E+13	6.47E+12	15.7	3.53E+11	5.60E+10	1.19E+13	1.88E+12	153.37
T7	2.38E+15	6.25E+14	26.3	8.48E+12	2.31E+12	5.24E+14	1.43E+14	45.76
T8	1.70E+15	2.67E+14	15.7	5.70E+12	9.63E+11	3.53E+14	5.98E+13	45.54
T9	3.55E+15	7.89E+14	22.2	1.14E+13	2.59E+12	7.04E+14	1.59E+14	36.95
T10	3.29E+15	6.83E+14	20.8	1.04E+13	2.21E+12	6.46E+14	1.37E+14	36.65
T11	7.56E+13	1.46E+13	19.3	6.18E+11	1.20E+11	2.08E+13	4.05E+12	137.46
T12	2.25E+13	3.81E+12	16.9	1.78E+11	3.05E+10	5.96E+12	1.03E+12	137.59
T13	1.63E+14	3.35E+13	20.6	1.24E+12	3.33E+11	4.21E+13	1.19E+13	134.42
T14								135.49
T15	3.21E+15	5.78E+14	18.0	9.95E+12	1.81E+12	6.10E+14	1.11E+14	37.27
T16	2.23E+15	3.41E+14	15.3	6.78E+12	1.06E+12	4.13E+14	6.47E+13	37.73
T17	1.77E+15	4.65E+14	26.2	6.31E+12	1.71E+12	3.83E+14	1.04E+14	47.04
T18	1.57E+15	3.08E+14	19.7	5.37E+12	1.10E+12	3.30E+14	6.80E+13	45.99
T19	6.47E+13	1.90E+13	29.3	5.40E+11	1.58E+11	1.83E+13	5.36E+12	150.13
T20	3.64E+13	6.21E+12	17.1	3.26E+11	5.80E+10	1.10E+13	1.96E+12	152.55
Average[f]			**20.0**					

a. EF = fuel-specific emission factor.
b. ER = emission rate.
c. EM = distance-specific emission factor.
d. 1 g/mi = 0.621 g/km.
e. PRL = road load power.
f. arithmetic average.

Table 9-6.   Test Average PM Particle Number Results Obtained from the ELPI

Test No.	EF[a] (count/kg fuel)			ER[b] (count/s)		EM[c] (g/km)[d]		P_RL[e]
	Ave	SD	RSD (%)	Ave	SD	Ave	SD	kW
T5	5.82E+15	8.67E+14	14.9	5.02E+13	7.60E+12	1.68E+15	2.56E+14	153.50
T6	6.50E+15	8.90E+14	13.7	5.63E+13	7.91E+12	1.89E+15	2.66E+14	153.37
T7	8.03E+15	2.33E+15	29.0	2.87E+13	8.60E+12	1.77E+15	5.32E+14	45.76
T8	7.89E+15	1.70E+15	21.6	2.64E+13	5.93E+12	1.64E+15	3.68E+14	45.54
T9	1.00E+16	2.72E+15	27.1	3.23E+13	8.84E+12	1.99E+15	5.45E+14	36.95
T10	9.97E+15	2.65E+15	26.6	3.17E+13	8.50E+12	1.96E+15	5.27E+14	36.65
T11	3.16E+14	6.31E+13	19.9	2.58E+12	5.20E+11	8.67E+13	1.75E+13	137.46
T12	1.16E+14	2.76E+13	23.8	9.20E+11	2.23E+11	3.08E+13	7.49E+12	137.59
T13	4.26E+14	1.69E+14	39.7	3.29E+12	1.39E+12	1.11E+14	4.72E+13	134.42
T14								135.49
T15	1.47E+16	3.83E+15	26.1	4.55E+13	1.19E+13	2.79E+15	7.28E+14	37.27
T16	1.36E+16	2.58E+15	19.0	4.12E+13	7.96E+12	2.51E+15	4.86E+14	37.73
T17	1.10E+16	2.45E+15	22.2	3.95E+13	9.17E+12	2.39E+15	5.57E+14	47.04
T18	1.03E+16	2.22E+15	21.5	3.51E+13	7.80E+12	2.17E+15	4.85E+14	45.99
T19	1.73E+14	2.45E+13	14.1	1.47E+12	2.18E+11	5.00E+13	7.41E+12	150.13
T20	8.03E+13	9.85E+12	12.3	7.16E+11	9.23E+10	2.41E+13	3.11E+12	152.55
Average[f]			**22.1**					

a. EF = fuel-specific emission factor.

b. ER = emission rate.

c. EM = distance-specific emission factor.

d. 1 g/mi = 0.621 g/km.

e. PRL = road load power.

f. arithmetic average.
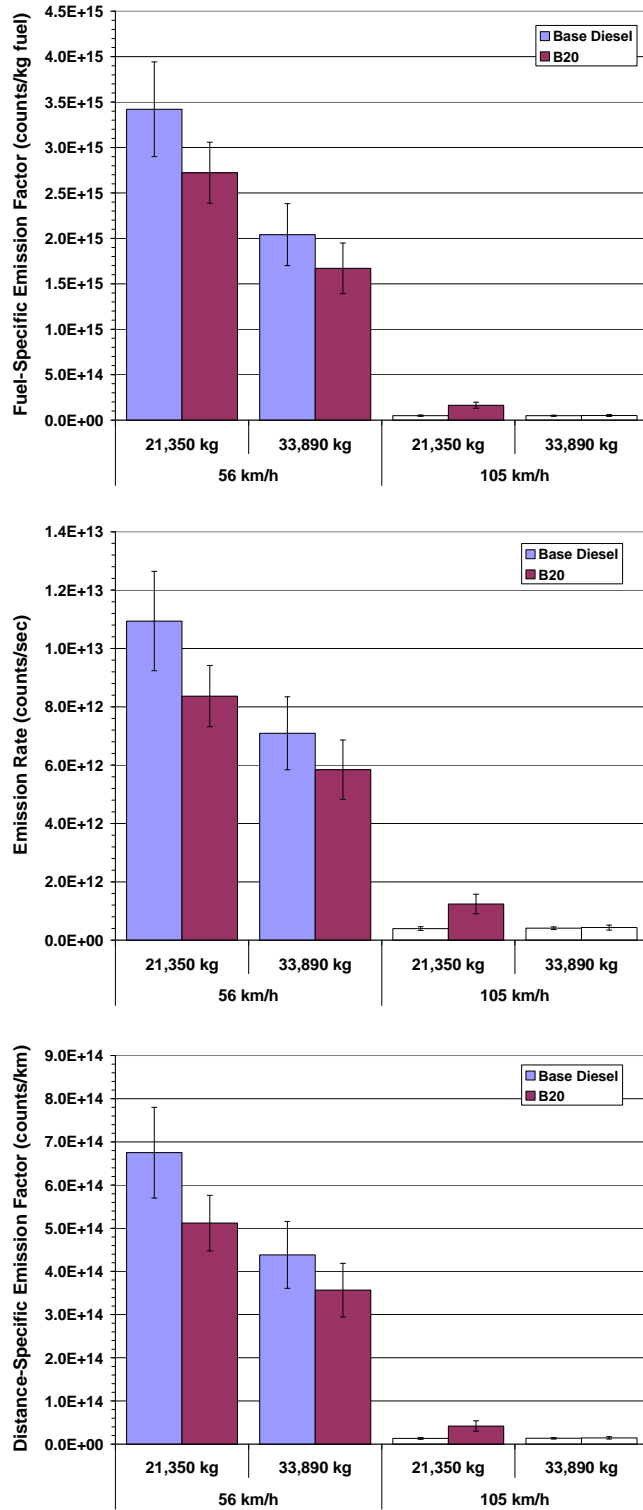
Figure 9-7. **Effects of Test Conditions on Particle Number Emissions Measured by SMPS: Fuel-Specific Emission Factor (top); Emission Rate (center); and Distance-Specific Emission Factor (bottom)**

The GVW had relatively less effect on the number of particles produced. In comparison to the unloaded truck, the fuel-specific particle number emission factor for both fuels at 56 km/h was lower by about 40% for the loaded truck. At the higher truck speed (105 km/h), the emissions were low and, therefore, the load effect was not significant.

The use of B20 showed an advantage in PM number emissions at the lower truck speed (56 km/h). An approximate 20% reduction in PM number count emissions was achieved by using B20 in comparison to the base fuel. However, at the higher truck speed, there was no notable improvement in PM number reduction observed by using B20.

The particle number emission factor results obtained from the SMPS data are plotted against truck power demand in Figure 9-8. The figure shows that the emission factors for base fuel and B20 can be correlated to the power demand separately by a power function as described in the Equations 9-3 and 9-4.

For base fuel:

$$EF_N = 4 \times 10^{20} \cdot P_{RL}^{-3.2003}$$ (9-3)

For B20:

$$EF_N = 5 \times 10^{19} \cdot P_{RL}^{-2.7189}$$ (9-4)
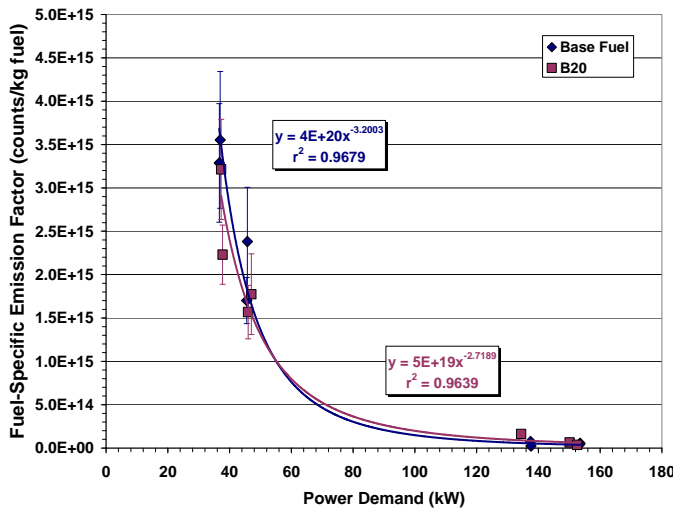
Figure 9-8.   Correlation between Fuel-Specific Particle Count Emission Factor Determined by SMPS and Truck Power Demand

The curve for B20 in the figure is slightly lower than that for the base fuel when the power demand was below 50 kW, indicating the improvement in particle number emissions by B20 under low power demand. Comparing the fuel compositions in Table 7-4, the B20 contains about

3% oxygen by weight. Adding oxygen into the fuel decreases the fuel/air equivalence ratio and promotes better combustion efficiency.

Table 9-7 is the three-way ANOVA results for the fuel-specific PM number emission factor obtained from the SMPS measurement. As indicated by the values of DLS (Pr > F) in the table, the truck speed, GVW, and their interaction are factors that had significant impact on the PM number emissions. The DLS for the factor of fuel type is greater than 0.1 because of the interference of measurement errors at the lower truck speed. The ELPI ANOVA results presented in Table 9-8 show the same trend. The interactions of fuel type with truck speed and with GVW all much less than 0.0001.

In order to evaluate the results from the two instruments used in this study, the test-average fuel-specific particle number emission factors obtained by the ELPI were compared with the SMPS data in Figure 9-9. The data in the figure show that the results by all instruments are basically proportional to one another except for the ELPI results for T5 and T6 (two points in the figure that are identified by red squares), which were conducted under the same test conditions: base fuel, GVW = 33,890 kg, and 105 km/h. Compared to the SMPS, the ELPI recorded much higher PM number concentrations for T5 and T6, which is consistent with the Teflon filter results. Because of the apparent anomaly between the T5 & T6 runs and the rest of the data set, T5 and T6 should have been repeated, which was not possible due to resource limitations.

Table 9-7.   Three-way ANOVA Results for Fuel-specific PM Number Emission Factor by the SMPS

Source	SS[a]	df[b]	MS[c]	F[d]	Pr > F[e]
Fuel	2.27E+29	1	2.27E+29	2.345	0.1642
Speed	2.28E+31	1	2.28E+31	235.519	0.0000
GVW	1.62E+30	1	1.62E+30	16.744	0.0035
Fuel x Speed	3.52E+29	1	3.52E+29	3.637	0.0930
Speed x GVW	1.34E+30	1	1.34E+30	13.886	0.0058
Fuel x GVW	1.18E+28	1	1.18E+28	0.122	0.7360
Fuel x Speed x GVW	4.83E+28	1	4.83E+28	0.499	0.4999
Error	7.74E+29	8	9.67E+28		
Total	**2.71E+31**	15			

a. SS = sum of squared measurement deviations from the overall mean.

b. df = degrees of freedom (for each source, number of parameters considered −1).

c. MS = SS/dt.

d. F = ratio of MS of the source to MS of the error.

e. Pr = probability of obtaining an F value equal to or greater than the calculated F (= DLS).

Table 9-8. **Three-way ANOVA Results for Fuel-specific PM Number Emission Factor by the ELPI**

Source	SS[a]	df[b]	MS[c]	F[d]	Pr > F[e]
Fuel	2.48E+29	1	2.48E+29	1.760	0.2212
Speed	3.21E+32	1	3.21E+32	2273.139	0.0000
GVW	7.10E+27	1	7.10E+27	0.050	0.8281
Fuel x Speed	4.00E+31	1	4.00E+31	283.720	0.0000
Speed x GVW	3.10E+31	1	3.10E+31	219.581	0.0000
Fuel x GVW	1.46E+31	1	1.46E+31	103.859	0.0000
Fuel x Speed x GVW	5.85E+30	1	5.85E+30	41.511	0.0002
Error	1.13E+30	8	1.41E+29		
Total	**4.13E+32**	15			

a. SS = sum of squared measurement deviations from the overall mean.

b. df = degrees of freedom (for each source, number of parameters considered –1).

c. MS = SS/dt.

d. F = ratio of MS of the source to MS of the error.

e. Pr = probability of obtaining an F value equal to or greater than the calculated F (= DLS).
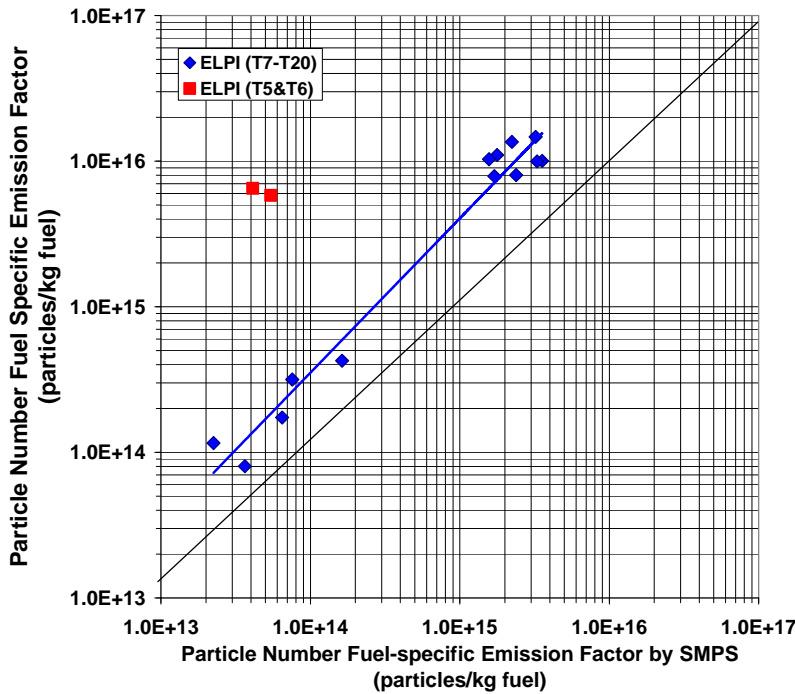
Figure 9-9. **Comparison of Fuel-Specific Particle Number Emission Factors Between Instruments**

9.3 PM Particle Size Distribution

As specified earlier, the particle size distributions (PSDs) in this study were characterized based on the results obtained from the long DMA SMPS and nano SMPS. Also note that the nano SMPS results are of interest only for particle sizes less than 100 nm due to its effective operating range.

In order to investigate the effects of fuel type, truck speed, and truck GVW, the PSDs under the different experimental conditions in this study were expressed and compared by plotting $d(EF)/dlogD_p$ vs. particle size. The values of $d(EF)/dlogD_p$ were the fuel-specific particle number emission factors for the individual bins, which were calculated from the particle number concentrations, $dN/dlogDp$, for the same bins recorded by the instrument.

The average PSDs obtained by SMPS under vehicle speeds of 56 and 105 km/h of truck speed are plotted separately in Figure 9-10. In the figure, the dark blue lines represent the particle size distributions for the base fuel and the dashed red lines for the B20. By comparing the results, it was found that the PSD was greatly affected by the truck speed. When the truck was travelling at 56 km/h, a unimodal size distribution was generally observed with the mean particle sizes in the range of 20–30 nm. When the truck was operated at 105 km/h, however, the particle size distribution became bimodal with a nuclei mode centered at 10 nm or less and an accumulation mode of 40 nm or larger. Similar trends were also observed both during prior testing of this particular engine as well as in the open literature (Kinsey et al., 2006b; Kittleson et al., 2006)

Similar trends were observed by the nano-SMPS under the same test conditions as presented in Figure 9-11. Though the particle numbers measured by the nano SMPS were slightly different from those obtained by the SMPS under the same experimental conditions, the mean particle sizes determined for the nuclei and accumulation modes were essentially the same for both instruments.

To reveal how the average particle size of diesel exhaust in this study was affected by the experimental conditions, the particle geometric mean diameter (GMD) and their standard deviations were calculated for each particle size distribution. The results from both SMPS and nano SMPS measurements are summarized in Table 9-9. It can be seen that the GMDs obtained from the nano SMPS were generally smaller than those obtained from the SMPS due to its limited size range. The overall average RSD for the SMPS measurement is 4.9%, which is better than the average RSD of 18.2% for the nano SMPS.
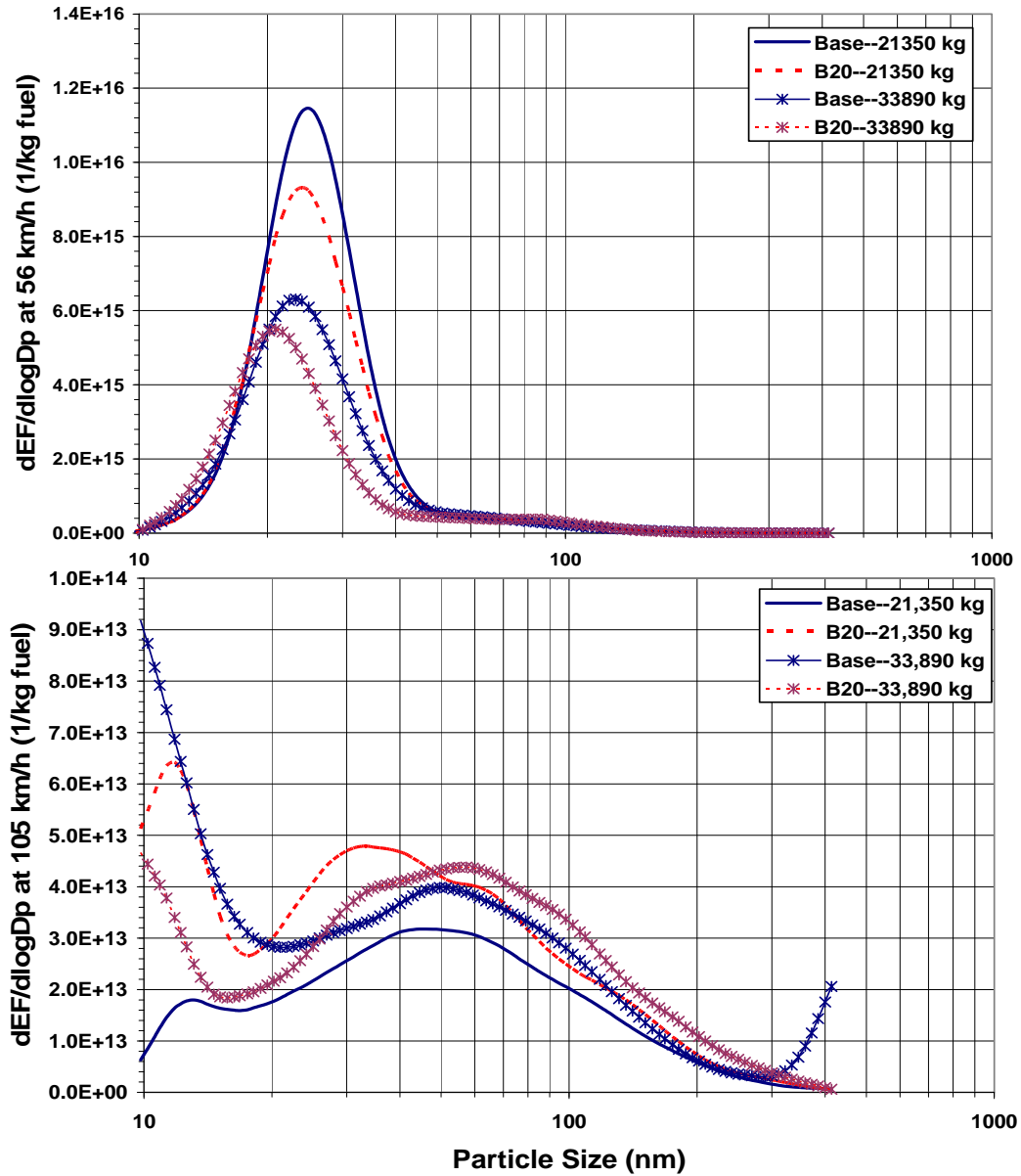
Figure 9-10. **Particle Size Distributions by SMPS Measurements under Various Test Conditions: 56 km/h (top); 105 km/h (bottom)**
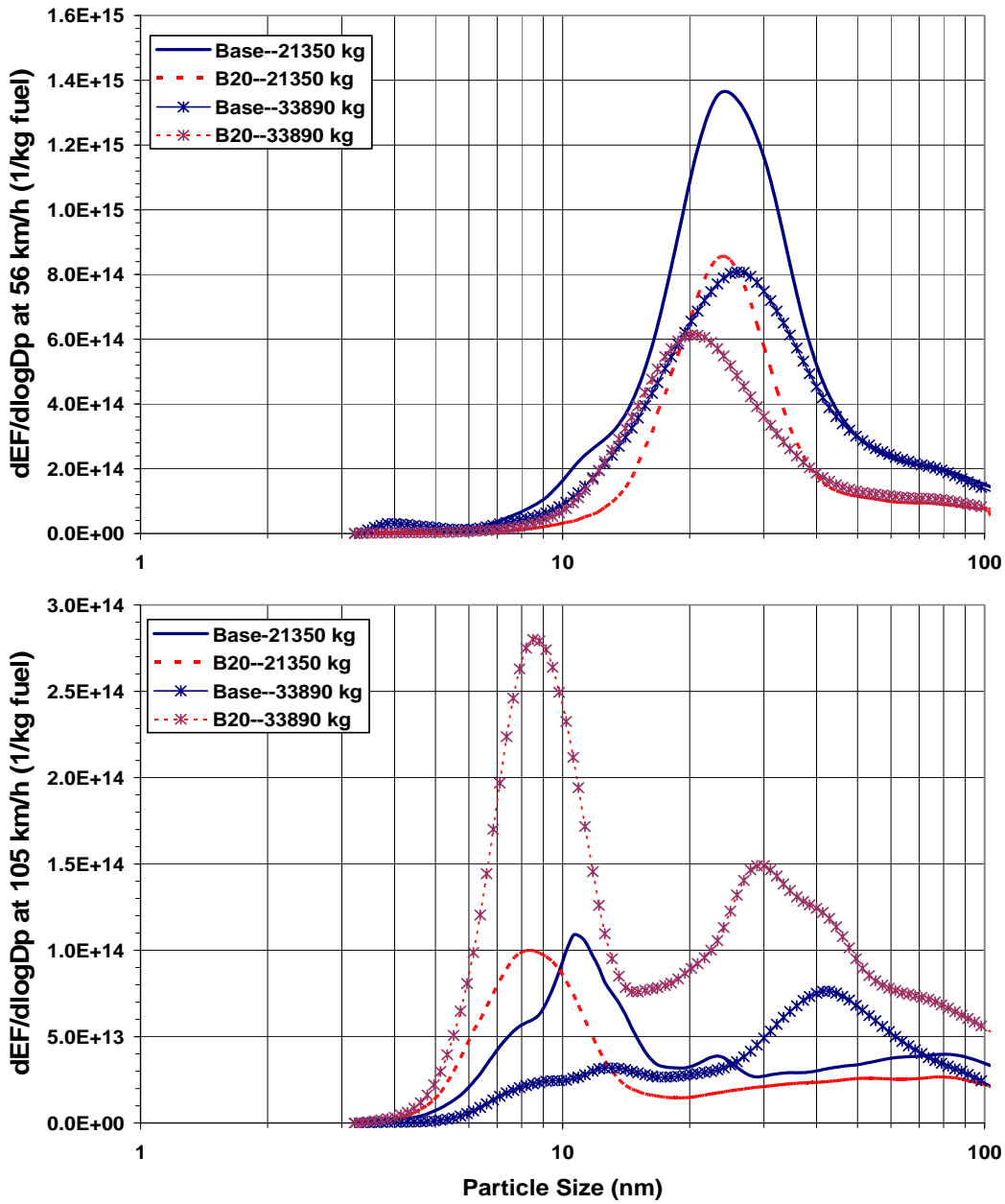
Figure 9-11.   Particle Size Distributions by Nano SMPS under Various Test Conditions: 56 km/h (top); 105 km/h (bottom)

Table 9-9.   GMD Results from the SMPS and Nano SMPS

Test No.	SMPS			nano SMPS		
	Ave[a]	SD[b]	RSD[c] (%)	Ave	SD	RSD (%)
T5	44.4	2.6	5.9	28.4	10.9	38.5
T6	37.9	2.9	7.6	30.3	7.0	23.0
T7	25.7	1.0	3.9	28.8		
T8	25.1	0.7	2.9	30.4	6.5	21.5
T9	25.3	0.9	3.5			
T10	26.4	0.8	2.9	28.4	4.1	14.4
T11	23.9	2.1	8.9	30.0	12.2	40.8
T12	46.2	1.8	4.0	28.9	11.0	38.2
T13	21.8	2.0	9.3	23.5	1.3	5.5
T14	38.6	2.7	7.0	17.1	1.2	6.7
T15	26.6	0.7	2.5	34.6	5.4	15.6
T16	26.9	0.7	2.7	30.9	2.6	8.5
T17	22.4	0.9	3.8	29.4	1.1	3.9
T18	24.5	0.6	2.6	26.1	3.0	11.5
T19	26.6	2.0	7.5	12.3	1.0	8.4
T20	47.6	1.7	3.6			
Average			**4.9**			**18.2**

a. Ave = average.

b. SD = standard deviation.

c. RSD = relative standard deviation.

Figure 9-12 provides the comparison of the GMDs obtained under different experimental conditions. It shows that the GMD increased with truck speed. The particle GMD is around 25 nm (unimodal) for 56 km/h and increased to 30–40 nm (bimodal) when the truck was operated at 105 km/h. This is due to the fact that the PSD has both nuclei and accumulation modes under the higher truck speed. From the results in the figure, we found that both truck load and fuel type had some effect on the GMD.

Figure 9-13 plots the diesel exhaust GMD against the truck power demand. It can be seen that, within the experimental range of this study, the average particle size of diesel exhaust increased with truck power demand for both fuels. However, if the two data sets are conjoined, the plot shows that the GMD varies linearly with the truck power with a correlation coefficient of 0.82.

Table 9-10 is the results of the three-way ANOVA for GMD analysis. The DLS in the table for truck speed is 0.0459, indicating that the truck speed has significant impact on the GMD. The effects of the rest of factors and their interactions on the GMD are insignificant in comparison to the experimental errors.
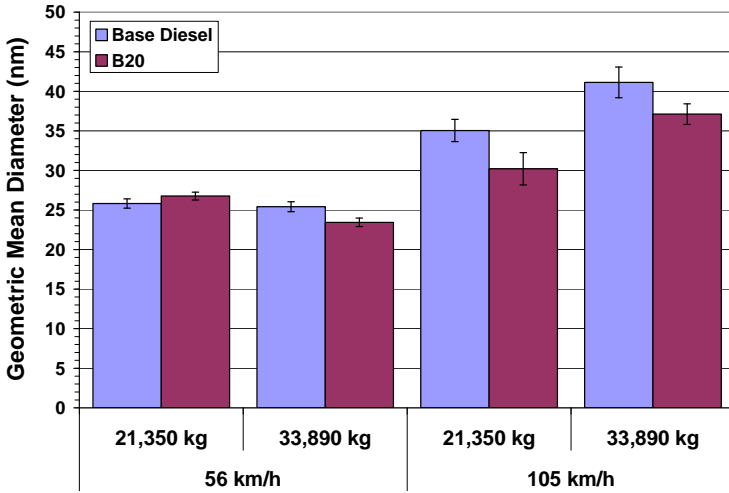
Figure 9-12.   Particle Geometric Mean Diameters by SMPS under Various Test Conditions
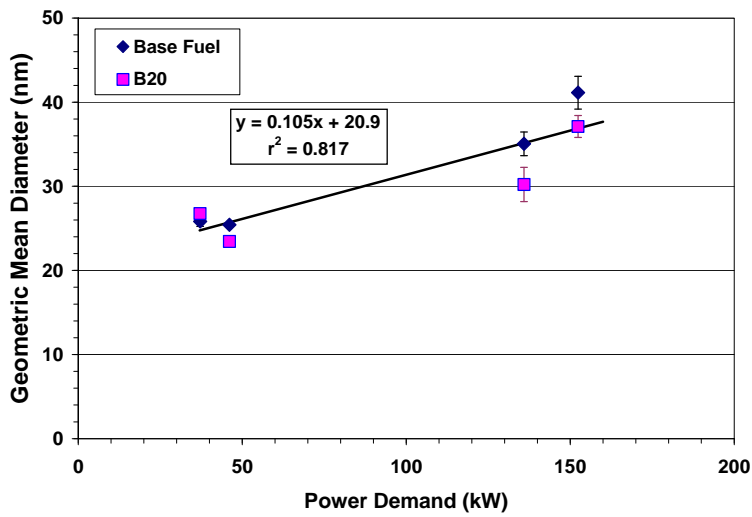
Figure 9-13.   Correlation between Particle GMD and Truck Power Demand under Steady-state Driving Conditions

Table 9-10.   Three-Way ANOVA Results for GMD

| Source	SS[a]	df[b]	MS[c]	F[d]	Pr > F[e]
Fuel	24.5	1	24.5	0.309	0.5937
Speed	442.1	1	442.1	5.574	0.0459
GVW	21.4	1	21.4	0.270	0.6174
Fuel x Speed	15.3	1	15.3	0.192	0.6725
Speed x GVW	69.8	1	69.8	0.880	0.3758
Fuel x GVW	1.1	1	1.1	0.014	0.9091
Fuel x Speed x GVW	3.5	1	3.5	0.044	0.8392
Error	634.6	8	79.3		
Total	**1212.2**	**15**			

a. SS = sum of squared measurement deviations from the overall mean.

b. df = degrees of freedom (for each source, number of parameters considered –1).

c. MS = SS/dt.

d. F = ratio of MS of the source to MS of the error.

e. Pr = probability of obtaining an F value equal to or greater than the calculated F (= DLS).

Chapter 10
Quality Assurance and Quality Control

The DQI (Data Quality Indicator) goals referenced in the QAPP are presented in Table 10-1. This table includes a correction to the CO_2 range because the Horiba Model 210 was replaced with the CAI Model 300. In addition, the QAPP has a typographical error that lists a CO_2 range of 0–2000 ppm; this 0–2000 ppm range should have been labeled CO_L, indicating low range carbon monoxide, instead of CO_2. The CO range of 0–1% in the QAPP is deleted because all the CO data was within the 0–2000 ppm range. The THC analyzer has a range of 0–100 ppm assuming a one carbon gas is used; the upper range becomes a multiple of the number of carbon atoms in the gas. For example, this study used propane, which resulted in an upper range of 300 ppm.

The accuracy completeness goal based on an accuracy value of 2% was too stringent for these types of measurements. To determine most appropriate DQI goal for these analyzers, completeness was recalculated for several slightly elevated DQI goals. The pre-test direct calibration checks were all 100% complete with a DQI of $\pm$ 5% for all instruments. With one exception, this was the case for the post-test checks as well when the DQI goal was raised to $\pm$ 8%, the NO_X analyzer was 93% complete. The values for the bias accuracy completeness were also recalculated at slightly elevated values for the bias DQI accuracy goals since they too are believed to have been too stringent. The pre-test bias checks were 96% complete with a DQI goal of $\pm$ 5% and the post-test bias checks were 94% complete with an accuracy DQI goal of $\pm$ 9%.

The calculated DQI values for the gas phase CEM measurements are presented in Section 10.1. The DQIs for the photoacoustic analysis, thermocouple, mass flow controllers, transducers, and gravimetric analysis are discussed in Sections 10.2 through 10.6, respectively.

10.1 CEM Calibrations

10.1.1   Multipoint CEM Calibration

Multipoint CEM calibrations were performed once before the sampling campaign started to establish appropriate calibration curves for the data acquisition system. Table 10-2 presents the multipoint CEM calibration curves for each of the gases.

Table 10-1.   Data Quality Indicator Goals

Experimental Parameter	Measurement Method	Precision[a]	Accuracy[b]	Completeness	Detection Limit or Range
Gas phase measurements (THC, NO/NO$_X$, O$_2$ CO$_2$, CO)	CEMs	± 2%	± 2%	95%	THC: 0–100 ppm NO$_X$: 0–3000 ppm O$_2$: 0–25% CO$_2$: 0–20% CO$_L$: 0–2000 ppm
1,1,1,2,3,3,3 heptafluoropropane	Photoacoustic analysis	± 5%	± 5%	95%	0–10 ppmv
Temperature	Thermocouple	5%	± 5%	95%	K-type: −200 °C to 1250°C J-type: 0 °C to 750 °C
Volumetric air flow rate	Mass flow controllers[c]	5%	± 10%	95%	0–2 L/min 0–15 L/min 0–50 L/min
Differential pressure	Transducers	5%	± 10%	95%	0–17.5 inches H$_2$0
PM mass[d]	Gravimetric analysis	3 µg[e]	± 15 µg	90%	1 µg

a. Calculated as the relative standard deviation of the reference measurements obtained at a constant instrument set point.

b. Average variation between the reference measurements and instrument readings as determined over the entire operating range.

c. Includes all on-line and time-integrated instruments as well as sampling tunnels.

d. For time-integrated sampling only.

e. Determined as the standard deviation of the results of multiple analyses of the same filter on the same microbalance.

Table 10-2.   CEM Calibration Curves

Gas	Calibration Gas Quantities (% Full Scale)	Instrument Range	Scaling Equation	Date of Calibration	r^2
THC	0, 29, 59, 90	300 ppm	y = 60.106 x − 0.2011	11/21/2003	1
NO$_X$	0, 30, 60, 91	3000 ppm	y = 300.66 x + 3.2978	12/03/2003	0.9999
O$_2$	0, 30, 60, 90	25%	y = 5.0163 x − 0.0756	11/18/2003	1
CO$_2$	0, 12, 24, 36, 49, 62, 73	20%	y = 1.9951 x − 0.078	10/31/2003	1
CO	0, 15, 31, 45, 60, 75, 89	2000 ppm	y = 200.85 x − 5.7935	12/03/2003	1

10.1.2 Daily CEM Calibration Checks

Quality control checks for gas phase measurements were performed before and after each test per the QAPP. The DQI values were calculated from these calibration checks using the formulas listed in Section 7.2.7 of the QAPP (U.S. EPA, 2004) and are presented here. Tables 10-3 through 10-7 present the DQI values for THC, NO, O_2, CO_2 and CO, respectively for each day of testing and include the direct and bias calibration checks.

The QAPP did not reference a separate DQI goal for the CEM system bias checks, which could have been made less stringent (higher) than the direct calibration checks.

Accuracy and precision were calculated each time direct instrument calibration checks and bias system checks were performed, both of which were done twice per test day. The first check was performed in the morning before testing was begun, and the second was done after testing was completed for the day. Because any gas can be used for the bias check, it is redundant and a waste of time and resources to run every gas, so there are some blanks where the bias calibration check DQI values are presented in Tables 10-3 through 10-7. However, more than one gas was always run.

Nearly all of the DQI values for THC measurements shown in Table 10-3 that exceeded the goals were, nonetheless, very close to those goals and occurred when conducting the post-test calibration checks. These errors are due to small drifts in the instrumentation. The bias results show that some values for accuracy were as high as 8.7% but the problem was not consistent through all tests. This may have been a result of "cold" spots in the heated sampling system.

Table 10-4 lists the DQI values for NO_X measurements. About half of the instances when measurements exceeded the goals occurred during the post test direct measurements and half occurred during the system bias measurements. In all but one instance the values were less than 10% and are believed to be due to instrument drift. On two consecutive days (Tests 15-18), the bias values indicate a drop of 30–50% in the instrument readings that is not reflected in the direct DQI values, nor was such a large drop noted in the bias readings of the other CEMs. The problem was suspected to be isolated to the NO_X sampling system rather than the instrument. The lines were cleaned in the field, and the problem readings improved.

DQI values for O_2 gas measurements are listed in Table 10-5. All instances when O_2 measurements violated goals occurred when conducting the direct midrange calibration checks. This instrument performed very well, and all DQI values exceeding the DQI goals were marginal.

DQI values for CO_2 gas measurements are shown in Table 10-6. Nearly all instances when CO_2 measurements violated goals occurred when conducting the direct midrange calibration checks. This instrument performed very well, and all DQI values exceeding the DQI goals were marginal.

DQI values for carbon monoxide gas measurements are listed in Table 10-7. This multirange instrument was used only in its low range and performed very well All DQI values exceeding the DQI goals were marginal.

Table 10-3.   DQI Values for Total Hydrocarbon Gas Measurements for All Tests

Test	Direct Calibration Check				Bias Calibration Check			
	Pretest		Post Test		Pretest		Post Test	
	Accuracy (% bias)	Precision (% RSD)	Accuracy (% bias)	Precision (% RSD)	Accuracy (% bias)	Precision (% RSD)	Accuracy (% bias)	Precision (% RSD)
Full Span Range								
1	–0.21%	0.32%	–3.28%	0.04%	–2.71%	0.04%	–3.86%	0.05%
2	0.02%	0.03%	–1.66%	0.04%	1.08%	0.08%	–5.47%	0.17%
3	–0.08%	0.02%	–0.20%	0.04%	—	—	—	—
4	–0.28%	0.03%	0.83%	0.03%	—	—	–8.74%	0.04%
5	0.03%	0.03%	–0.35%	0.03%	—	—	–6.30%	0.08%
6	–0.21%	0.03%	0.65%	0.04%	—	—	–3.70%	0.11%
7 & 8	0.02%	0.03%	1.13%	0.03%	—	—	—	—
9 & 10	0.41%	0.51%	0.41%	0.03%	—	—	—	—
11 & 12	–0.25%	0.04%	2.03%	0.03%	—	—	—	—
13 & 14	0.04%	0.08%	3.09%	0.03%	0.63%	0.05%	—	—
15 & 16	–0.08%	0.03%	1.60%	0.02%	0.47%	0.08%	—	—
17 & 18	0.04%	0.05%	0.98%	0.02%	—	—	—	—
19	0.00%	0.06%	3.09%	0.03%	—	—	2.33%	0.04%
20	–0.77%	0.87%	4.52%	0.04%	—	—	2.97%	0.07%
Midrange								
1	0.14%	0.04%	—	—	—	—	—	—
2	0.32%	0.05%	–1.53%	0.05%	—	—	—	—
3	0.10%	0.07%	–0.10%	0.06%	—	—	—	—
4	–0.23%	0.03%	1.04%	0.04%	—	—	—	—
5	0.16%	0.04%	0.31%	0.12%	—	—	—	—
6	0.34%	0.02%	0.80%	0.03%	—	—	—	—
7 & 8	0.47%	0.03%	1.62%	0.03%	—	—	1.32%	0.03%
9 & 10	0.23%	0.03%	1.23%	0.05%	—	—	—	—
11 & 12	0.36%	0.02%	2.95%	0.05%	0.40%	0.04%	—	—
13 & 14	0.40%	0.09%	4.02%	0.04%	—	—	3.26%	0.04%
15 & 16	0.24%	0.04%	2.30%	0.04%	—	—	—	—
17 & 18	0.72%	0.07%	2.07%	0.06%	—	—	—	—
19	0.24%	0.21%	3.11%	0.04%	—	—	—	—
20	0.62%	0.05%	5.93%	0.03%	—	—	—	—

Table 10-4.　DQI Values for Oxides of Nitrogen Gas Measurements for All Tests

Test	Direct Calibration Check				Bias Calibration Check			
	Pretest		Post Test		Pretest		Post Test	
	Accuracy (% bias)	Precision (% RSD)	Accuracy (% bias)	Precision (% RSD)	Accuracy (% bias)	Precision (% RSD)	Accuracy (% bias)	Precision (% RSD)
Full Span Range								
1	–0.02%	0.04%	–1.45%	0.02%	–3.77%	10.04%	–0.90%	0.09%
2	0.02%	0.05%	–3.84%	0.18%	–3.55%	0.02%	–8.53%	0.06%
3	–0.86%	0.05%	–1.00%	0.03%	–1.25%	0.11%	—	—
4	0.13%	0.03%	–1.13%	0.03%	—	—	–2.49%	0.04%
5	0.05%	0.04%	3.87%	0.19%	4.85%	0.03%	—	—
6	0.06%	0.02%	–0.07%	0.11%	–8.12%	0.11%	—	—
7 & 8	–0.03%	0.11%	–1.49%	0.09%	–1.91%	0.10%	—	—
9 & 10	0.00%	0.15%	–1.89%	0.07%	—	—	—	—
11 & 12	0.06%	0.07%	–2.24%	0.06%	—	—	–2.08%	0.22%
13 & 14	0.01%	0.13%	–2.28%	0.12%	—	—	—	—
15 & 16	0.14%	0.06%	–1.68%	0.05%	0.10%	0.41%	–51.07%	31.69%
17 & 18	–0.25%	0.71%	–7.97%	0.08%	—	—	—	—
19	–0.02%	0.24%	–10.05%	0.11%	–0.87%	0.07%	–7.84%	0.38%
20	0.00%	0.05%	–5.01%	0.12%	3.35%	0.28%	–2.91%	0.11%
Midrange								
1	1.38%	0.05%	0.37%	0.06%	—	—	—	—
2	2.63%	0.05%	–1.10%	0.08%	—	—	—	—
3	–0.32%	0.03%	0.73%	0.06%	—	—	—	—
4	2.27%	0.45%	0.81%	0.09%	0.19%	0.07%	—	—
5	–2.20%	0.10%	6.31%	0.06%	—	—	–22.27%	0.26%
6	2.29%	0.09%	1.96%	0.08%	—	—	—	—
7 & 8	1.44%	0.11%	1.14%	0.07%	—	—	–6.22%	0.08%
9 & 10	1.98%	0.10%	–0.15%	0.06%	2.12%	0.08%	–0.11%	0.09%
11 & 12	1.73%	0.09%	0.44%	0.07%	—	—	—	—
13 & 14	1.93%	0.10%	–0.39%	0.07%	—	—	—	—
15 & 16	2.14%	0.05%	1.18%	0.19%	—	—	—	—
17 & 18	3.46%	0.14%	–5.57%	0.08%	—	—	–33.14%	0.09%
19	2.57%	0.16%	–7.10%	0.06%	–1.07%	0.09%	—	—
20	4.31%	0.17%	–1.97%	0.12%	4.16%	0.15%	—	—

Table 10-5.   DQI Values for Oxygen Gas Measurements for All Tests

Test	Direct Calibration Check				Bias Calibration Check			
	Pretest		Post Test		Pretest		Post Test	
	Accuracy (% bias)	Precision (% RSD)	Accuracy (% bias)	Precision (% RSD)	Accuracy (% bias)	Precision (% RSD)	Accuracy (% bias)	Precision (% RSD)
Full Span Range								
1	0.33%	0.15%	0.34%	0.12%	—	—	0.13%	0.16%
2	–0.33%	0.14%	0.05%	0.16%	—	—	—	—
3	0.01%	0.13%	0.00%	0.13%	–0.62%	0.16%	—	—
4	–0.22%	0.15%	0.16%	0.13%	–0.57%	0.13%	—	—
5	0.10%	0.18%	0.24%	0.14%	—	—	—	—
6	0.03%	0.13%	–0.59%	0.16%	—	—	–1.68%	0.57%
7 & 8	0.09%	0.15%	–0.26%	0.14%	–0.01%	0.15%	–0.05%	0.15%
9 & 10	0.29%	0.36%	0.26%	0.14%	–0.25%	0.19%	—	—
11 & 12	–0.08%	0.17%	–0.04%	0.17%	—	—	—	—
13 & 14	0.19%	0.19%	0.42%	0.15%	—	—	—	—
15 & 16	0.09%	0.15%	0.17%	0.15%	0.08%	0.13%	0.36%	0.14%
17 & 18	0.16%	0.13%	0.41%	0.13%	—	—	–0.05%	0.15%
19	0.30%	0.14%	–0.42%	0.18%	–0.38%	0.33%	—	—
20	0.11%	0.13%	0.03%	0.14%	—	—	—	—
Midrange								
1	2.10%	0.21%	2.53%	0.14%	—	—	—	—
2	0.40%	0.23%	0.97%	0.15%	—	—	—	—
3	1.26%	0.16%	1.64%	0.19%	—	—	—	—
4	2.37%	0.16%	3.08%	0.18%	—	—	—	—
5	1.89%	0.14%	2.24%	0.30%	—	—	—	—
6	0.52%	0.19%	-0.83%	0.21%	—	—	—	—
7 & 8	1.03%	0.18%	0.14%	0.16%	—	—	—	—
9 & 10	0.85%	0.21%	1.17%	0.15%	—	—	0.07%	0.13%
11 & 12	1.15%	0.17%	0.97%	0.13%	—	—	—	—
13 & 14	0.98%	0.83%	2.37%	0.18%	—	—	—	—
15 & 16	0.59%	0.32%	-0.26%	0.18%	—	—	—	—
17 & 18	1.27%	0.19%	1.54%	0.20%	0.45%	0.15%	—	—
19	1.59%	0.18%	0.78%	0.14%	—	—	0.39%	0.39%
20	2.34%	0.20%	2.07%	0.15%	1.22%	0.33%	1.17%	0.23%

Table 10-6.   DQI Values for Carbon Dioxide Gas Measurements for All Tests

| Test | Direct Calibration Check | | | | Bias Calibration Check | | | |
| | Pretest | | Post Test | | Pretest | | Post Test | |
	Accuracy (% bias)	Precision (% RSD)	Accuracy (% bias)	Precision (% RSD)	Accuracy (% bias)	Precision (% RSD)	Accuracy (% bias)	Precision (% RSD)
Full Span Range								
1	0.27%	0.04%	0.42%	0.06%	1.96%	0.08%	–0.13%	0.09%
2	0.07%	0.04%	1.60%	0.05%	0.21%	0.04%	—	—
3	0.18%	0.04%	0.53%	0.05%	1.10%	0.09%	—	—
4	–0.05%	0.05%	0.62%	0.05%	—	—	–0.14%	0.05%
5	0.02%	0.05%	1.17%	0.04%	1.96%	0.10%	—	—
6	0.14%	0.04%	–1.12%	0.04%	–3.80%	1.46%	—	—
7 & 8	–0.14%	0.05%	0.29%	0.06%	–0.73%	—	—	—
9 & 10	0.10%	0.22%	1.06%	0.04%	1.78%	—	—	—
11 & 12	–0.03%	0.04%	–2.41%	0.04%	—	—	–2.88%	0.10%
13 & 14	–0.47%	0.27%	–1.11%	0.05%	–1.20%	0.04%	—	—
15 & 16	0.18%	0.04%	–0.60%	0.04%	—	—	–3.70%	0.05%
17 & 18	0.08%	0.06%	1.92%	0.04%	–0.14%	0.07%	—	—
19	0.48%	0.66%	–1.77%	0.05%	1.46%	0.12%	—	—
20	-0.18%	0.04%	–0.36%	0.04%	2.29%	0.14%	—	—
Midrange								
1	4.17%	0.06%	4.09%	0.08%	—	—	—	—
2	3.96%	0.07%	5.17%	0.13%	—	—	5.74%	0.13%
3	3.86%	0.07%	4.19%	0.08%	—	—	—	—
4	3.37%	0.08%	4.15%	0.07%	—	—	—	—
5	3.81%	0.08%	5.30%	0.07%	—	—	–0.43%	0.20%
6	4.14%	0.07%	2.62%	0.06%	—	—	—	—
7 & 8	4.03%	0.09%	4.47%	0.07%	—	—	—	—
9 & 10	4.19%	0.06%	5.63%	0.07%	—	—	5.67%	0.06%
11 & 12	4.39%	0.07%	1.93%	0.06%	5.82%	0.06%	—	—
13 & 14	4.28%	0.07%	3.36%	0.07%	—	—	1.81%	0.07%
15 & 16	4.57%	0.07%	3.78%	0.07%	—	—	—	—
17 & 18	3.98%	0.09%	6.07%	0.07%	—	—	—	—
19	4.22%	0.07%	1.89%	0.07%	—	—	2.75%	2.04%
20	3.75%	0.06%	3.83%	0.06%	—	—	4.71%	0.16%

Table 10-7.   DQI Values for Carbon Monoxide Gas Measurements for All Tests

Test	Direct Calibration Check				Bias Calibration Check			
	Pretest		Post Test		Pretest		Post Test	
	Accuracy (% bias)	Precision (% RSD)	Accuracy (% bias)	Precision (% RSD)	Accuracy (% bias)	Precision (% RSD)	Accuracy (% bias)	Precision (% RSD)
Full Span of the Low Range								
1	0.13%	0.93%	0.63%	0.94%	0.84%	0.97%	0.72%	0.97%
2	−0.42%	0.91%	1.07%	1.11%	−0.25%	0.93%	—	—
3	−0.58%	0.93%	−0.28%	0.92%	−0.08%	0.88%	—	—
4	−0.26%	0.93%	0.43%	0.93%	—	—	−0.10%	0.92%
5	0.50%	0.90%	1.25%	0.97%	1.07%	0.98%	—	—
6	−0.83%	0.90%	−1.29%	0.90%	−3.35%	1.86%	—	—
7 & 8	−0.13%	0.91%	0.15%	0.90%	−0.42%	0.91%	—	—
9 & 10	0.57%	0.94%	1.44%	0.96%	1.56%	1.00%	—	—
11 & 12	0.06%	0.93%	−1.26%	0.92%	—	—	−1.79%	0.96%
13 & 14	−0.22%	0.89%	−0.64%	0.91%	−0.68%	0.90%	—	—
15 & 16	0.48%	0.93%	−0.02%	0.89%	—	—	−1.56%	0.92%
17 & 18	0.25%	0.92%	1.49%	0.96%	0.11%	0.89%	—	—
19	1.06%	0.95%	−0.02%	0.89%	1.84%	1.03%	—	—
20	−0.03%	0.89%	0.80%	0.90%	1.14%	0.97%	—	—
Middle of the Low Range								
1	−1.75%	1.28%	−1.57%	1.32%	—	—	—	—
2	−1.83%	1.26%	−0.20%	1.45%	—	—	−0.63%	1.39%
3	−2.05%	1.26%	−1.85%	1.27%	—	—	—	—
4	−2.50%	1.28%	−1.20%	1.34%	—	—	—	—
5	−1.06%	1.29%	0.29%	1.28%	—	—	−3.68%	1.32%
6	−2.52%	1.28%	−2.89%	1.29%	—	—	—	—
7 & 8	−1.87%	1.29%	−1.48%	1.29%	—	—	—	—
9 & 10	−1.08%	1.27%	0.86%	1.20%	—	—	0.74%	1.24%
11 & 12	−1.54%	1.27%	−1.61%	1.25%	−0.65%	1.36%	—	—
13 & 14	−1.64%	1.30%	−0.71%	1.21%	—	—	−1.13%	1.20%
15 & 16	−0.90%	1.25%	−0.22%	1.18%	—	—	—	—
17 & 18	−1.37%	1.27%	0.63%	1.22%	—	—	—	—
19	−0.71%	1.29%	−1.79%	1.25%	—	—	−2.32%	2.60%
20	−1.71%	1.27%	0.27%	1.23%	—	—	0.45%	1.20%

10.1.3 CEM Span Drift

Table 10-8 (pump diesel and low sulfur diesel) and Table 10-9 (biodiesel) list values for the CEM gas analyzer's span drift and zero drift calculated for each test day. The drift was calculated per CFR 86.315-79, which states that the drift shall be less than 2% of full-scale over a 1-hour period. All the percent drifts in the tables were measured over a much longer period than 1-hour. The period of time that the gas analyzers were operated between the morning and evening calibration checks was at least 8 hours or more every test day. Nearly all of the values for percent drift in the two tables below are less than 2% while most of the remaining values are between 2% and 4%. Percent drift was calculated using Equation 10-1:

$$\% \: Drift = \left(\frac{Average \: of \: PM \: Calibration \: Check - Avgerage \: of \: AM \: Calibration \: Check}{Gas \: Analyzer \: Full \: Scale} \right) \quad (10\text{-}1)$$

Table 10-8. CEM Span & Zero Drift for the Pump Diesel and the Low Sulfur Diesel Fuel Tests

	Test # 1	Test # 2	Test # 3	Test # 4	Test # 5	Test # 6	Test # 7 & 8	Test # 9 & 10	Test # 11 & 12
	9/2/2004	10/1/2004	10/13/2004	10/14/2004	10/19/2004	10/20/2004	10/21/2004	10/22/2004	10/23/2004
Span Drift									
CO	0.44%	1.32%	0.26%	0.61%	0.66%	−0.41%	0.24%	0.77%	−1.17%
CO_2	0.11%	1.11%	0.25%	0.48%	0.84%	−0.91%	0.31%	0.70%	−1.73%
O_2	0.01%	0.34%	−0.01%	0.34%	0.13%	−0.56%	−0.32%	−0.02%	0.04%
NO_X	−1.31%	−3.53%	−0.13%	−1.15%	3.48%	−0.12%	−1.34%	−1.73%	−2.10%
THC	−2.77%	−1.51%	−0.11%	1.00%	−0.34%	0.78%	1.00%	0.00%	2.01%
Zero Drift									
CO	−0.14%	0.42%	−0.06%	0.20%	0.29%	0.00%	0.12%	1.31%	0.72%
CO_2	−0.08%	0.03%	−0.07%	−0.05%	0.04%	−0.03%	0.00%	0.21%	0.13%
O_2	0.17%	−0.32%	0.03%	0.46%	0.20%	0.00%	−0.17%	−0.25%	−0.20%
NO_X	0.01%	0.00%	0.01%	−0.01%	0.00%	−0.01%	0.00%	0.00%	0.00%
THC	−0.55%	19.03%	−0.03%	0.13%	0.04%	0.00%	0.05%	0.30%	0.27%

Table 10-9.   CEM Span and Zero Drift for the Biodiesel Fuel Tests

	Test # 13 & 14	Test # 15 & 16	Test # 17 & 18	Test # 19	Test # 20
	10/26/2004	10/27/2004	10/28/2004	10/29/2004	10/30/2004
Span Drift					
CO	–0.38%	–0.44%	1.10%	–0.96%	0.73%
CO_2	–0.46%	–0.56%	1.34%	–1.64%	–0.13%
O_2	0.21%	0.08%	0.23%	–0.64%	–0.07%
NO_X	–2.08%	–1.66%	–7.04%	–9.14%	–4.57%
THC	2.75%	1.51%	0.85%	2.79%	4.78%
Zero Drift					
CO	1.24%	1.00%	0.58%	0.39%	0.94%
CO_2	0.31%	0.20%	0.15%	0.09%	0.20%
O_2	0.93%	–0.28%	–0.18%	–0.20%	0.20%
NO_X	0.00%	–0.01%	–0.07%	0.00%	–0.01%
THC	0.35%	0.43%	0.37%	1.14%	0.55%

10.2 Photoacoustic Multigas Analyzer

Prior to beginning the testing campaign, a new INNOVA 1314 Photoacoustic Multigas Analyzer for sampling the FM-200 tracer gas in the exhaust plume was substituted for the Bruell and Kjaer (B&K) 1302 Multigas analyzer referenced in the QAPP. The main difference between the two devices is that the INNOVA model allows the operator to change the integration time to achieve a faster sampling rate. Table 10-10 lists the calibrations that were performed on the INNOVA analyzer, and the calibration data sheets are included in Appendix C.

The analyzer uses two channels to measure concentrations of propane and the tracer gas, FM-200, in the plume. Quality control checks for FM-200 and propane measured by the photoacoustic analyzer were performed before and after each test per the QAPP. The propane concentration used in the daily pretest and post test calibration checks was 29.4 ppm, and the concentration of FM-200 used in the two checks was 20.0 ppm. The DQI values for propane and FM-200 in Table 10-11 were calculated from these calibration checks using the formulas listed in Section 7.2.7 of the QAPP (U.S. EPA, 2004). Measurements for the photoacoustic analyzer were 100% complete.

10.3 Thermocouples

The Metrology Lab (met lab) calibrations of the DEAL thermocouples are listed in Table 10-12, and the calibration files are included in Appendix D. The thermocouple DQIs can be addressed using the information in the met lab reports. The reports include a "combined expanded uncertainty" value that is applicable over the calibration range of that thermocouple. As long as there were no observations of a thermocouple responding with unexpected values, it is assumed that the true value is +/- that uncertainty of the recorded value. No observations found unexpected values. Met lab experience has determined that thermocouple results are consistent

and reliable within one year of the calibration date. Thermocouple measurements were 100% complete.

Table 10-10. INNOVA 1314 Photoacoustic Multigas Analyzer Calibrations

Optical Filter	Gas Name	Date(s) of Zero Calibration	Date(s) of Humidity Interference Calibration	Date(s) of Span Calibration
UA0971	FM-200	10/7/2004	10/7/2004	10/11/2004, 10/19/2004
UA0987	Propane	10/7/2004	10/7/2004	10/8/2004, 10/19/2004
Water	Water	10/7/2004	NA	10/8/2004

Table 10-11. DQI Values for FM-200 and Propane Gas Measurements for All Tests

Test	FM-200				Propane			
	Pretest		Post Test		Pretest		Post Test	
	Accuracy (% bias)	Precision (% RPD)	Accuracy (% bias)	Precision (% RPD)	Accuracy (% bias)	Precision (% RPD)	Accuracy (% bias)	Precision (% RPD)
1	—	—	—	—	—	—	—	—
2	—	—	—	—	—	—	—	—
3	1.00%	0.70%	-0.44%	0.68%	1.90%	1.11%	2.04%	0.58%
4	2.71%	0.84%	-0.83%	1.27%	-0.26%	1.52%	1.90%	0.93%
5	0.10%	0.22%	-1.90%	0.23%	0.68%	0.00%	0.82%	0.30%
6	0.00%	0.00%	-1.25%	0.28%	0.26%	0.17%	0.53%	0.27%
7 & 8	0.69%	0.26%	-1.75%	0.28%	0.00%	0.22%	1.19%	0.25%
9 & 10	0.73%	0.26%	-1.68%	0.26%	0.04%	0.38%	1.25%	0.24%
11 & 12	1.00%	0.00%	-1.63%	0.24%	-0.53%	0.27%	0.97%	0.13%
13 & 14	0.25%	0.50%	-2.56%	0.18%	-0.23%	0.24%	1.19%	0.28%
15 & 16	1.29%	0.80%	-2.06%	0.17%	-0.48%	0.29%	0.82%	0.30%
17 & 18	0.40%	0.22%	-1.71%	0.27%	-0.94%	0.24%	0.94%	0.24%
19	0.00%	0.00%	-1.75%	0.43%	-0.57%	0.28%	0.40%	0.26%
20	-1.50%	0.51%	-1.64%	0.24%	0.23%	0.28%	0.49%	0.27%
21	NA	NA	NA	NA	NA	NA	NA	NA
22	NA	NA	NA	NA	NA	NA	NA	NA

Table 10-12. Thermocouple Calibrations

Location	Description	Met Lab ID	Calibration Range (°C)	Uncertainty (°C)	Calibration Date	
Background Tunnel	K-Type	02802	20–100	0.9	11//3/2003	2/15/2005
Ambient	K-Type	02803	20–100	0.9	11//3/2003	2/16/2005
Plume Tunnel	K-Type	02804	20–120	0.9	11//3/2003	2/14/2005
Stack	K-Type	02796	25–265	0.8	11/12/2003	—
Exhaust	K-Type	02797	25–265	0.8	11/12/2003	—
Water	K-Type	02798	25–120	0.7	11/12/2003	—
Intake	K-Type	02799	25–120	0.7	11/12/2003	—
Oil	K-Type	02800	25–120	0.8	11/12/2003	—

10.4 Mass Flow Controllers

The met lab calibrations for the DEAL mass flow meters, and the DEAL mass flow controllers are listed in Table 10-13. The calibration files are included in Appendix E. The flow DQIs can be addressed using the information in the met lab reports. The reports include a "combined expanded uncertainty" value that is applicable over the calibration range of that flow device. As long as there were no observations of a flow device responding with unexpected values, it is assumed that the true value is +/- the uncertainty of the recorded value. No observations found unexpected values. Met lab experience has determined that the flow calibrations are consistent and reliable within one year of the calibration date. Mass flow measurements were 100% complete.

10.5 Pressure Transducer

A Dietrich Standard Annubar was used to sense a differential pressure (dP) signal in the tractor exhaust stack, and then the Validyne pressure transducer was used to convert the dP to an analog voltage that could be recorded in the DAS. After completing the study, it was decided that data from the pressure transducer would not be used to determine the exhaust flow, but the exhaust flow would be calculated from the exhaust gas composition instead.

On 10/31/03, the met lab calibrated the DEAL pressure transducer as having an uncertainty of $\forall$0.04 in. of water over its range of 0 to 17.5 in. of water (met lab ID 02801), and the calibration file is included in Appendix F. The DQIs can be addressed using the information in the met lab report. The report includes a "combined expanded uncertainty" value that is applicable over the calibration range of the transducer. As long as there were no observations of the device responding with unexpected values, it is assumed that the true value is +/- the uncertainty of the recorded value. Met lab experience has determined that the transducer calibrations are consistent and reliable within one year of the calibration date. The pressure measurements were 99.1% complete.

Table 10-13. Flow Calibrations

Location[a]	Description	Met Lab ID	Calibration Range	Uncertainty	Calibration Date
Plume FTP1	Mass Flow Controller	02805	0–30 SLPM	0.33 SLPM	11/14/2003
Plume FTP2	Mass Flow Controller	02806	0–30 SLPM	0.31 SLPM	04/08/2004
Background Teflon	Mass Flow Controller	02807	2–15 SLPM	0.07 SLPM	11/14/2003
Background Quartz	Mass Flow Controller	02808	2–15 SLPM	0.12 SLPM	11/05/2003
Background Bypass	Mass Flow Controller	02809	2–15 SLPM	0.08 SLPM	11/05/2003
Background Bag	Mass Flow Controller	02810	0–1.4 SLPM	0.01 SLPM	11/05/2003
Plume TD[b] Quartz	Mass Flow Meter	02212	0–18 SLPM	0.16 SLPM	11/05/2003
Plume TD Teflon	Mass Flow Meter	02214	0–18 SLPM	0.13 SLPM	05/17/2004
Plume Minor	Mass Flow Meter	02812	0–5 SCFM	1%	11/13/2003
Plume Major	Mass Flow Meter	02813	0–38 SCFM	2.2%	11/13/2003

[a] Refer to Figures 2-5, 2-6, and 2-8 for schematics of the Plume and Background Sampling Systems.
[b] TD = thermal denuder

10.6 Post-Test Laboratory Analysis

The data quality objectives, measurement acceptance criteria, and quality assurance and control used for the post-test laboratory analysis have been provided in detail in the Fine PM Characterization Laboratory QAPP (U.S.EPA, 2005). The post-test laboratory analysis of the on-road samples was conducted carefully in accordance with the guidelines set in the QAPP.

As described in MOP No. 2503 in the DEAL QAPP (U.S.EPA, 2004), the working standard weights, the lab control Teflon filter, and random re-weighing were used in this study to insure the quality of gravimetric analysis of the on-road Teflon filter samples. Although the results of individual weighing satisfy the data quality indicator goal (precision < 3 µg), it was found that the weights of the on-road samples were affected by the vaporization losses of volatiles in the samples.

Several quality control checks were performed on the balance used to obtain filter weights. During each weigh session, standard weights of 100.000 mg and 200.000 mg were weighed to demonstrate balance accuracy. Acceptance criteria for accuracy was a difference between the obtained and the standard of less than 0.015 mg. Table 10-14 shows values obtained and the differences from the standard weights. Differences were all less than 0.015 mg in all cases. Teflon control filters were weighed repeatedly to demonstrate balance precision. The control filter was weighed a total of 13 times over 3 weigh sessions with a minimum value of 172.621 mg and a maximum value of 172.629 mg. The average weight for the control filter was 172.626 mg with a standard deviation of 0.003 mg, which meets the acceptance criteria for precision of 0.003 mg. DQI goals were met for accuracy and precision making these measurements 100% complete.

Table 10-14. Balance Variations from Standard Weights

Date	Standard Weight			
	100.000 mg	Absolute Differences, mg	200.000 mg	Absolute Differences, mg
12/7/2004	99.994	0.006	200.003	0.003
1/13/2005	99.997	0.003	200.001	0.001
4/6/2005	99.998	0.002	200.007	0.007

Table 10-15 displays the PM mass results on the Teflon filters weighed on the two different days, which demonstrates the vaporization losses. It can be seen that the PM weights obtained on 2/18/2005 are always lower than those obtained on 12/7/2004 for the same filters. The PM weight results of 2/18/2005 were found linearly correlated with the results of 12/7/2004 as shown in Figure 10-1, indicating a consistently 7% sample loss on all the filters. Since the on-road diesel PM samples contain 30–90% volatile (see Section 6.10), the sample losses occurred during the overnight equilibrium required for Teflon filter samples in the weighing room.

Table 10-15. Comparison of the PM Mass Results Weighed On Two Different Days

Test No.	Sample ID	PM mass (mg)	
		12/7/2004	2/18/2005
5	T020504W	2.088	1.867
6	T020504C	1.662	1.544
7	T092904A	0.196	0.190
8	T092904D	0.871	0.860
9	T020504H	0.890	0.877
10	T020504G	0.560	0.546
11	T092904G	0.448	0.441
12	T092904Y	0.366	0.352
13	T092904N	0.352	0.344
14	T092904L	0.299	0.294
15	T092904W	0.427	0.422
16	T092904U	0.442	0.435
17	T092904R	0.290	0.288
18	T092904T	0.310	0.304
19	T020504K	0.261	0.238
20	T020504O	0.309	0.272
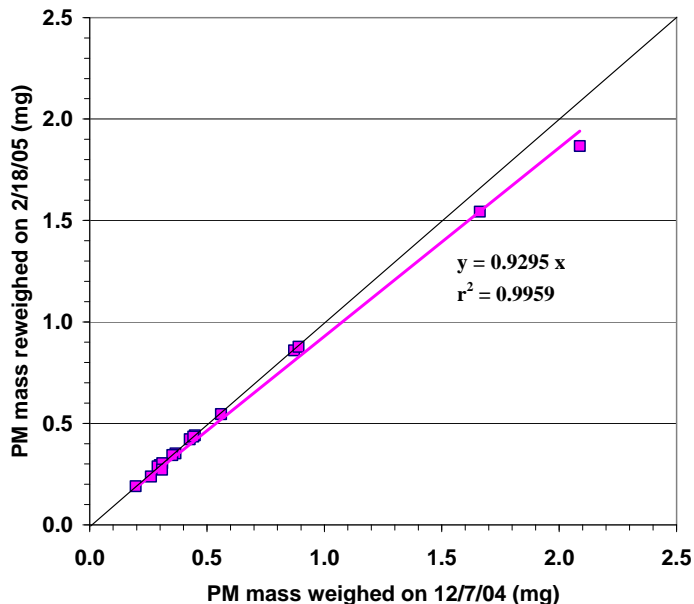
Figure 10-1.   PM Mass Affected by Sample Losses

The best OC/EC analyzer range of deposit concentration is 5–400 µg/cm^2 for organic carbon and 1–15 µg/cm^2 for elemental carbon. However, quite a number of quartz filters collected in this study were found to have less OC and EC than the best OC/EC analyzer range. The concentrations in some of them, such as those behind the thermal denuder, were even below the lower detection limit (0.2 µg/cm^2). To evaluate the data quality of OC/EC results at low concentrations, a second punch (specimen from the filter sample) was taken from the selected quartz filters and analyzed. The OC and EC results from the two samples for the selected filters are plotted in Figure 10-2. It can be seen that, when the OC concentration on the filter is greater than 5 µg/cm^2, the results from the two samples are almost identical. It also shows that the EC results of two samples are close each other when the EC concentration is greater than 1 µg/cm^2. As the OC and EC concentrations on the filters decrease, the quality of OC results becomes less satisfactory.

For the PM speciation, it was found that the percentage of organic compounds in the PM that could be detected by the GC/MS with the currently practiced solvent-extraction protocol depended on the type of PM being measured. Table 10-16 gives some of the results obtained by the laboratory for the samples of different sources. In the table, the mass of organic carbon on the quartz filter determined by the OC/EC analyzer is compared with the mass of organic compounds detected by the GC/MS on the same filter. It can be seen that the diesel truck samples had lowest percentage of organic compound detection.

10-15
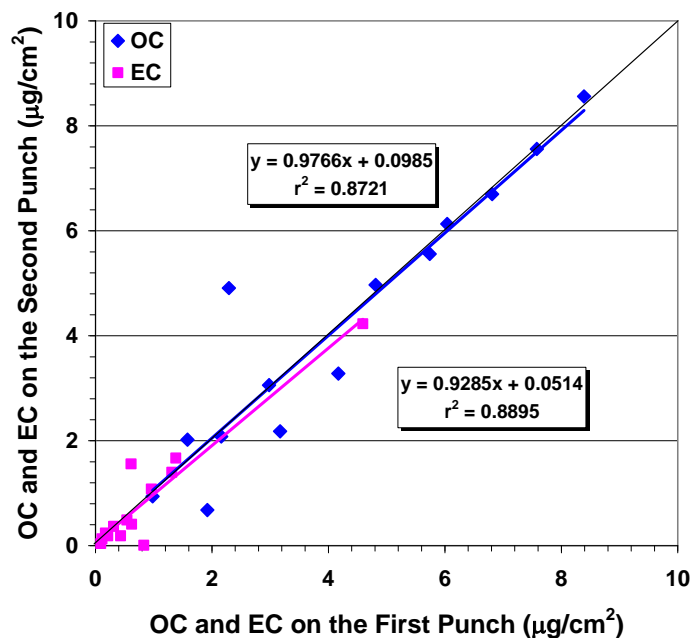
Figure 10-2. Repeatability of OC/EC Analysis

Table 10-16. Effect of Sample Source on Organic Compound Speciation

Sample Source	OC by Analyzer	OC by GC/MS	Detected
	(μg/filter)	(μg/filter)	(%)
On-road diesel truck (this study)	2670	29.5	1.1
Jet engine (APEX-2)	366.5	6.0	1.6
Residential oil boiler	288	51.8	18.0
Industrial oil-fired boiler (NC A&T2)	1020	97.5	9.6

The quality of the on-road inorganic ion analysis was evaluated by comparing the results of three replicate injections of the sample extracts. Table 10-17 provides the relative standard deviation for the filter samples analyzed. All the RSDs in the table are below the measurement acceptance criteria, ± 15%, set for the IC analysis.

In the XRF analytical report, the concentrations of elements were reported together with their uncertainties. In order to insure the quality of emission data calculated accordingly, a criterion was set to discriminate the data reported. Only the element with the concentration three times greater than its uncertainty was considered acceptable for further emission factor estimation.

Table 10-17. Relative Standard Deviation in Inorganic Ions Analysis

Filter ID	RSD (%)				
	K^+	NH_4^+	SO_4^{-2}	NO_3^{-1}	NO_2^-
T020504W		3.46	2.38	0.00	1.40
T020504Y			1.30		
T020504X	3.77		1.10		
T020504C		3.77	1.33		
T020504B					
T020504A			3.01		
T020504K		4.28	4.45		
T020504J					
T020504L			1.90		
T020504O		2.20	0.81		
T020504N		6.19	0.46		
T020504M		1.27	3.67		

Chapter 11
Comparison to Historical Data

A fairly large number of studies on the use of biodiesel fuels have been conducted over the past 10–15 years. Most of these involved dynamometer measurements employing standard test cycles such as those used for engine certification. Some of the more pertinent results using an ultra-low sulfur base fuel and a B20 blend are shown in Table 11-1 for criteria pollutants. As can be seen from this table, no other studies were found in the literature that duplicate the one described in this report.

The results of this study were compared to those of Rosenblatt and Rideout (2007) at Environment Canada (EC) that most closely match the experimental conditions of the current work. The EC study used a chassis dynamometer to determine the emissions from a Cummins ISX 435 ST heavy duty engine installed in an International 9200i tractor (24,000 kg GVW) burning a B20 blend of canola oil and ultra-low sulfur diesel fuel while operating at steady speeds of 50 and 110 km/h. Figure 11-1 shows the percent difference in emissions from the base fuel calculated for all four criteria pollutants as compared to the DEAL at similar operating conditions. Also shown is a single value for the percent change in emissions for a variety of different base and biofuel blends as compiled by EPA in 2001. (U.S. EPA, 2002)

As shown in the figure, all data sets indicate an emissions reduction of up to 20% for THC. In the case of CO, however, only the EC study for the 50 km/h operation found an increase in emissions. For NO_X, the EPA historical database indicated a small increase in emissions whereas the other data indicated up to a 16% decrease. Finally, although significant decreases in PM were consistently reported from all three data sources, the amount of decrease determined in the current study during low speed operation was up to 15 times greater. It should be noted, however, that the Rosenblatt and Rideout data were collected under similar vehicle speeds but on a dynamometer instead of on-road and with a different type of engine, sampling system, and biodiesel fuel blend, which could help explain at least some of this variation.

There are also very limited data available for the PSD generated from burning ultra-low sulfur and biodiesel blends. Only one study was found in the literature which provides a typical PSD for burning low sulfur (50–100 ppm) fuel while operating on-road under conditions generally similar to that of the current program. Kittelson et al. (2006) measured a bimodal PSD with modes at approximately 10 and 60 nm for a Caterpillar 3406E engine, which is comparable to that shown in Figure 9-10 for high speed on-road operation during this study.

Table 11-1. Comparison of Emission Factors for Criteria Pollutants

| Reference	Engine Type	Operating Cycle/Mode	Fuel Type	Fuel Sulfur Content	Reported Emissions Factor/Rate[a]							
					g/bph×h				g/mi			
					THC	CO	NO$_X$	PM	THC	CO	NO$_X$	PM
McCormick et al., 2002	1991 DD60[b]	HD-FTP Transient[c]	Fischer-Tropsch (F-T)	<10	0.007	3.84	4.03	0.17				
			B20: F-T/soy	14	0.005	3.61	4.25	0.146				
Lin et al., 2006	2006 2.8-L 4M40-2AT1	HD-FTP Transient (<300 hr)[c,d]	Petroleum	30	0.280	1.47	3.82	0.125				
			B20: Petroleum/ palm oil	<10	0.250	1.46	3.77	0.117				
Ropkins et al., 2007	1.8-L EURO I light duty diesel[e]	On-road urban driving route (~0 to 70 km/h)	Petroleum	<50	0.122	0.195	0.760	N/A[f]				
			B5: Petroleum/ rape seed	Low not specified	0.118	0.238	0.823	N/A				
Durbin et al., 2007[g]	6.5-L GM	Light duty FTP[h]	ULSD CARB (petroleum)[i]	Low not specified					0.020	0.66	7.2	0.048
			B20: ULSD/soy	Low not specified					0.042	0.84	7.1	0.045
	1993 5.9-L Cummins	AVL 8-mode	ULSD CARB (petroleum)[i]	Low not specified					0.30	0.90	6.5	0.150
			B20: ULSD/soy	Low not specified					0.31	0.92	6.8	0.146
	1999 Caterpillar 3126[j]		ULSD CARB (petroleum)[i]	Low not specified					0.10	0.94	5.3	0.030
			B20: ULSD/soy	Low not specified					0.11	0.88	5.1	N/A
Yang et al., 2007	Mitsubishi 4M40-2AT1	Light duty FTP transient (0 km accumulated operation)[j]	Low S petroleum	22	0.061	0.859	3.91	~0.06				
			B20: Petroleum/ waste cooking oil	21	0.055	0.823	4.35	~0.05				
Rosenblatt and Rideout, 2007	Cummins ISX 435 ST	Steady-state 50 km/h; 24,000 kg GVW	Low S petroleum	<15 ppm					0.50	1.02	14.9	0.166
			B20: Petroleum/ canola oil	Not specified					0.43	1.07	13.1	0.159
		Steady-state 110 km/h; 24,000 kg GVW	Low S petroleum	<15 ppm					0.25	0.61	5.23	0.117
			B20: Petroleum/ canola oil	Not specified					0.27	0.57	5.16	0.104
			B5: Petroleum/ canola oil	Not specified					0.26	0.56	5.11	0.103
			B20: Petroleum/ canola oil	Not specified					0.23	0.58	5.07	0.105
			B2: Petroleum/ tallow	Not specified					0.24	0.60	5.04	0.108
			B5: Petroleum/ tallow	Not specified					0.24	0.61	4.83	0.110

(Table notes on next page)

a. All data in most commonly used units and not converted to SI

b. DD60 = Detroit Diesel Series 60

c. HD-FTP Transient = Heavy Duty-Federal Test Procedure transient cycle per 40 CFR Part 86, Subpart N.

d. Tested after 300 hrs of engine operation.

e. Light-duty Ford Mondeo LX TD automobile.

f. N/A = not available

g. All emissions factors taken from graphs presented in paper. Therefore, all emission values are approximate.

h. Per 40 CFR Part 86, Subpart N.

i. ULSD = ultra-low sulfur diesel fuel; CARB = California Air Re-sources Board.

j. Emissions for B20 rose above base fuel after 20,000 km for THC, CO, and PM
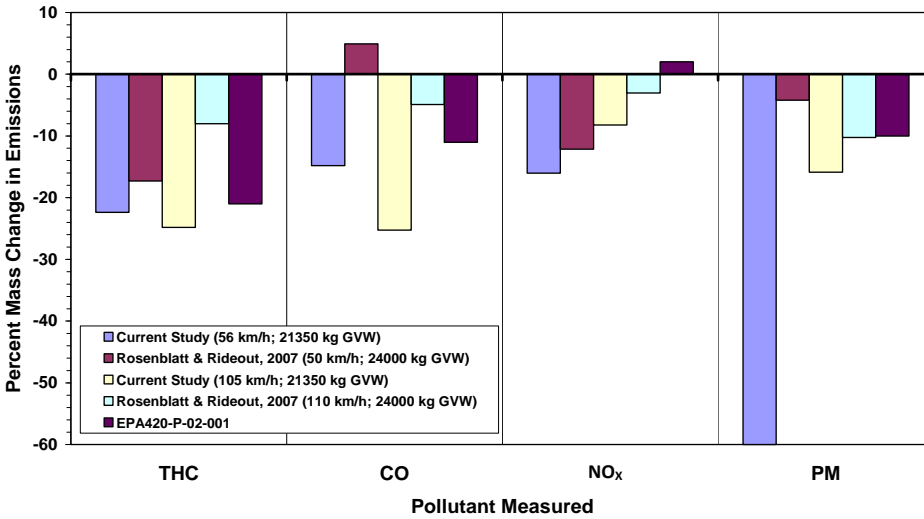
Figure 11-1. **Percent Change in Distance-Specific Emission Factor for B20 Relative to the Base Fuel**

With regard to PM chemical composition, the greatest amount of information available is for total PAHs. Figure 11-2 provides a comparison of PAH analyzer results from this study to data obtained in three other studies that used filter sampling and subsequent GC/MS analysis. The PAH analyzer results from this study were used for comparison in the figure since they are more complete than those derived from the quartz filter analyses. As shown in Figure 11-2, the percent change in PAH emissions for a B20 blend were similar except for the two low speed conditions in the present study. In these cases, there was either no change or a small increase in PAH emissions. This trend is consistent with the gas phase THC emissions measured in the current study, which also tended to decrease with increasing speed as shown above.
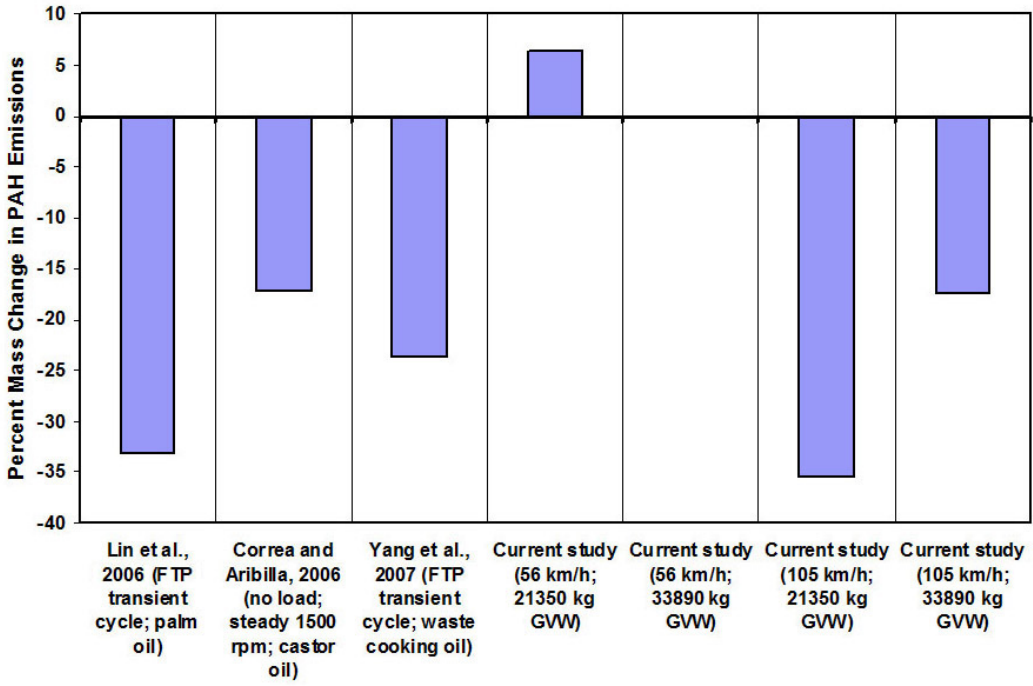
Figure 11-2. **Percent Change in Distance-Specific PAH Emission Factor when Using B20 Relative to the Emission Factor when Using Base Fuel (data for current study taken from continuous PAH analyzer not chemical analysis of the quartz filters)**

Chapter 12
Research Findings

The following conclusions were reached as a result of the research conducted in the study:

1. The emissions of NO_X from the DD60 heavy duty diesel engine tested increases linearly with power demand. Only a relatively small difference in NO_X was observed between the use of the low-sulfur base fuel and B20.

2. Emissions of CO and THC decreased linearly with increasing power demand for the steady-state, near-zero grade tests. Some differences were seen for the two fuels, however, especially at higher power demand.

3. With the exception of the high speed/high load conditions at near-zero grade, the total PM-2.5 mass emissions also decrease linearly with increasing power demand. Substantial differences were observed, however, between the various instruments used to measure this parameter and for the two fuels during low speed (56 km/h) operation.

4. PM-2.5 number emissions decrease exponentially with increasing power demand in the steady-state, near-zero grade tests for both fuels. This was accompanied by the development of an accumulation mode in the PSD with an associated increase in the GMD for the high speed (105 km/h) tests.

5. At the high speed/high load condition, the amount of semi-volatile organic compounds in the PM decreased through the use of B20. These organics appear to be dominated by C17 to C31 alkanes.

6. Using B20 in place of the base fuel reduced nearly all emissions under nearly all operating conditions but the greatest reduction was in the PM-2.5 emission factors.

Based on the study results, the following recommendations are offered for future research:

1. Since the PM-2.5 emission factors determined from the Teflon filter samples for Tests 5 and 6 did not decrease linearly with increasing power demand as was found in other tests, at least a portion of the test matrix should be repeated to verify these results. Also, additional investigation is needed to reconcile the results determined by the filter measurements as compared to the TEOM and QCM.

2. In future on-road investigations, CO_2 and not a tracer gas should be used in the plume measurements. The use of CO_2 would allow a direct determination of fuel-specific emission factors without the use of dilution ratio thus substantially improving the reliability of the data collected.

3. The experimental results are limited to only one diesel engine burning two fuel types. Additional measurements are recommended to determine if the emission vs. power demand relationships developed in the current study also hold true for other engines and fuels.

4. Since only criteria gas emissions were determined in the uphill grade tests, additional measurements should be made for PM-2.5 and its constituents. This work should also include multiple fuel types to provide emission factors with a wider range of application.

Chapter 13
References

Abdul-Khalek, I.S.; Kittelson, D.B.; Graskow, B.R.; and Wei, Q. (1998) Diesel Exhaust Particle Size: Measurement Issues and Trends, SAE Paper No. 980525, Society of Automotive Engineers, Warrendale, PA.

ASTM (2007) Standard Specification for Biodiesel Fuel Blend Stock (B100) for Middle Distillate Fuels, ASTM D6751-07b, ASTM International, West Conshohocken, PA.

Brodrick, C-J.; Laca, E.A.; Burke, A.F.; Farshchi, M.; Li, L.; and Deaton, M. (2004) Effect of Vehicle Operation, Weight, and Accessory Use on Emissions from a Modern Heavy-Duty Diesel Truck, Transport Research Record No. 1880, *J. of the Trans. Res. Board*, pp.119–125.

Brown, J.E.; King, F.G.; Mitchell, W.A.; Squier, W.C.; Harris, D.B.; and Kinsey, J.S. (2002) On-Road Facility to Measure and Characterize Emissions from Heavy-Duty Diesel Vehicles, *J. Air & Waste Manage. Assoc*. **52**(4):388–395.

Canagaratna, M.R.; Jayne, J.T.; Ghertner, D.A.; Herndon, S.; Shi, Q.; Jimenez, J.L.; Silva, P.J.; Williams, P.; Lanni, T., Drewnick, F.; Demerjian, K.L.; Kolb, C.E.; and Worsnop, D.R. (2004) Chase Studies of Particulate Emissions from In-Use New York City Vehicles, *Aerosol Sci. & Tech.* **38**(6):555–573.

Clark, N.N. and Lyons, D.W. (1999) Class 8 Truck Emissions Testing: Effects of Test Cycles And Data On Biodiesel Operation. *Trans. of ASAE* **42**:1211–1219.

Corrêa, S.M. and Arbilla, G. (2006) Aromatic hydrocarbons emissions in diesel and biodiesel exhaust. *Atmos. Environ*. **40**(35):6821–6826.

Dreher, D.B. and Harley, R.A. (1998) A Fuel-Based Inventory for Heavy-Duty Diesel Truck Emissions, *J. Air & Waste Manage. Assoc*. **48**:352–358.

Durbin, T.D. and Norbeck, J.M. (2003) Comparison of Emissions for Medium-Duty Diesel Trucks Operated on California In-Use Diesel, ARCO's EC-Diesel, and ARCO EC-Diesel with a Diesel Particulate Filter, Final Report, Contract No. ACL-1-30110-01, National Renewable Energy Laboratory, Golden CO.

Durbin, T.D., Cocker, D.R.; Sawant, A.A.; Johnson, K.; Miller, J.W.; Holden, B.B.; Helgeson, N.L.; and Jack, J.A. (2007). Regulated Emissions from Biodiesel Fuels from On/Off-Road Applications. *Atmos. Environ.* **41**(27), 5647–5658.

Hays, M.D. and Lavrich, R.J. (2007) Developments in Direct Thermal Extraction Gas Chromatography-Mass Spectrometry of Fine Aerosols, *Trends in Analy. Chem*. **26**(2):88–102.

Kinsey, J.S.; Mitchell, W.A.; Squier, W.C.; Wong, A.; Williams, C.D.; Logan, R.; and Kariher, P.H. (2006a) Development of a New Mobile Laboratory for Characterization of the Fine Particulate Emissions from Heavy-Duty Diesel Trucks, *J. of Auto. Eng*. D3, 220:335–345.

Kinsey, J.S.; Mitchell, W.A.; Squier, W.C.; Linna, K.; King, F.G.; Logan, R.; Dong, Y.; Thompson, G.J.; and Clark, N.N. (2006b) Evaluation of Methods for the Determination of Diesel-Generated Fine Particulate Matter: Physical Characterization Results, *J. of Aerosol Sci.* **37**(1):63–87.

Kittelson, D.B., Watts, W.F.; and Johnson, J.P. (2006) On-Road and Laboratory Evaluation of Combustion Aerosols—Part1: Summary of diesel engine results. *J. of Aerosol Sci*. **37**(8):913–930.

Kweon, C-B.; Okada, S.; Stetter, J.C.; Christenson, C.G.; Shafer, M.M.; Shaver, J.J.; and Foster, D.E. (2003) Effect of Fuel Consumption on Combustion and Detailed Chemical/Physical Characteristics of Diesel Exhaust, SAE Paper 2003-01-1899 Society of Automotive Engineers, Warrendale, PA.

Lin, Y-C.; Lee, W-J.; Wu, T-S.; and Wang, C-T. (2006a) Comparison of PAH and Regulated Harmful Matter Emissions from Biodiesel Blends and Paraffinic Fuel Blends on Engine Accumulated Mileage Test. *Fuel*, **85**(17/18):2516–2523.

McCormick, R.L.; Alvarez, J.R.; Graboski, M.S.; Tyson, K.S.; and Vertin, K. (2002) Fuel Additive and Blending Approaches to Reducing NO_X Emissions from Biodiesel. SAE Paper No. 2002-01-1658, Society of Automotive Engineers, Warrendale, PA.

NIOSH (2003) Diesel Particulate Matter (as Elemental Carbon), Method 5040, Issue 3, National Institute of Occupational Safety and Health, 15 March.

Pierson, W. R. and Brachaczek, W.W. (1982) Particulate matter associated with vehicles on the road. II, *Aerosol Sci. Tech.*, **2**(1):1–40.

Pierson, W.R., Gertler, A.W., Robinson, N.F., Sagebiel, J.C., Zielinska, B., Bishop, G.A., Stedman, D.H., Zweidinger, R.B., and Ray, W.D. (1996) Real-World Automotive Emissions—Summary of Studies in the Fort McHenry and Tuscarora Mountain Tunnels, *Atmos. Environ*. **30**(12):2233–2256.

Ramamurthy, R., Clark, N.N., Atkinson, C.M., and Lyons, D.W. (1998) Models for Predicting Transient Heavy-Duty Vehicle Emissions, SAE Paper 982652, Society of Automotive Engineers, Warrendale, PA.

Ropkins, K., Quinn, R.; Beebe, J.; Li, H.; Daham, B.; Tate, J.; Bell, M. and Andrews, G. (2007) Real-World Comparison of Probe Vehicle Emissions and Fuel Consumption Using Diesel and a 5% Biodiesel (B5) Blend. *Sci. of the Tot. Environ*. **376**(1–3):267–284.

Rosenblatt, D., and Rideout, G. (2007) *Effects of modified drive cycles and biodiesel blends on criteria air contaminant emissions and fuel consumption from a Class 8 highway truck*. Draft

ERMD Report 06-40, Environmental Science and Technology Centre, Environment Canada, Ottawa.

Singer, B.C. and Harley, R.A. (1996) A Fuel-Based Motor Vehicle Emission Inventory, *J. Air & Waste Manage. Assoc*. **46**:581–593.

Society of Automotive Engineers (SAE) (1996a) Road Load Measurement and Dynamometer Simulation Using Coast-Down Techniques, Surface Vehicle Recommended Practice, J1263, February.

Society of Automotive Engineers (SAE) (1996b) Road Load Measurement Using On-Board Anemometry and Coast-Down Techniques, Surface Vehicle Recommended Practice, J2263, October.

Society of Automotive Engineers (SAE) (2003) Procedure for the Analysis and Evaluation of Gaseous Emissions from Aircraft Engines, Aerospace Recommended Practice, ARP1533, August 21.

Turpin, B.J., Saxena, P., and Andrews, E. (2000) Measuring and Simulating Particulate Organics in the Atmosphere: Problems and Prospects, *Atmos. Environ.* **34**(18): 2983–3013.

U.S. EPA (1999) Determination of Metals in Ambient Particulate Matter Using X-Ray Fluorescence (XRF) Spectroscopy, Method IO-3.3, in *Compendium of Methods for the Determination of Inorganic Compounds in Ambient Air*, report No EPA/625/R-96/010a, Office of Research and Development, Cincinnati, OH, June.

U.S. EPA (2002) A Comprehensive Analysis of Biodiesel Impacts on Exhaust Emissions, report No. EPA/420/P-02/001, Office of Transportation and Air Quality. October

U.S. EPA (2004) *Mobile Diesel Laboratory Fine PM Emissions Support: Steady-State Experiments, EPA Quality Assurance Project Plan, Category III/Applied Research, Revision 0*, (QTRAK #2051) Air Pollution Prevention and Control Division, January.

U.S. EPA (2005) *Chemical Analysis of Fine Particulate Matter, EPA Quality Assurance Project Plan, Category III/Applied Research, Revision 7*, (QTRAK #99002) Air Pollution Prevention and Control Division, August.

Yang, H-H., Chien, S-M.; Lo, M-Y.; Lan,, J. C-W.; Lu, W-C; and Ku; Y-Y. (2007) Effects of Biodiesel on Emissions of Regulated Air Pollutants and Polycyclic Aromatic Hydrocarbons under Engine Durability Testing. *Atmos. Environ*. **41**(34):7232–7240.

Yanowitz, J., McCormick, R.L., and Graboski, M.S. (2000) In-Use Emission from Heavy-Duty Diesel Vehicles, *Environ. Sci. & Tech*. **34**(5):729–740.

Appendix A
Chemical Composition

A.1 Black Carbon and PAH Emissions

The recorded black carbon (BC) and particle surface PAH concentration data from the aethalometer and PAH analyzer were used to calculate the average emission factors to investigate their dependence on test conditions. It should be noted that because their emissions were only monitored in the plume, the emission factors obtained from these instruments could not be background corrected and, thus, are probably high.

The test-average fuel-specific emission factors obtained for black carbon and PAH are summarized in Table A-1. The average RSD is 44.1% for BC and 21.9% for PAH, indicating that the quality of the PAH data measured is better than that of BC measurements.

Figures A-1 and A-2 show comparisons of the fuel-specific emission factor results obtained under the different test conditions. The error bars in the figure represent the uncertainties in the emission factor determination. It can be seen that, despite large uncertainties, truck speed exhibits strong effects on these emissions. The increase in unloaded truck speed from 56 to 105 km/h resulted in about a 78% reduction in the BC emission factor with the base fuel and about 84% reduction when fueled with the B20. When the truck was loaded (GVW = 33,890 kg), the increase in truck speed resulted in a BC reduction of 73% for the base fuel and 78% for B20. The increase in truck speed also reduced the PAH emission factor. With the base fuel, a 38% reduction in the fuel-specific PAH emission factor was observed for the unloaded truck and about 45% for the loaded truck. When B20 was used, a greater PAH reduction was observed. The increase in truck speed resulted in a 63% reduction in PAH emission factor for the unloaded truck and a 56% reduction for the loaded truck.

However, a reduction in black carbon and PAH emissions from a change in fuel type was only observed at the higher truck speed (105 km/h). For the unloaded truck, the use of B20 resulted in a reduction by 24% for BC and 33% for PAH. When the truck was loaded, the reduction from using B20 was 28% for BC and 21% for PAH. The truck GVW was found to have little impact on the BC and PAH emissions.

Table A-1.   Black Carbon and PM Surface PAH Emission Factors

| Test No.	EF (mg/kg fuel) BC			EF (mg/kg fuel) PAH		
	Ave[a]	SD[b]	RSD[c] (%)	Ave	SD	RSD (%)
T5	0.324	0.126	38.8	0.546	0.058	10.6
T6	0.268	0.098	36.5	0.417	0.039	9.4
T7	1.097	0.348	31.7	0.776	0.247	31.8
T8	1.075	0.281	26.1	0.966	0.239	24.8
T9	1.117	0.566	50.7	0.698	0.265	37.9
T10	0.928	0.462	49.8	0.738	0.289	39.2
T11	0.181	0.126	69.3	0.387	0.050	12.8
T12	0.268	0.150	56.0	0.504	0.059	11.6
T13	0.171	0.142	82.7	0.299	0.055	18.5
T14						
T15	0.884	0.370	41.9	0.616	0.202	32.8
T16	1.260	0.333	26.4	0.998	0.207	20.7
T17	1.071	0.384	35.8	1.006	0.296	29.4
T18	0.892	0.290	32.5	0.735	0.208	28.3
T19	0.192	0.086	44.6	0.337	0.030	9.0
T20	0.234	0.090	38.6	0.428	0.051	12.0
Average			**44.1**			**21.9**

a. Ave = average.

b. SD = standard deviation.

c. RSD = relative standard deviation.
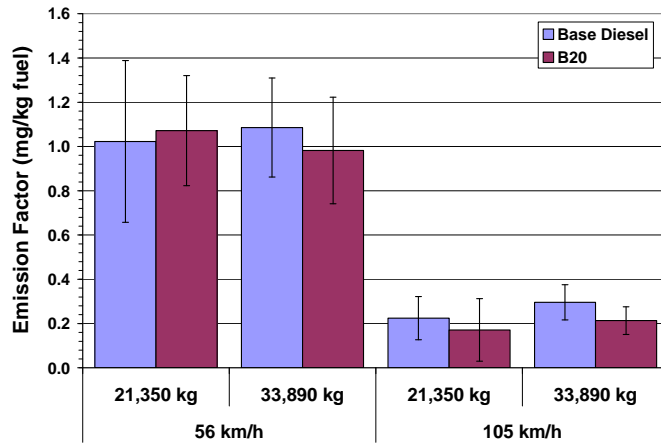
Figure A-1.   Effects of Test Conditions on Fuel-Specific Black Carbon Emission Factor
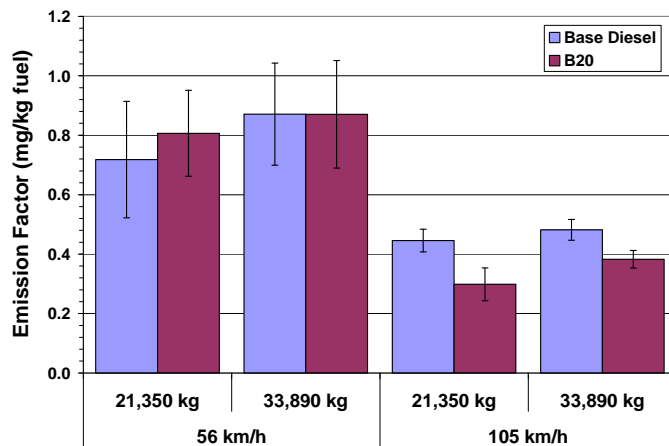
Figure A-2.   Effects of Test Conditions on Fuel-Specific PAH Emission Factor

The three-way ANOVA results for the BC and PAH data are presented in Tables A-2 and A-3. In Table A-2, the only parameter that had significant impact on the BC emission factor was found to be truck speed with a DLS less than 0.0001. Table A-3 shows that the truck speed was also the only parameter affecting the PAH emission factor. The effects of fuel type on BC and PAH emissions were not shown by the ANOVA analysis because of their mixed influences at the higher truck speed.

The effects of experimental conditions on the black carbon and PAH emission factors mentioned above can be explained by the truck power demand. In Figures A-3 and A-4, the fuel-specific emission factors of BC and PAH are plotted against truck power demand, showing that the emission factors are reduced as the power demand increases. This trend is consistent with the finding discussed in Section 9 of this report on PM mass and number emissions.

Table A-2.   Three-Way ANOVA Results for Black Carbon

Source	SS[a]	df[b]	MS[c]	F[d]	Pr > F[e]
Fuel	0.0091	1	0.0091	0.658	0.4407
Speed	2.6525	1	2.6525	190.886	0.0000
GVW	0.0019	1	0.0019	0.137	0.7212
Fuel x Speed	0.0016	1	0.0016	0.118	0.7398
Speed x GVW	0.0049	1	0.0049	0.355	0.5676
Fuel x GVW	0.0083	1	0.0083	0.598	0.4616
Fuel x Speed x GVW	0.0038	1	0.0038	0.273	0.6157
Error	0.1112	8	0.0139		
Total	**2.7933**	**15**			

a. SS = sum of squared measurement deviations from the overall mean.
b. d*f* = degrees of freedom (for each source, number of parameters considered –1).
c. MS = SS/d*t*.
d. F = ratio of MS of the source to MS of the error.
e. Pr = probability of obtaining an F value equal to or greater than the calculated F (= DLS).

Table A-3.   Three-Way ANOVA Results for PAH

| Source	SS[a]	df[b]	MS[c]	F[d]	Pr > F[e]
Fuel	0.0091	1	0.0091	0.658	0.4407
Speed	2.6525	1	2.6525	190.886	0.0000
GVW	0.0019	1	0.0019	0.137	0.7212
Fuel x Speed	0.0016	1	0.0016	0.118	0.7398
Speed x GVW	0.0049	1	0.0049	0.355	0.5676
Fuel x GVW	0.0083	1	0.0083	0.598	0.4616
Fuel x Speed x GVW	0.0038	1	0.0038	0.273	0.6157
Error	0.1112	8	0.0139		
Total	**2.7933**	**15**			

a. SS = sum of squared measurement deviations from the overall mean.
b. d*f* = degrees of freedom (for each source, number of parameters considered –1).
c. MS = SS/d*t*.
d. F = ratio of MS of the source to MS of the error.
e. Pr = probability of obtaining an F value equal to or greater than the calculated F (= DLS).

Figure A-3.   Plot of Black Carbon Emission Factor against Truck Power Demand
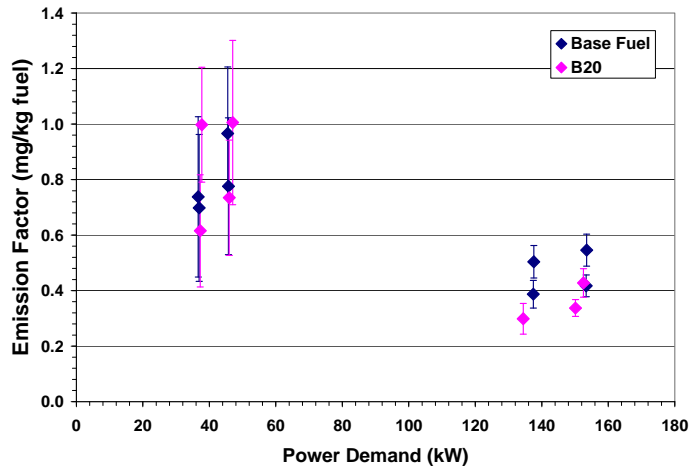
Figure A-4.   Plot of PAH Emission Factor against Truck Power Demand

A.2   PM Organic and Elemental Carbon

The organic and elemental carbon collected on the quartz fiber filters during the tests were determined by the Sunset Laboratory OCEC carbon aerosol analyzer using National Institute for Occupational Safety and Health (NIOSH) Method 5040. (NIOSH, 2003) Because quartz fiber filters have a large specific surface area for adsorbing gases, the particle-phase organics measured on them is increased by gaseous and condensable organics. To minimize these artifacts in the quartz filter sampling, the approach developed by Turpin et al. (2000) was used in this study. According to Turpin's approach, backup quartz filters were installed behind the Teflon filters in both plume and background sampling systems to correct for the gas adsorption artifact by the primary quartz filters. The concentration of PM organic carbon was determined by subtracting the concentration of gaseous organic carbon found on the backup quartz filter from the overall concentration of particulate and adsorbed gaseous organic carbon on the primary

quartz filter. The background-corrected emission factor for particulate OC was then calculated from the backup filter corrected plume and background OC concentrations. The elemental carbon is always considered as particulate; therefore, no backup filter correction was needed in the elemental carbon emission factor calculation. The fraction of non-volatile OC was determined from the analysis of the quartz filters installed behind the TD.

The quartz fiber filters collected for T5, T6, T19, and T20 were analyzed for OC and EC contents. These four tests were conducted at the same truck driving conditions (105 km/h and GVW = 33,890 kg) but with the different diesel fuels. The base diesel was used in T5 and T6, while B20 was used for T19 and T20. Thus, by comparison of the OC and EC emission factors from these tests, the effects of fuel type on OC and EC emission factors could be obtained. Table A-4 presents the backup and background corrected fuel-specific particulate OC and EC emission factors for each type of fuel as well as their weight percentages in the PM. As shown, a large reduction in organic carbon emissions, from 462 mg/kg fuel to 23 mg/kg fuel, was achieved by switching to B20. The percentage of organic carbon in the PM was found to be 52% for the base fuel and 29% for B20, respectively.

Table A-4.   Effects of Fuel Type on OC and EC Emissions for Speciated Tests

| Parameter	Base Fuel	B20
Test	T5 & T6	T19 & T20
Vehicle Speed (km/h)	105	105
GVW (kg)	33,890	33,890
PM EF (mg/kg fuel)	872.2	78.1
OC EF (mg/kg fuel)	462.1	23.0
EC EF (mg/kg fuel)	ND[a]	ND
PM-OC-EC[b] (mg/kg fuel)	410.1	55.1
OC/PM (%)	52.3	29.2
EC/PM (%)	ND	ND

a. ND = not detected.
b. PM-OC-EC = The part of PM excluding OC and EC.

As can be seen from Table A-4, the PM collected on the quartz filters for both fuels contains very little elemental carbon, which is unusual for a diesel engine. However, the elemental carbon emission factors determined by the aethalometer measurement for these two fuels are in the range of 0.2–0.3 mg/kg fuel. The discrepancy in EC results between the quartz filters and the aethalometer is probably due to the different techniques used. The black carbon was measured by the aethalometer based on light-absorption, and the elemental carbon was measure by the OC/EC analyzer based on thermal refraction.

The results of very low fraction of EC in the PM observed in this study do not appear to agree with that reported by some of other investigators using low-sulfur fuel in dynamometer studies (Durbin and Norbeck, 2003; Kweon et al., 2003).

A.3 Semi-Volatile Organic Compounds in Particulate Emissions

The material collected on quartz filters during the four speciated test in this study were composited as shown in Table 5-2 of the main report. The back-up and background correction discussed in Section A.2 for the OC emission factor calculation was also used in calculating the backup and background-corrected emission factors for individual organic compounds from the GC/MS analysis of the quartz filters. Figure A-5 shows the difference in the fuel specific PM organic emission factors obtained from the two fuels at high speed and load. As can be seen, the PM emitted from the truck contained many more organic compounds when using the base fuel (T5 and T6) than when using B20, which is consistent with the observations for organic carbon discussed in the previous section. Figure A-5 also shows that PM from the use of base fuel was dominated by C17–C31 alkanes. This agrees well with the observations by other investigators. (Canagaratna et al., 2004)
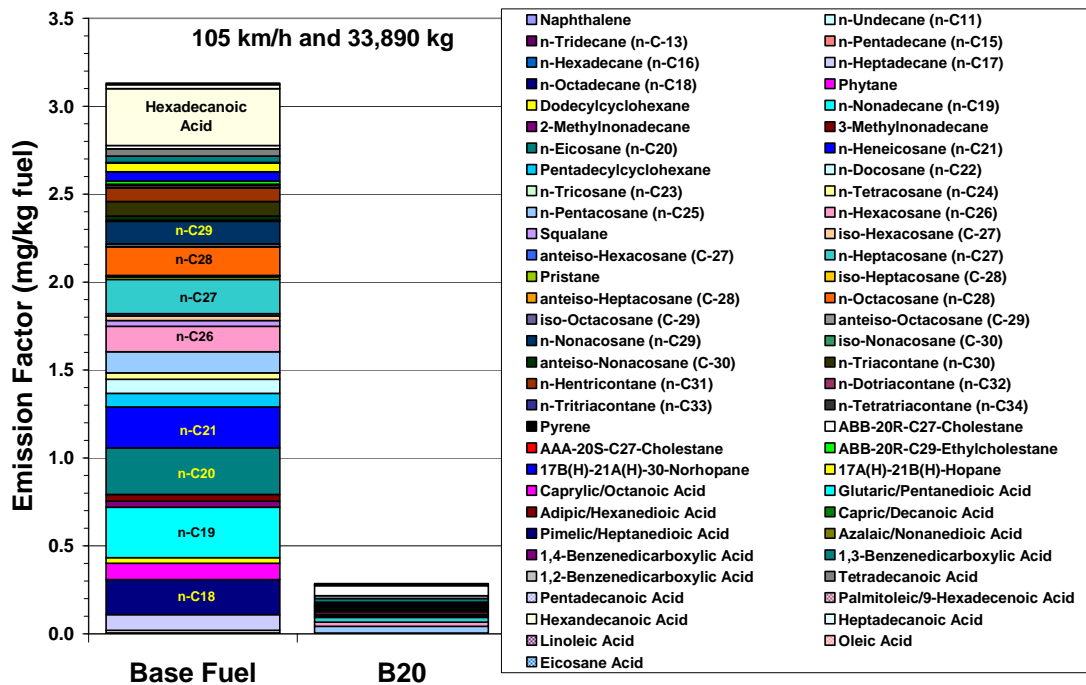
Figure A-5.   Effects of Fuel Type on Emission Factors of PM Organic Species

In comparison to the base fuel, burning B20 produced less alkanes. Since both the diesel fuel and lubricating oil contain high concentrations of alkanes, this suggests that the B20 has higher combustion efficiency than the base fuel.

In addition to alkanes, the PM from burning the base fuel also contained a small amount of PAHs and notable quantities of organic acids. For the B20, on the other hand, the PM contained approximately equal amounts of alkanes and acids. To further investigate the speciation results, the fuel-specific emission factors of the compound groups for the two fuels are compared in Table A-5. The table includes the results with and without the backup quartz filter correction. As discussed in Section A.2, the backup quartz filters installed behind the Teflon filters were used to

correct the sampling artifact caused by adsorption of gas-phase organics on the surface of quartz filters. Therefore, by comparing the results with and without backup filter correction, the effects of gas-phase organic compounds can be identified. For the base fuel, about 31% of the alkanes and 60% of the acids were gas-phase organics adsorbed on the primary quartz filters. For the B20, 4% of the alkanes and 69% of the acids were in the gas-phase. However, for both fuels, very little amount of gas-phase PAH was found in the PM collected by the primary quartz filters.

Table A-5. Effects of Quartz Filter Sampling Artifact for 105 mkm/h and 33,890 kg GVW

| Organic Group | Emission Factor (mg/kg fuel) | | | | Gas-Phase Organics on Primary Quartz Filter (%) | |
| | No Backup Correction | | With Backup Correction | | | |
	Base Fuel	B20	Base Fuel	B20	Base Fuel	B20
Alkanes	3.69	0.13	2.54	0.13	31.3	4.4
PAH	0.14	0.01	0.14	0.01	1.8	
Acids	1.15	0.48	0.46	0.15	60.4	68.9

A.4 Elements and Ions in Diesel Truck Particulate Emissions

Various trace elements in the PM are considered to originate from the presence of the elements in fuels, from the organometallic additives in lubricating oils, and from the wear and corrosion of engine and exhaust system. In this study, the background corrected fuel-specific emission factors for the elements found in PM were determined from the XRF (U.S.EPA, 1999) analytical results of the Teflon filters collected from both plume and background sampling systems in tests T5, T6, T19, and T20. Note again the unusually high PM-2.5 emission factors obtained for T5 and T6.

The emission factor calculation found that the total fuel-specific emission factor for all the elements detected by the XRF was about 35.4 mg/kg of base fuel, which is almost eight times higher than the total elemental emission factor of 4.5 mg/kg of the B20. The higher elemental emissions for the base fuel is consistent with the higher PM mass emissions obtained from the Teflon filter gravimetric analysis and with the higher OC and semi-volatile organics obtained from quartz filter analyses for the same tests. It is also in agreement with the higher particle number emissions obtained by the ELPI for T5 and T6.

The XRF analytical results show that about 98% of the detected element mass was silicon (Si) for T5 and T6 and about 85% for T19 and T20. Since soil dust from ambient air that gets mixed in with the plume is usually considered to account for all of the silicon found in the PM (Pieson and Brachaczek, 1983), the Si is excluded in the comparison of element emission factors for the two fuels as shown in Figure A-6. The figure shows that, sulfur (S) was the primary component existing in the PM, accounting for 36% of the total elements for the base fuel and 71% for the B20. It was also seen that there was notable amount of aluminum (Al) and chlorine (Cl) in the PM samples from the base fuel. Most Al found in the PM can be considered to originate from soil dust. The Cl in the PM may come from either soil or a fuel additive. However, it should be

pointed out that, except for Si, the emission factors for the rest of detected elements were insignificant in comparison to the total PM mass. This probably indicates that the Teflon filters in this study collected a lot of soil dust. The lower emission factor of sulfur (less than 0.5 mg/kg fuel) observed for both base fuel and B20 is consistent with the low sulfur content of the two fuels used in this study.
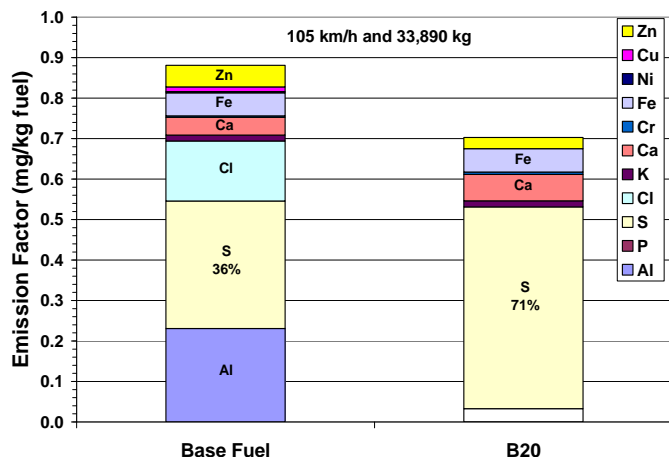
Figure A-6.   Fuel-Specific Element Emission Factors by XRF (Si component removed)

The low sulfur emissions were verified by an IC analysis of the Teflon filter samples. The concentration in the PM samples from both fuels was so low that water-soluble sulfates (SO_4^{-2}) could not be detected by the IC. Figure A-7 compares the ion emission factors for the two diesel fuels, showing a higher ion content in emissions from use of the base fuel. According to the IC results, the detected water soluble ions in the base fuel PM consisted of 44.5% ammonium (NH_4^+), 24.6% nitrates (NO_3^{-1}), and 30.8% nitrites (NO_2^-), whereas only NH_4^+ was detected in the B20 PM.
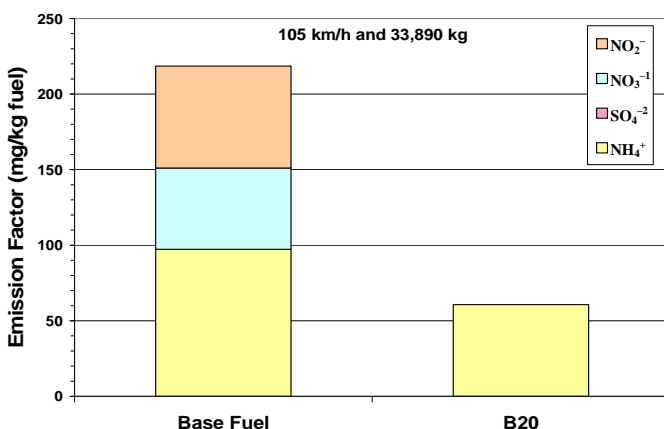
Figure A-7.   Fuel-specific Ion Emission Factors by IC

A.5 Composition of PM Emissions

The fuel-specific emission factor results obtained for PM mass, organic carbon, black carbon, semi-volatile organic compounds, inorganic ions, and elements from the combustion of each diesel fuel are summarized in Table A-6. The table shows that only a small fraction of the total organic carbon determined by the OC/EC analyzer could be ascertained by solvent extraction and GC/MS analysis. For the samples from the base fuel, for example, the fuel-specific OC emission factor determined by the OC/EC analyzer is 462 mg/kg fuel, but the organics detected by solvent extraction analysis could only account for 0.8% of this total. This difference occurs partly because not all organic compounds in the sample can be solvent extracted and resolved and not all those organic compounds extracted can evolve at the GC operating temperature of 300 EC. Moreover, the difference is consistent with previous analyses by EPA and others and highlights the limitations of solvent extraction discussed in Hays and Lavrich (2007).

**Table A-6.   Emission Factors of PM Components from Base Fuel and B20 for 105 km/h and 33,890 kg GVW**

PM Component		Instrument	Media	Emission Factor (mg/kg fuel)			
				Base Fuel		B20	
Component	Component Constituent			Component	Component Constituent	Component	Component Constituent
Soluble NH_4^+		IC	Teflon filters	97.4		60.7	
Soluble NO_3^{-1}		IC	Teflon filters	53.8			
Soluble NO_2^-		IC	Teflon filters	67.4			
Elements		XRF		35.4		4.6	
	Si	XRF	Teflon filters		34.5		3.9
	Others	XRF	Teflon filters		0.9		0.7
Total OC		OC/EC analyzer	Quartz filters	462.1		23.0	
	Alkanes	GC/MS	Quartz filters		2.54		0.13
	PAH	GC/MS	Quartz filters		0.14		0.01
		UV analyzer			0.5		0.4
	Acid	GC/MS	Quartz filters		0.46		0.15
	Undefined	OC/EC analyzer	Quartz filters		458.6		22.3
Total BC		OC/EC analyzer	Quartz filters				
		Aethalometer		0.3		0.2	
Undetermined (ND)				155.8			
Total PM		**Gravimetric**	**Teflon filters [a]**	**872.2**		**78.1**	

a. Note that this emission factor fell outside of the trend observed for the other tests conducted. See Figure 9-2 of the main report.

Figure A-8 illustrates the mass percentage of each component in the PM from the base fuel and B20. The figure shows that the base fuel PM consists of 53% OC, 11% NH_4^+, 14% NO_3^{-1}, 8%

NO_2^-, and 4% Si. The undetermined compounds account for 18% of PM. For the B20, its PM contains approximately 26% OC, 69% NH_4^+, and 4% Si.

Because very limited experimental conditions were studied, the results of emission factors obtained are valid only under these specified operating conditions and fuels. In order to establish a complete emission inventory, more studies are required with other types of engines under additional levels of vehicle speed and GVW, and different road grades.
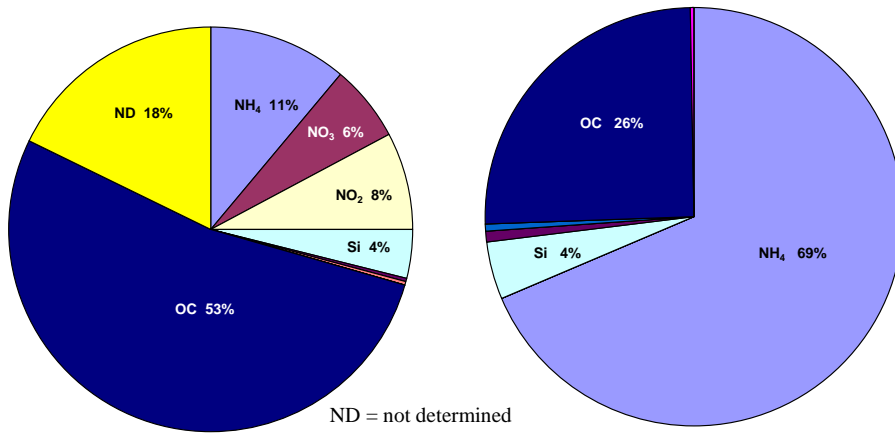
Figure A-8.   Percentage of Each Component in the PM for Base fuel (left) and B20 (right)